Exotic Contributions to Double Beta Decay

Research Thesis

by

Guilherme Ruiz Ferreira

August 2020

1st Supervisor: Frank Deppisch

2nd Supervisor: Ruben Saakyan

A Dissertation submitted in part fulfilment of the

Degree of Master of Science in Physics

Department of Physics & Astronomy

University College London

Abstract

Searching for exotic contributions to double beta ($\beta\beta$) decay is paramount for probing the nature of neutrino masses and beyond the Standard Model physics. In this study, in addition to considering Majorana neutrinos, we introduce a hypothetical Majoron particle ϕ which couples only to neutrinos via both right and left-handed currents. This particle is assumed massive and scalar. After a brief review of neutrino physics, we discuss the theory and experiments behind $\beta\beta$ decay, including the key concepts of nuclear physics and experimental constraints which rule such reactions. We also discuss corrections and realistic approximations needed to be made throughout the calculation of the theoretical amplitudes. We then investigate three of the most promising $\beta\beta$ decay modes: the standard neutrinoless double beta ($0\nu\beta\beta$) decay, the simplest Majoron emitting neutrinoless double beta ($0\nu\beta\beta\phi$) decay, and as an extension to the known literature, we mainly investigate the two peculiar modes of the simplest Majoron induced double beta ($2\nu_\phi\beta\beta$) decay. We name the first mode s-Channel. It is an extension to ($0\nu\beta\beta\phi$) decay, in which the Majoron is virtual and decays into a pair of neutrinos. The second mode is called t+u-channel. It is a very distinct process, similar to $2\nu\beta\beta$ decay, in which the two emitted neutrinos are scattered via a Majoron exchange. We show that the neutrino emitting processes favour emitting electrons with total energy less than half of the decay's kinetic energy release. Both $0\nu\beta\beta\phi$ and $2\nu_\phi\beta\beta$ are demonstrated to be heavily suppressed by the Majoron mass m_ϕ. Also, for $2\nu_\phi\beta\beta$ decay, we show that increasing m_ϕ shifts the electron energy distribution to a higher share of the kinetic energy release. This behaviour makes the normalised energy distribution of both $2\nu_\phi\beta\beta$ and the standard double beta ($2\nu\beta\beta$) decays overlap and become almost indistinguishable for a large enough m_ϕ. Our results motivate further theoretical dedication and experimental searches for such exotic $\beta\beta$ decay modes.

Contents

1 Introduction **3**

2 Neutrinos **4**

2.1 Neutrinos in the Standard Model 4

2.2 Dirac versus Majorana Nature of the Neutrinos 5

3 Double Beta Decay **7**

3.1 Neutrinoless Double Beta Decay 7

3.2 Majoron Induced Double Beta Decay 8

3.3 Principles of Nuclear Physics 9

3.4 Calculating Double Beta Decay Amplitudes 11

4 Neutrinoless Amplitudes **14**

4.1 $0\nu\beta\beta$ Leptonic Current 15

4.2 $0\nu\beta\beta\phi$ Leptonic Current with Scalar ϕ Emission 19

4.3 Neutrinoless Phase Space and Decay Rates 24

4.4 Neutrinoless Energy Distribution 26

5 $2\nu_\phi\beta\beta$ with Virtual Scalar ϕ Exchange **29**

5.1 s-Channel Leptonic Current 29

5.2 t+u-Channel Leptonic Current 30

5.3 Phase Space and Decay Rates 36

5.3.1 s-Channel 36

5.3.2 t+u-Channel 39

5.4 Energy Distribution 43

5.4.1 s-Channel 44

5.4.2 t+u-Channel 47

6 Conclusion **50**

A $W^+W^- \to e^+e^-$ Matrix Element **51**

B The Standard Double Beta Decay **52**

References **54**

1 Introduction

After the discovery of the Higgs boson [1][2], the Standard Model has been completed. Every predicted particle has been observed, and the theory is, in the physicists' jargon, self-consistent. However, in a more sceptical point of view, we have also stumbled across many discrepancies from its original formulation. In fact, the very Higgs mechanism was developed to fix one of these discrepancies, namely, the mass of the gauge bosons. Another unpredicted phenomenon is the oscillation of neutrino flavours, which requires that neutrinos have tiny, yet finite, masses [3][4]. The mere existence of neutrino masses, and their peculiar magnitudes, is a sign that, perhaps, there is more to discover beyond the Standard Model. Introduced by Wolfgang Pauli in his "Dear radioactive Ladies and Gentlemen" letter [5] in 1930, the neutrino (ν) was postulated to be a massless, spin-$\frac{1}{2}$, neutral fermion. Its inclusion to the Standard Model was meant to explain the continuous energy spectra observed in beta decay via a direct coupling to the positron (e^+) through the weak charged current. Although exceptionally simple in its original formulation, the neutrino has proven itself to be full of surprises. We are still far from truly knowing all of its properties. For this, and many more reasons, neutrino physics is currently at the forefront for searching for new physics.

The so-called double beta ($\beta\beta$) decay, akin to how single beta decay unveiled the neutrino, is arguably the most promising process to reveal the remaining mysteries behind the neutrino, as will be shown in this study. The standard double beta ($2\nu\beta\beta$) decay consists of two neutrons simultaneously decaying into two protons, two electrons and two electron antineutrinos. Conserving lepton number, $2\nu\beta\beta$ decay is an allowed process in the Standard Model and has already been detected by numerous experiments [6][7]. The simplest neutrinoless double beta ($0\nu\beta\beta$) decay, on the contrary, is a lepton number violating process. It consists of a $\beta\beta$ decay in which the neutrino emitted by one nucleon is absorbed by the other nucleon. The exchanged neutrino is a virtual particle and must be its own antiparticle. This is a forbidden process in the Standard Model. However, if neutrinos are indeed Majorana particles, they are their own antiparticles and such process is allowed, opening the doors to a beyond the Standard Model physics.

Following this introduction, in Section 2 we present a brief overview of neutrino physics, encompassing the latest experimental and theoretical knowledge. Then, in Section 3, we discuss the importance of double beta decay, both standard and neutrinoless, as a probe to the very nature of neutrino masses. However, as the title of this work suggests, we are not limiting ourselves to Standard Model particles. We use this freedom to introduce, in Section 3.2, a hypothetical Majoron particle, which could allow prominent double beta decay modes, as well as being a decent candidate for dark matter. Later, in Section 3.3 we summarise the basic required principles of nuclear physics to deal with double beta decay. Finally, using particle physics techniques described in Section 3.4, we calculate the theoretical amplitudes for the specified double beta decay processes in Sections 4 and 5. These amplitudes tell us what an experimentalist should expect to measure and highlight what traits are more advantageous in each process. Our ultimate goal is to bring to the spotlight processes beyond the Standard Model, both well known in the literature and newly proposed, which could be waiting for us right behind the background spectrum.

2 Neutrinos

In this section, we first introduce the neutrino as it is currently formulated in the Standard Model. Then, we address the open dilemma regarding the nature of neutrino masses.

2.1 Neutrinos in the Standard Model

Today, we know from the Cowan–Reines neutrino experiment in 1956 [8][9], and the Lederman, Schwartz and Steinberger experiment in 1962 [10], that the neutrino is real and a member of three families of particles together with a charged lepton counterpart. It couples to its counterpart via the weak charged current, which is mediated by the W-boson. Said boson is a doublet of charge ± 1 member of the $SU(2)_L$ group, where the subscript L denotes that only left-handed currents are present, as discovered by Wu in 1957 [11]. Such parity violation implies that a massless neutrino has only left-handed components in the Standard Model. A neutral current interaction between neutrino and antineutrino is also possible via the Z-boson, a neutral singlet of the same group. These properties alone would make the neutrino quite simple and dull. Reality is much more complicated and, we dare say, deeply interesting. The surprise, and reason behind this study, came when neutrinos were observed to oscillate.

First proposed by Bruno Pontecorvo in 1957 [12], neutrino oscillation is a quantum mechanical phenomenon where a neutrino created with a specific lepton flavour can later change to another flavour. It is of extreme interest in both theoretical and experimental physicists as it implies that neutrinos must have non-zero and distinct masses. However, it was not until the experimental discovery of neutrino oscillations in 2002 [4] by the Sudbury Neutrino Observatory (SNO) [13] and later in 2015 [3] by the Super-Kamiokande Observatory [14] that Pontecorvo's prediction was confirmed.

The mechanism for neutrino oscillation emerges from a mixing between flavour and mass eigenstates. That is, the weak eigenstates, which are the ones that couple to the charged leptons, are each a different superposition of mass eigenstates. This mixing of eigenstates leads us to the Pontecorvo-Maki–Nakagawa–Sakata (PMNS) mixing matrix [15]:

$$\begin{pmatrix} \nu_e \\ \nu_\mu \\ \nu_\tau \end{pmatrix} = \begin{pmatrix} U_{e1} & U_{e2} & U_{e3} \\ U_{\mu 1} & U_{\mu 2} & U_{\mu 3} \\ U_{\tau 1} & U_{\tau 2} & U_{\tau 3} \end{pmatrix} \begin{pmatrix} \nu_1 \\ \nu_2 \\ \nu_3 \end{pmatrix} \tag{2.1}$$

Where the matrix elements U_{ij} result from the neutrino mixing angles θ_{ij} and an imaginary phase δ. This mixing allows neutrinos to change flavour over time, once that each superposed mass eigenstate evolve in time as a plane wave

$$\nu_k(t) = \nu_k(0) e^{-iE_k t}, \quad k = 1, 2, 3 \tag{2.2}$$

If neutrinos were massless, the phases would be all the same as they would all be propagating at the speed of light. We cannot measure the individual neutrino masses directly, but from the latest experimental

results [16] we have the mass splits and mixing angles

$$\Delta m^2_{21} = 2.5 \times 10^{-3}\text{eV}^2, \qquad |\Delta m^2_{31}| = 7.5 \times 10^{-5}\text{eV}^2$$
$$\theta_{12} = 34.3^\circ, \qquad \theta_{23} = 48.8^\circ, \qquad \theta_{13} = 8.6^\circ, \qquad \delta = \begin{cases} 216^\circ, \ \Delta m^2_{31} > 0 \\ 277^\circ, \ \Delta m^2_{31} < 0 \end{cases} \tag{2.3}$$

Moreover, to account for the addition of the PMNS matrix to the Standard Model, we must adapt the Feynman rules when calculating charged currents involving neutrinos. The convention is to add these extra terms to the vertex factor, leaving spinors and propagators unchanged. This results in the relevant Feynman rules

$$-i\frac{\not{q} + m_k}{q^2 - m_k} \qquad \nu_k \tag{2.4}$$

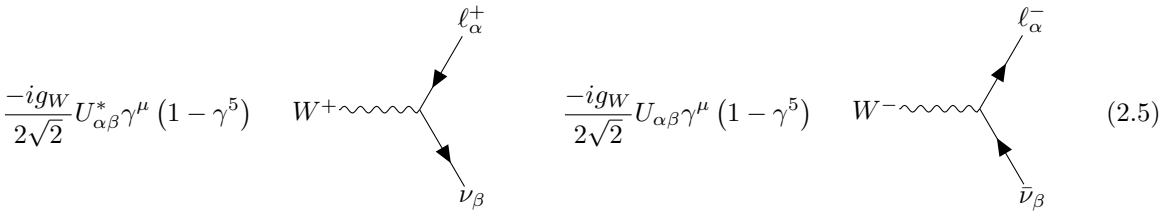

(2.5)

which we will be using in Sections 4 and 5.

The nature of neutrino masses is still an open question and also the most palpable link between the Standard Model and a theory beyond. Furthermore, lepton flavour number violating processes suggest us that perhaps lepton number itself might not be a fundamental quantity at all, being rather a theoretical workaround to justify the large suppression of such processes. This and other questions arising from neutrino masses are addressed in Section 2.2.

2.2 Dirac versus Majorana Nature of the Neutrinos

The formerly believed properties of massless neutrinos led many authors, as Krane [17] and Pontecorvo [18], to argue that neutrinos and antineutrinos must be distinct particles differentiated only by their helicity. Today this interpretation does not hold any more. Neutrinos (antineutrinos) have both left and right-handed components due to their masses, thus, they cannot be differentiated by this property. This opens the highly enticing possibility that neutrinos are their own antiparticles. The concept of a particle being its own antiparticle dates back to 1937 [19], when Ettore Majorana suggested that neutral spin-$\frac{1}{2}$ particles could be described by a real wave equation and would, consequently, be their own antiparticle. Thus, we call a particle that is its own antiparticle a Majorana particle. Now, we shall see the significance it would have in lepton number and neutrino masses.

Charged particles are evidently not their own antiparticles. These particles are known as Dirac particles and have $2n$ degrees of freedom, being n the number of spin projections and the 2 factor to account for both particles ψ and antiparticles $\bar{\psi}$. By contrast, Majorana particles have only n degrees of freedom, with

$$\psi = \psi^c = \hat{C}\psi \tag{2.6}$$

Where ψ^c is the charge (C) conjugate field to ψ. As usual, the chiral projections are $\psi_{L,R} = P_{L,R}\psi$.

In the Quantum Field Theory point of view, these two types of particles generate two distinct mechanisms for generating mass: the Dirac mechanism and the Majorana mechanism. In the former case, the Lagrangian mass term would have the form

$$\mathcal{L}_D = -m_D(\bar{\psi}_R\psi_L + \bar{\psi}_L\psi_R) \tag{2.7}$$

with the Dirac mass, m_D, being of the same order of the mass of other fermions. In the later case, the Lagrangian mass term would have the form

$$\mathcal{L}_M = -\frac{1}{2}M(\bar{\psi}^c_R\psi_R + \bar{\psi}_R\psi^c_R) \tag{2.8}$$

with M being the Majorana mass. This Lagrangian has a direct coupling between a particle and antiparticle, allowing the process $\psi \to \bar{\psi}^c$ and violating lepton number. For the charged fermions it would not be possible, but for the neutrino there is no theoretical or experimental reason, so far, to impose lepton number conservation, apart for the lack of detection of any lepton number violating process. Moreover, this Majorana mass term also gives an compelling hypothesis for the smallness of neutrino masses. We can take both the Dirac Eq. (2.7) and Majorana Eq. (2.8) mass terms and write a general Lagrangian of the form

$$\mathcal{L}_{DM} = -\frac{1}{2}(\bar{\psi}_L, \bar{\psi}^c_R)\begin{pmatrix} 0 & m_D \\ m_D & M \end{pmatrix}\begin{pmatrix} \psi^c_L \\ \psi_R \end{pmatrix} \tag{2.9}$$

Diagonalizing this matrix to find the physical masses and states of the neutrinos, and taking the Majorana mass M to be much greater than the Dirac Mass m_D, we obtain the physical masses

$$m_\pm \approx \frac{M}{2} \pm \frac{1}{2}\left(M + \frac{2m_D^2}{M}\right) \tag{2.10}$$

However, we must include the hermitian conjugate half of Eq. 2.9 to obtain the physical neutrino fields. Doing so yields a light physical eigenstate (ν) and a heavy physical eigenstate (N)

$$\begin{aligned} \nu \approx &(\psi_L + \psi^c_L) - \frac{m_D}{M}(\psi_R - \psi^c_R), \quad m_\nu \approx \frac{m_D^2}{M} \\ N \approx &(\psi_R + \psi^c_R) + \frac{m_D}{M}(\psi_L + \psi^c_L)), \quad m_N \approx M \end{aligned} \tag{2.11}$$

The resulting states are a superposition of left and right-handed states, ν being the mostly left-handed observed neutrinos and N the sterile, mostly right-handed neutrinos.

This is the so-called type-I seesaw model. It provides a compelling, but yet speculative, explanation for the generation of neutrino masses. The best way to probe the nature of neutrinos experimentally is to look for processes that are only possible to occur in one scenario, the most studied being the so-called neutrinoless double beta decay, which will be discussed in Section 3, including a brief review of the essential nuclear physics concepts which rule such processes.

3 Double Beta Decay

Being the most prominent process to probe the true nature of the neutrinos, we dedicate this section to double beta ($\beta\beta$) decay. We begin by reviewing the standard neutrinoless double beta ($0\nu\beta\beta$) decay as it is the most renowned process which would be allowed only for Majorana neutrinos. We then venture through exotic variations of $\beta\beta$ decay involving a hypothetical Majoron particle, which yields fascinating analogous processes to both $0\nu\beta\beta$ and the standard double beta ($2\nu\beta\beta$) decay. As a necessary digression, we present the fundamental principles of nuclear physics that govern $\beta\beta$ decay and, finally, close this section with the steps and assumptions needed to obtain the theoretical amplitudes for $\beta\beta$ processes.

3.1 Neutrinoless Double Beta Decay

The process known as $0\nu\beta\beta$ decay, depicted in the Feynman diagram in Figure 1 (left), could be the best way of probing whether neutrinos are Majorana or Dirac particles. This reaction is a nuclear decay in which 2 neutrons decay into 2 electrons and 2 protons, without changing the mass number (A) of the nucleus, or in short $(A, Z) \to (A, Z+2) + 2e^-$. This process is, however, forbidden in the Standard Model, as it requires that a left-handed particle emitted in one W^- vertex is absorbed as a right-handed antiparticle in the other W^- vertex. However, if neutrinos are actually Majorana particles, this is not a problem anymore as their mass allows them to flip helicity.

$0\nu\beta\beta$ decay has a remarkable experimental sensitivity as processes which could compete with it can be avoided. As we will soon discuss, some nuclei are stable against single beta decay, so this mode can be eliminated. As for $2\nu\beta\beta$ decay, it can be avoided via the energy spectrum of the emitted electrons. $0\nu\beta\beta$ decay would produce a mono-energetic electron pair with energy $E_e = [M(A, Z) - M(A, Z+2)]$, being $M(A, Z)$ and $M(A, Z-2)$ the masses of the parent and daughter nucleus respectively. Conversely, $2\nu\beta\beta$ decay produces a continuous spectrum alike that of a single beta decay, as shown in Figure 1 (right). Furthermore, the half life for $0\nu\beta\beta$ decay is given in the form of [20]

$$\left[T^{0\nu}_{1/2}\right]^{-1} = \frac{|m_{\beta\beta}|^2}{m_e^2} G_{0\nu} |\mathcal{M}|^2 \tag{3.1}$$

where $\mathcal{M}$ is a nontrivial nuclear matrix element, $G_{0\nu}$ the phase space factor, and $m_{\beta\beta}$ the effective

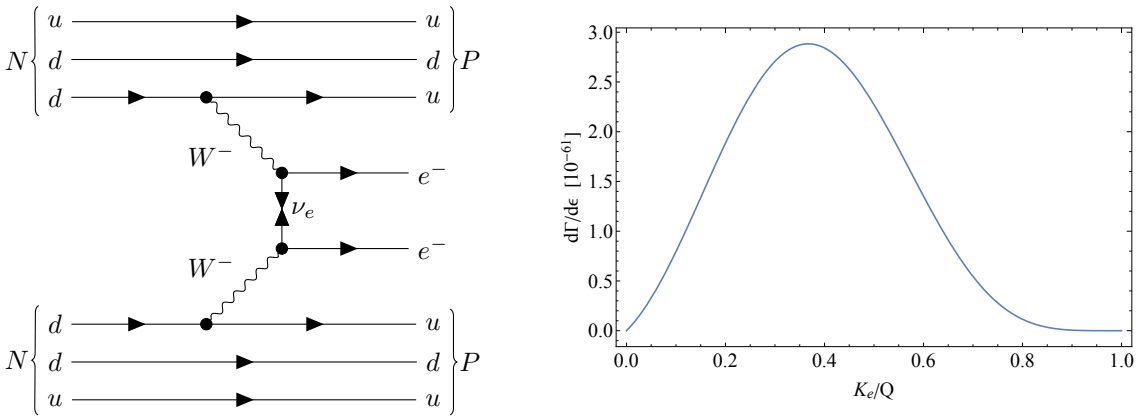

Figure 1: *Left:* $0\nu\beta\beta$ Feynman Diagram with Majorana neutrino exchange. *Right:* Standard $2\nu\beta\beta$ total electron energy spectrum.

mass for $0\nu\beta\beta$ decay. Assuming only left-handed currents and neutrino masses small compared to the momentum transfer in $0\nu\beta\beta$ decay (≈ 100 MeV) [21], $m_{\beta\beta}$ can be written as

$$m_{\beta\beta} = \sum_{k=1}^{3} |U_{ek}|^2 m_k \tag{3.2}$$

which depends only on the PMNS matrix elements in Eq. 2.1 and the neutrino masses. Since U_{ek} are elements of a unitary matrix, $m_{\beta\beta}$ is limited to the heaviest neutrino mass. Hence, the observation of $0\nu\beta\beta$ decay wound impose a lower bound on neutrino masses.

A number of experiments aimed at observing $0\nu\beta\beta$ decay have already been conducted, the first one dating back to 1948 [22], and, although no evidence for a signal has been found so far, they provided constraints to $0\nu\beta\beta$ decay half-life ($T^{0\nu}_{1/2}$). In table 1, we briefly list the current best limits for the main studied isotopes.

Isotope	^{130}Te	^{76}Ge	^{138}Xe	^{100}Mo	^{82}Se
Experiment	CUORE	GERDA	KamLAND-Zen 400	NEMO-3	NEMO-3
$T^{0\nu}_{1/2}$ [10^{24} y]	>2.7	> 90	> 110	> 1.1	> 0.25
Q-value [MeV]	2.528	2.039	4.268	3.034	2.998
Reference	2019 [23]	2019 [24]	2019 [25]	2015 [26]	2018 [27]

Table 1: Best measured limits on $T^{0\nu}_{1/2}$ from $0\nu\beta\beta$ search experiments for the most common Isotopes.

We have, so far, discussed only the importance of the standard $0\nu\beta\beta$ decay but, as the title of this work suggests, we are interested in exotic processes, hence, we are not limited to the particles in the standard model. Among numerous theorised exotic particles, we have selected the notorious Majoron to study, which we shall now present in Section 3.2.

3.2 Majoron Induced Double Beta Decay

After various generalisations from the original concept, the term Majoron became an umbrella and might spark a lot of confusion on its definition. In this section we present what a Majoron is in the context of this work and why it is the emphasis of this study.

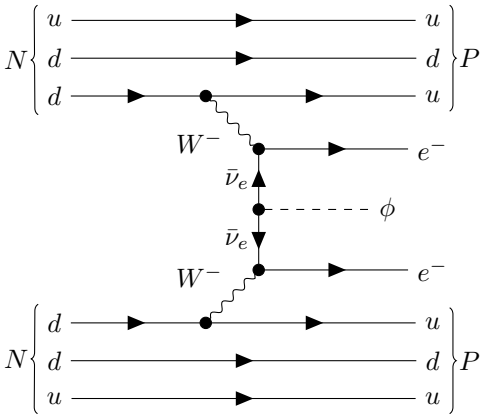

Figure 2: Neutrinoless Double Beta Decay with Majoron emission Feynman diagram .

A extensively analysed set of theories involve the emission of one or more scalar particles in $\beta\beta$ decay. The first such proposed particle was a Goldstone boson ϕ associated with the spontaneous breaking of lepton number symmetry, coupling to neutrinos ν as $g_\phi \nu\nu\phi$. This particle was eventually named Majoron. Although the name Majoron originates from Majorana, Majorons are simply exotic charge-neutral scalar particles. Originally they were considered to be massless, but massive Majoron are also currently considered, providing an riveting candidate for Dark Matter [28]. The diagram depicted in Figure 2 shows the simplest Majoron-induced neutrinoless double beta ($0\nu\beta\beta\phi$) decay, which will be explicitly calculated in Section 4.2. From the diagram it is immediately noticeable that this process violates lepton number conservation. However, such process would be possible even for the deprecated Standard Model massless neutrino as the coupling between them and ϕ has no helicity mismatch.

Coupling only to neutrinos, ϕ would not be directly detectable, appearing only as a missing energy in the energy spectrum of the decay. The same way as the non-observation of $0\nu\beta\beta$ decays give us constraints to work with, the non-observation of $0\nu\beta\beta\phi$ decays translates to constraints on the effective $\nu - \phi$ coupling constant g_ϕ. The strongest experimental limit obtained at 90%C.L. assuming ϕ massless is, so far, $|g_\phi| \leq (0.8 - 1.7) \times 10^{-5}$ from EXO-200 [28].

Still, we have just presented the simplest Majoron-induced $0\nu\beta\beta$ decay model. In this work, we construct two classes of models for Majoron induced $\beta\beta$ decay, the first violating lepton number ($0\nu\beta\beta\phi$) and the second conserving it ($2\nu_\phi\beta\beta$), each of which leads to distinct energy spectra. These spectra are key to understanding the feasibility of experimental searches to such processes. Before going to the specifics of each model, we shall first discuss what is common to them all, and that is the hadronic part of $\beta\beta$ decay. To begin with, we must understand what criteria make such processes possible from a nuclear physics standpoint. We dedicate Section 3.3 to introduce the basic concepts which rule $\beta\beta$ decay.

3.3 Principles of Nuclear Physics

In this section, we will cover the fundamental principles from nuclear physics needed to deal with $\beta\beta$ decay. To do so, we present key concepts and how they govern $\beta\beta$ decay without any particular order:

- Q value: Is defined as the initial mass energy minus the final mass energy, or equivalently, the excess kinetic energy of the final state

$$Q = (m_i - m_f) = (T_f - T_i) \tag{3.3}$$

- The binding energy B of a nucleus is the difference in mass between the nucleus ${}^A_Z\mathrm{X}_N$ and its constituent Z protons and N neutrons:

$$B = Zm_P + Nm_n - [m({}^A_Z\mathrm{X}_N - Zm_e)] \tag{3.4}$$

  where $m({}^A\mathrm{X})$ is the mass of the whole atom, including the electrons.

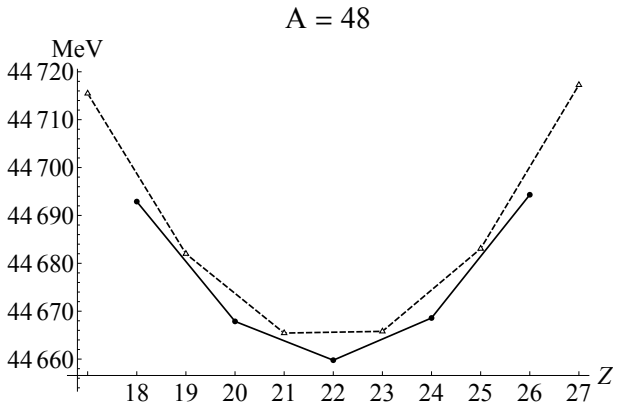

Figure 3: Mass parabola for A=48. $Z_{min} = 22$ ($^{48}_{22}$Ti). Odd Z nuclei are represented by the dashed parabola. Even Z nuclei are represented by the solid parabola.

Expressing the binding energy as a function of A and Z is a rather complicated process. In [17], the formula

$$B(Z,A) = \left[15.5A - 16.8A^{\frac{2}{3}} - 0.72Z(Z-1)A^{-\frac{1}{3}} - 23\frac{(A-2Z)^2}{A} + \delta\right] \text{MeV} \tag{3.5}$$

$$\delta = \begin{cases} +34A^{-\frac{3}{4}}, & \text{Z and N even} \\ -34A^{-\frac{3}{4}}, & \text{Z and N odd} \\ 0, & \text{A odd} \end{cases} \tag{3.6}$$

is derived and substituted into Eq. 3.6 to give the semi-empirical mass formula

$$M(Z,A) = Z(^1\text{H}) + Nm_n - B(Z,A) \tag{3.7}$$

The term δ is called the pairing term, which comprises the effect of spin-coupling. For a constant A, Eq. 3.7 represents a parabola in Z, the so-called mass parabola. Its minimum is found to be at

$$Z_{min} \approx \frac{A}{2}\frac{1}{\left(1 + \frac{0.72}{92}A^{\frac{1}{3}}\right)} \tag{3.8}$$

So that unstable nuclei approach stability (the minimum of the parabola) by converting Z into N or vice versa. For even A, $M(Z,A)$ results in two parabolas displaced by 2δ. This causes two effects: Some odd Z odd N nuclei can decay by converting Z to N and vice-versa, and certain $\beta\beta$ decays become energetically allowed, changing 2 protons into 2 neutrons directly. Now let us focus our attention back to the beta decay. Being a quantum mechanic process, the parent nucleus must satisfy a number of selection rules. These rules allow us to classify beta decays in 2 groups: Allowed decays and forbidden decays.

In the allowed approximation, we replace the electron and neutrino wave-functions by their values at origin. In this case they cannot have any orbital angular momentum and any change in the angular momentum of the nucleus must be due to their spins. Also, as parity P is associated with angular momentum by $(-1)^l$, it cannot change. We shall use the notation I^P, where I is the total angular

momentum and P the parity of the nucleus. Allowed decays must then satisfy the rules

$$\Delta S = 0, 1; \quad \Delta P = 0 \tag{3.9}$$

an example is ${}^{6}_{2}\mathrm{He} \to {}^{6}_{3}\mathrm{Li}$, a $0^+ \to 1^+$ decay.

Forbidden decays are less probable to happen but are not strictly forbidden. An easy way to define a forbidden decay is to see when the selection rules for allowed decays in Eq. 3.9 are violated. Doing so, the first selection rules obtained are

$$\Delta I = 0, 1, 2; \quad \Delta P = \pm 1 \tag{3.10}$$

An example is ${}^{76}_{35}\mathrm{Br} \to {}^{76}_{34}\mathrm{Se}$, a $1^- \to 0^+$ decay. Transitions with $\Delta I \geq 2$ but no change in parity are not possible for first-forbidden decays. In this case, we would have to escalate to second-forbidden decays.

These selection rules make to selecting candidate nuclei for experiments searching for $\beta\beta$ decay a lot easier. For instance, take ${}^{48}_{20}\mathrm{Ca} \to {}^{48}_{21}\mathrm{Sc} + e^- + \bar{\nu_e}$ decay, with its mass parabola shown in Figure 3. ${}^{48}_{20}\mathrm{Ca}$ is a 0^+ state with $Q = 0.28$ MeV, nonetheless, it would require at least a fourth-forbidden decay, as the only accessible states of ${}^{48}_{21}\mathrm{Sc}$ for ${}^{48}_{20}\mathrm{Ca}$ are $4^+, 5^+$ and 6^+ states. Nonetheless, the process ${}^{48}_{20}\mathrm{Ca} \to {}^{48}_{22}\mathrm{Ti} + 2e^- + 2\bar{\nu_e}$ is an allowed $(0^+ \to 0^+)$ $\beta\beta$ decay with $Q = 4.27$ MeV. Hence, it does not require transitioning through the intermediate state ${}^{48}_{21}\mathrm{Sc}$. As a matter of fact, the CANDLES experiment at Kamioka Observatory [14] was planned to study $\beta\beta$ decay of ${}^{48}_{20}\mathrm{Ca}$.

Another way of having $\beta\beta$ decays while avoiding single beta decays is when the latter is energetically forbidden. As an example, take ${}^{130}_{52}\mathrm{Te} \to {}^{130}_{53}\mathrm{I} + e^- + \bar{\nu}_e$ decay. It has a negative Q-value of -0.419 MeV, therefore it is energetically forbidden. However, the $\beta\beta$ decay ${}^{128}_{52}\mathrm{Te} \to {}^{128}_{53}\mathrm{I} + 2e^- + 2\bar{\nu}_e$ has a Q-value of 2.530 MeV, which makes ${}^{130}_{52}\mathrm{Te}$ ideal to study $\beta\beta$ decay processes. It is in fact the isotope selected for study at SNO+ [13].

Observing $\beta\beta$ decays is, unfortunately, exceptionally hard since these have immensely long half-lives of the order of 10^{24} years. Still, pursuing these decays is of paramount importance for neutrino physics.

3.4 Calculating Double Beta Decay Amplitudes

From a theorist standpoint, experimental searches mean nothing if there are no theoretical results to serve as baseline. These are translated by cross-sections, decay rates and energy distributions. Obtaining these theoretical results is precisely the goal of this work and consists, as usual, of following a recipe. The whole procedure is extremely complex, depending on many assumptions and approximations due to the structure of the decaying nucleus. We will eventually discuss some of these assumptions when pertinent, but, in general, we will be following the recipe described in [21].

It is convenient to start by decomposing the decay rate, as done in [29] and [30]:

$$\Gamma = |\langle \mathcal{G} \rangle|^2 \, |\mathcal{M}|^2 \, G(p_j) \tag{3.11}$$

where $\mathcal{G}$ is a coupling constant, $\mathcal{M}$ the nuclear matrix element, and $G(\phi)$ the kinematic phase space factor. p_j represents the momenta of the final state particles. This decomposition looks familiar to that

in Eq. 3.1 and this is no accident as the former is a special case of the latter. The nuclear matrix element is nothing but the scattering matrix element of the process taking into account the quarks' confinement within the nucleons and all the nuclear physics principles we would be leaving behind if following just the standard text book Feynman rules. To derive this matrix element we must depart from the interaction Lagrangian:

$$\mathcal{L}_{\text{int}} = \mathcal{L}_{CC} + \mathcal{L}_{\phi} \tag{3.12}$$

In this expression, $\mathcal{L}_{CC}$ represents the weak charged-current that couples hadrons to leptons.

$$\mathcal{L}_{CC} = \frac{G_F}{\sqrt{2}} J_{H\mu} J_L^{\mu\dagger} + \text{h.c.}, \quad J_{H\mu} = \bar{u}\gamma_\mu(1-\gamma^5)d, \quad J_L^{\mu\dagger} = \bar{e}\gamma^\mu(1-\gamma^5)\nu \tag{3.13}$$

The hadronic current $J_{H\mu}$ does not change for the exotic processes we will be considering. Conversely, the leptonic current $J_L^{\mu\dagger}$ will change and, for Majoron induced processes, we will also have an exotic current interaction Lagrangian $\mathcal{L}_\phi$, which we define as

$$\mathcal{L}_\phi = -\frac{1}{2}\bar{\nu}\left(\alpha + \beta\gamma^5\right)\nu\phi^* + \text{h.c.} \tag{3.14}$$

to account for both left and right-handed currents. The scattering matrix is now obtained from calculating the time ordered product $\mathcal{T}$ from initial i to final f states [31]

$$S_{fi} = \int dx\ dy\ dz\, \langle f|\, \mathcal{T}\left[\mathcal{L}_{CC}(x)\mathcal{L}_{CC}(y)\mathcal{L}_\phi(z)\right]|i\rangle \tag{3.15}$$

Since we have a double decay, we have 2 charged-currents depending on 2 different positions. Although Eq. 3.13 might give the wrong impression that this scattering matrix is easily obtainable from the text book approach, the particles interacting are not really free fields. The emitted electrons are affected by the Coulomb potential of the nuclei, while the quarks are confined in hadrons. Therefore, to proceed with this calculation, a deep understanding on the quantum level structure of the initial and final states is needed.

From now on, some approximations must be made. With regard to the hadronic current, the first is the so-called impulse approximation: The assumption that the nucleon transition is induced by the lowest order quark transition and the nucleons are free. Through this assumption we can convert the quark currents to nucleon currents. The second is the closure approximation: it builds up on an observation that the momentum transfer must be of the order of the average inverse spacing between nucleons (~ 100 MeV). This approximation is extremely powerful as it allows us to eliminate the need of summing over every intermediate state. To better understand this, we must recall that a $\beta\beta$ decay is composed of two consecutive decays. In principle, we would have to consider every possible intermediate state but, within the closure approximation [21], we can simply write

$$\sum_a f(E_a)\,\langle f|\,\hat{O}_2\,|N_a\rangle\,\langle N_a|\,\hat{O}_1\,|i\rangle \to f(\langle E_a\rangle)\,\langle f|\,\hat{O}_2\hat{O}_1\,|i\rangle \tag{3.16}$$

where we have used the closure relation $\sum_a |N_a\rangle\langle N_a| = \mathbb{1}$ from quantum mechanics after assuming that

the energy eigenvalues E_a can be considered approximately equal to their average $\langle E_a \rangle$.

These approximations elucidated, we will move forward to the leptonic part of the process. The detailed derivation of the nuclear matrix element is not discussed any further and can be found in [21]. The leptonic part for our chosen exotic contributions to double beta decay will be calculated in detail in Sections 4 and 5. However, the standard Feynman rules assume Dirac fermions. To calculate processes involving Majorana fermions, we will be using the following adapted Feynman rules, as derived in [32]:

$$\left[i\frac{C^{-1}(\not{p}+M)}{p^2-M}\right]_{\alpha\beta} \quad \beta \bullet\!\!\longrightarrow\!\!\longleftarrow\!\!\bullet \alpha \qquad \left[-i\frac{(\not{p}+M)C}{p^2-M}\right]_{\alpha\beta} \quad \beta \bullet\!\!\longleftarrow\!\!\longrightarrow\!\!\bullet \alpha \tag{3.17}$$

$$-ig^M\left[C^{-1}\Gamma_M\right]_{\alpha\beta} \quad \psi_\beta \searrow \sim\!\!\sim \swarrow \lambda_\alpha \qquad i(g^M)^*\left[(\Gamma_M C)^T\right]_{\alpha\beta} \quad \psi_\beta \nearrow \sim\!\!\sim \searrow \lambda_\alpha \tag{3.18}$$

where Γ_M is a combination of gamma matrices composing the vertex factor, g^M is the coupling constant, λ the Majorana fermion and ψ the Dirac fermion. The charge operator $\hat{C}$ is defined in such a way that it satisfies the following properties:

$$\hat{C}\bar{u}^T = v, \quad \hat{C}\bar{v}^T = u, \quad \hat{C}^2 = 1, \quad \hat{C}^{-1} = \hat{C}^\dagger, \quad \hat{C}^T = -\hat{C}, \quad \hat{C}\gamma^\mu = -(\gamma^\mu)^T\hat{C}, \quad \hat{C}\gamma^5 = (\gamma^5)^T\hat{C} \tag{3.19}$$

We will see further ahead how these rules will be used not only in neutrinoless processes, in Section 4, but also in exotic neutrino emitting processes in Section 5. Moreover, to obtain realistic results, there are corrections and approximations we will consider due to the Coulomb potential of the involved particles. This attraction is stronger for heavier nuclei, causing the wave functions of electrons and nucleons to overlap. To account for this effect, we start by expanding the relativistic electron wave function in a uniform charged field in terms of spherical waves

$$\psi(\epsilon, r) = \psi^{(S)}(\epsilon, r) + \psi^{(P)}(\epsilon, r) + \psi^{(D)}(\epsilon, r) + \dots \tag{3.20}$$

with S and P representing the S- and P-waves respectively. Then, we expand the wave function in r and keep only the leading order term, that is, we neglect the finite de Broglie wave length correction. This approximation is permitted by the assumption that the electron wave-length is bigger than the nuclear radius, which is realistic for the small Q-values encountered in $\beta\beta$ decay. Also, this implies that the higher order terms in r would not yield a relevant correction to be considered, since the electron is most affected by the Coulomb potential while it is travelling inside the nucleus. By doing so, the radial components $\tilde{f}_{j_1}$ and $\tilde{g}_{j_2}$ that compose the overall wave function are given by [21]

$$S_{j=\frac{1}{2}} : \begin{pmatrix} \tilde{g}_{-1} \\ \\ \tilde{f}_1 \end{pmatrix} = \tilde{A}_{\mp 1} \tag{3.21}$$

$$P_{j=\frac{1}{2}}:\begin{pmatrix}\tilde{g}_1\\ \\ \tilde{f}_{-1}\end{pmatrix}=\pm\tilde{A}_{\pm1}[\alpha Z/2+(\epsilon\pm m_e)R/3](r/R),\quad P_{j=\frac{3}{2}}:\begin{pmatrix}\tilde{g}_{-2}\\ \\ \tilde{f}_2\end{pmatrix}=\tilde{A}_{\mp2}(|\vec{p}|r/3) \tag{3.22}$$

where α is the fine structure constant, Z is the atomic number of the daughter nucleus and R is the nuclear radius, and $\vec{p}$ the momentum of the electron. The reason why we have both $\tilde{f}_{j_1}$ and $\tilde{g}_{j_2}$ is because each is the radial part of a 2-component spinor, being the overall wave function a 4-component spinor. The normalisation constants $\tilde{A}_{\pm k}$ are explicitly calculated in [21] and can be approximated up to the order of $(\alpha Z)^2$ by

$$\tilde{A}_{\pm k}\approx\sqrt{(\epsilon\mp m_e)/\epsilon}\sqrt{F_{k-1}(Z,\epsilon)} \tag{3.23}$$

with $F_{k-1}(Z,\epsilon)$ being the so-called Fermi factor

$$F_{k-1}(Z,\epsilon)=\left[\frac{\Gamma(2k+1)}{\Gamma(k)\Gamma(2\gamma_k+1)}\right]^2(2|\vec{p}|R)^{2(\gamma_k-k)}|\Gamma(\gamma_k+iy)|^2e^{\pi y},\quad \gamma_k=\sqrt{k^2-(\alpha Z)^2},\quad y=\frac{\alpha Z\epsilon}{|\vec{p}|} \tag{3.24}$$

An additional Coulomb repulsive interaction between the two emitted electrons exists, but this effect is of the order of the fine structure constant α. Furthermore, the electron emitted first is influenced by the Coulomb field of the intermediate nucleus before it decays again. This correction is less than a few percent and, thus, both of these effects are too small and will not be considered.

The final step needed is to calculate the phase space, as it will be significantly different for each process considered. This is, perhaps, the most complicated step. The phase space can rarely be fully calculated without a certain amount of approximations. As we shall see in Sections 4 and 5, the matrix element squared is nothing more than an intricate combination of scalar products of the 4-momenta of initial and final states. To separate final from initial states in the scalar products, we implicitly use the so-called Fierz transformation [32]

$$\begin{aligned}&\psi\bar{\chi}=\frac{1}{4}\left(c_S\mathbb{1}_4+c_P\gamma^5+c_V^\mu\gamma_\mu+c_A^\mu\gamma_\mu\gamma_5+c_T^{\mu\nu}\sigma_{\mu\nu}\right),\quad \sigma^{\mu\nu}=[\gamma^\mu,\gamma^\nu]\\ &c_S=\bar{\chi}\psi,\quad c_P=\bar{\chi}\gamma^5\psi,\quad c_V^\mu=\bar{\chi}\gamma^\mu\psi,\quad c_A^\mu=-\bar{\chi}\gamma^\mu\gamma^5\psi,\quad c_T^{\mu\nu}=-\bar{\chi}\sigma^{\mu\nu}\psi\end{aligned} \tag{3.25}$$

It allows us to decompose bilinears of the product of two spinors as a linear combination of products of the bilinears of the individual spinors by using the completeness and orthogonality of the basis matrices. Also, since we will be integrating the phase space over the final states only, the main approximation we will be using is that the matrix element squared is constant in the 4-momenta of the initial states. Other approximations will be made when needed for each process. We now have all the preliminary information we need about $\beta\beta$ decay to start with the calculations.

4 Neutrinoless Amplitudes

In this section, we study two of the simplest and most notorious lepton number violating $\beta\beta$ decay modes. We begin by calculating the leptonic current for the standard neutrinoless double beta decay, but with a twist. Instead of solely calculating the current as done by numerous authors, we will pretend, as in a toy model, that a W-boson collider is experimentally feasible and compare how the lepton number violating

process $W^-W^- \to e^-e^-$ differs from the lepton number conserving analogous process $W^+W^- \to e^+e^-$. Although not realistic, this calculation will expose some key features of the lepton number violating process that would be hard to view with the uncontracted current only.

We then calculate the leptonic current for the majoron emitting neutrinoless double beta decay introduced in Section 3.1. This calculation will be done more formally as it will pave the way for one of the more complex processes we will discuss in Section 5. Nonetheless, this is also a process that has been extensively discussed by other authors. We will add our personal touch by considering a more general exotic interaction and compare some interesting special cases.

These leptonic currents obtained, we then proceed to calculating the phase space of such processes. The resulting phase spaces are then used to show the energy distribution of the emitted electrons and how they differ from that of a standard $2\nu\beta\beta$.

4.1 $0\nu\beta\beta$ Leptonic Current

For $W^-W^- \to e^-e^-$, as opposed to the lepton number conserving process $W^+W^- \to e^+e^-$, we must also consider the different permutations of the two identical emitted electrons, namely, the t and u-channels. Due to Pauli's exclusion principle, upon exchanging two fermions, the matrix element gains a relative minus sign, thus, we subtract the u-channel diagram from the t-channel diagram to obtain the total matrix element. We start our calculations by the t-channel diagram shown in Figure 4 (left). Using the standard Feynman rules in communion with the Majorana Feynman presented in Section 3.1, the matrix element is given by

$$\begin{aligned}\mathcal{M}_1 &= \frac{-g_W^2 (U_{ei}^*)^2 \epsilon_\mu(p_1)\epsilon_\nu(p_2)}{8(q^2 - m_{\nu_i}^2)} \left[\bar{u}_e(p_3)\right]_d \left[\gamma^\mu(\mathbb{1}_4 - \gamma^5)\right]_{dc} \left[(\gamma^\rho q_\rho + m_{\nu_i})\hat{C}\right]_{cb} \left[\gamma^\nu(\mathbb{1}_4 - \gamma^5)\right]_{ab} \left[\bar{u}_e(p_4)\right]_a \\ &= \frac{-g_W^2 (U_{ei}^*)^2 \epsilon_\mu(p_1)\epsilon_\nu(p_2)}{8(q^2 - m_{\nu_i}^2)} \bar{u}_e(p_3)\gamma^\mu(\mathbb{1}_4 - \gamma^5)(\not{q} + m_{\nu_i})\hat{C}(\mathbb{1}_4 - \gamma^5)^T(\gamma^\nu)^T \bar{u}_e^T(p_4) \end{aligned} \tag{4.1}$$

Using the commutation relations of the charge conjugation operator $\hat{C}$ as given in Eq. (3.19) and, subsequently, those of γ^5, we obtain

$$\begin{aligned}\mathcal{M}_1 &= \frac{g_W^2 (U_{ei}^*)^2 \epsilon_\mu(p_1)\epsilon_\nu(p_2)}{8(q^2 - m_{\nu_i}^2)} \bar{u}_e(p_3)\gamma^\mu(\mathbb{1}_4 - \gamma^5)(\not{q} + m_{\nu_i})(\mathbb{1}_4 - \gamma^5)\gamma^\nu v_e(p_4) \\ &= \frac{m_{\nu_i} g_W^2 (U_{ei}^*)^2 \epsilon_\mu(p_1)\epsilon_\nu(p_2)}{4(q^2 - m_{\nu_i}^2)} \bar{u}_e(p_3)\gamma^\mu(\mathbb{1}_4 - \gamma^5)\gamma^\nu v_e(p_4) \end{aligned} \tag{4.2}$$

Figure 4: $W^-W^- \to e^-e^-$ Feynman diagrams. *Left:* t-channel with $q = p_1 - p_3 = p_4 - p_2$. *Right:* u-channel with $q' = p_1 - p_4 = p_3 - p_2$.

Applying Casimir's trick [33] and defining the matrices Γ_1 and $\bar{\Gamma}_2$

$$\begin{aligned}\Gamma_1 &= \gamma^\mu(\mathbb{1}_4-\gamma^5)\gamma^\nu = \gamma^\mu\gamma^\nu(\mathbb{1}_4+\gamma^5)\\ \bar{\Gamma}_2 &= \gamma^0\left[\gamma^\rho(\mathbb{1}_4-\gamma^5)\gamma^\sigma\right]^\dagger\gamma^0 = \gamma^0(\gamma^\sigma)^\dagger(\mathbb{1}_4-\gamma^5)^\dagger(\gamma^\rho)^\dagger\gamma^0 = (\mathbb{1}_4-\gamma^5)\gamma^\sigma\gamma^\rho\end{aligned} \tag{4.3}$$

we obtain the averaged matrix element squared

$$\left\langle|\mathcal{M}_1|^2\right\rangle = \frac{m_{\nu_i}^2 g_W^4|U_{ei}|^4}{(2^6)(3^2)(q^2-m_{\nu_i}^2)^2}\left(-g_{\mu\rho}+\frac{p_{1\mu}p_{1\rho}}{m_W^2}\right)\left(-g_{\nu\sigma}+\frac{p_{2\nu}p_{2\sigma}}{m_W^2}\right)\mathrm{Tr}\left[\Gamma_1(\not{p}_4-m_e)\bar{\Gamma}_2(\not{p}_3+m_e)\right] \tag{4.4}$$

Considering only the term $\Gamma_1(\not{p}_4-m_e)\bar{\Gamma}_2$, we have

$$\gamma^\mu\gamma^\nu(\mathbb{1}_4+\gamma^5)(\not{p}_4-m_e)(\mathbb{1}_4-\gamma^5)\gamma^\sigma\gamma^\rho = 2(\mathbb{1}_4+\gamma^5)\gamma^\mu\gamma^\nu\not{p}_4\gamma^\sigma\gamma^\rho$$

Thus, remembering that only terms with an even number of γ^μ contribute to the trace, we can write

$$\left\langle|\mathcal{M}_1|^2\right\rangle = \frac{m_{\nu_i}^2 g_W^4|U_{ei}|^4}{(2^5)(3^2)(q^2-m_{\nu_i}^2)^2}\left(-g_{\mu\rho}+\frac{p_{1\mu}p_{1\rho}}{m_W^2}\right)\left(-g_{\nu\sigma}+\frac{p_{2\nu}p_{2\sigma}}{m_W^2}\right)Tr\left[(\mathbb{1}_4+\gamma^5)\gamma^\mu\gamma^\nu\not{p}_4\gamma^\sigma\gamma^\rho\not{p}_3\right] \tag{4.5}$$

Calculating the trace on Wolfram's Mathematica [34] using the package Feyncalc [35], we obtain

$$\begin{aligned}Tr\left[(\mathbb{1}_4+\gamma^5)\gamma^\mu\gamma^\nu\not{p}_4\gamma^\sigma\gamma^\rho\not{p}_3\right] =& -4p_3^\sigma p_4^\rho g^{\mu\nu}+4p_3^\rho p_4^\sigma g^{\mu\nu}-4p_3^\nu p_4^\mu g^{\rho\sigma}+4p_3^\mu p_4^\nu g^{\rho\sigma}-4p_3^\rho p_4^\mu g^{\nu\sigma}+4p_3^\rho p_4^\nu g^{\mu\sigma}\\ &-4p_3^\mu p_4^\rho g^{\nu\sigma}+4p_3^\nu p_4^\rho g^{\mu\sigma}+4p_3^\sigma p_4^\mu g^{\nu\rho}-4p_3^\sigma p_4^\nu g^{\mu\rho}+4p_3^\mu p_4^\sigma g^{\nu\rho}-4p_3^\nu p_4^\sigma g^{\mu\rho}\\ &+4g^{\mu\nu}g^{\rho\sigma}(p_3\cdot p_4)-4g^{\mu\sigma}g^{\nu\rho}(p_3\cdot p_4)+4g^{\mu\rho}g^{\nu\sigma}(p_3\cdot p_4)\\ &-4ig^{\mu\nu}p_{3\delta}p_{4\chi}\epsilon^{\rho\sigma\delta\chi}+4ig^{\rho\sigma}p_{3\delta}p_{4\chi}\epsilon^{\mu\nu\delta\chi}\\ &-4ip_{3\delta}p_4^\mu\epsilon^{\nu\rho\sigma\delta}+4ip_{3\delta}p_4^\nu\epsilon^{\mu\rho\sigma\delta}+4ip_{4\chi}p_3^\rho\epsilon^{\mu\nu\sigma\chi}-4ip_{4\chi}p_3^\sigma\epsilon^{\mu\nu\rho\chi}\end{aligned} \tag{4.6}$$

Contracting the indices in this trace with the indices from the W-bosons on Mathematica gives

$$\begin{aligned}\left\langle|\mathcal{M}_1|^2\right\rangle = \frac{m_{\nu_i}^2 g_W^4|U_{ei}|^4}{288(q^2-m_{\nu_i}^2)^2}\frac{4}{m_W^4}&\left[2\left(2m_W^2-p_1^2\right)(p_3\cdot p_2)(p_4\cdot p_2)+\left(2m_W^2-p_1^2\right)\left(2m_W^2-p_2^2\right)(p_3\cdot p_4)\right.\\ &\left.+(p_3\cdot p_1)\left(\left(4m_W^2-2p_2^2\right)(p_4\cdot p_1)+4(p_4\cdot p_2)(p_1\cdot p_2)\right)\right]\end{aligned} \tag{4.7}$$

Rewriting it in terms of the masses and Mandelstam variables

$$\begin{gathered}s=(p_1+p_2)^2=p_1^2+p_2^2+2(p_1\cdot p_2);\quad t=(p_1-p_3)^2=p_1^2+p_3^2-2(p_1\cdot p_3);\\ u=(p_1-p_4)^2=p_1^2+p_4^2-2(p_1\cdot p_4)\end{gathered} \tag{4.8}$$

we get rid of the scalar products, yielding

$$\begin{aligned}\left\langle|\mathcal{M}_1|^2\right\rangle =& \frac{m_{\nu_i}^2 g_W^4|U_{ei}|^4}{144(t-m_{\nu_i}^2)^2m_W^4}\\ &\times\left[m_W^4\left(s-2m_e^2\right)+2m_W^2\left(m_e^2+m_W^2-u\right)\left(m_e^2+m_W^2-t\right)+\left(m_e^2+m_W^2-t\right)^2\left(s-2m_W^2\right)\right]\end{aligned} \tag{4.9}$$

which is the final averaged matrix element squared for the t-channel.

Now, for the u-channel we have the diagram depicted in Figure 4 (right). It is evident that its matrix element will be perfectly symmetric to that of the t-channel. Instead of writing it from first principles, we simply swap the indices in the W-boson polarisation vectors, which is equivalent to swapping the 4-momenta of the two electrons, and change the internal momentum q to q'. This gives us

$$\mathcal{M}_2 = \frac{m_{\nu_i} g_W^2 (U_{ei}^*)^2 \epsilon_\nu(p_1)\epsilon_\mu(p_2)}{4(q'^2 - m_{\nu_i}^2)} \bar{u}_e(p_3)\gamma^\mu(\mathbb{1}_4 - \gamma^5)\gamma^\nu v_e(p_4) \tag{4.10}$$

hence, the total matrix element is

$$\mathcal{M} = m_{\nu_i} g_W^2 (U_{ei}^*)^2 \epsilon_\mu(p_1)\epsilon_\nu(p_2) \left[\frac{\bar{u}_e(p_3)\gamma^\mu(\mathbb{1}_4 - \gamma^5)\gamma^\nu v_e(p_4)}{4(q^2 - m_{\nu_i}^2)} - \frac{\bar{u}_e(p_3)\gamma^\nu(\mathbb{1}_4 - \gamma^5)\gamma^\mu v_e(p_4)}{4(q'^2 - m_{\nu_i}^2)} \right] \tag{4.11}$$

As for the averaged matrix element squared, we have

$$\begin{aligned} \left\langle |\mathcal{M}_2|^2 \right\rangle =& \frac{m_{\nu_i}^2 g_W^4 |U_{ei}|^4}{144(u - m_{\nu_i}^2)^2 m_W^4} \\ & \times \left[m_W^4 \left(s - 2m_e^2\right) + 2m_W^2 \left(m_e^2 + m_W^2 - u\right)\left(m_e^2 + m_W^2 - t\right) + \left(m_e^2 + m_W^2 - u\right)^2 \left(s - 2m_W^2\right) \right] \end{aligned} \tag{4.12}$$

Finally, we must also calculate the crossed term $2\mathrm{Re}\left[\mathcal{M}_1^* \mathcal{M}_2\right]$. This is done, again, by using the trace technique, but this time we must be more careful on how the spinors are positioned. Doing this calculation explicitly gives

$$\begin{aligned} \mathcal{M}_1^* \mathcal{M}_2 =& \frac{m_{\nu_i}^2 g_W^4 |U_{ei}|^4}{(2^6)(3^2)(t - m_{\nu_i}^2)(u - m_{\nu_i}^2)} \left(-g_{\mu\rho} + \frac{p_{1\mu} p_{1\rho}}{m_W^2}\right)\left(-g_{\nu\sigma} + \frac{p_{2\nu} p_{2\sigma}}{m_W^2}\right) \\ & \times \left[\bar{u}_e(p_3)\gamma^\mu(\mathbb{1}_4 - \gamma^5)\gamma^\nu v_e(p_4)\right]^\dagger \left[\bar{u}_e(p_3)\gamma^\sigma(\mathbb{1}_4 - \gamma^5)\gamma^\rho v_e(p_4)\right] \\ =& \frac{m_{\nu_i}^2 g_W^4 |U_{ei}|^4}{(2^6)(3^2)(t - m_{\nu_i}^2)(u - m_{\nu_i}^2)} \left(-g_{\mu\rho} + \frac{p_{1\mu} p_{1\rho}}{m_W^2}\right)\left(-g_{\nu\sigma} + \frac{p_{2\nu} p_{2\sigma}}{m_W^2}\right) \\ & \times \mathrm{Tr}\left[v_e(p_4)\bar{v}_e(p_4)\gamma^\nu(\mathbb{1}_4 - \gamma^5)\gamma^\mu u_e(p_3)\bar{u}_e(p_3)\gamma^\sigma(\mathbb{1}_4 - \gamma^5)\gamma^\rho\right] \end{aligned} \tag{4.13}$$

Now, summing over spin projections, eliminating terms with an odd number of gamma matrices and evaluating the trace like in the previous cases, we obtain

$$\begin{aligned} 2\mathrm{Re}\left[\langle \mathcal{M}_1^* \mathcal{M}_2 \rangle\right] =& \frac{m_{\nu_i}^2 g_W^4 |U_{ei}|^4}{(2^4)(3^2)(t - m_{\nu_i}^2)(u - m_{\nu_i}^2)} \left(-g_{\mu\rho} + \frac{p_{1\mu} p_{1\rho}}{m_W^2}\right)\left(-g_{\nu\sigma} + \frac{p_{2\nu} p_{2\sigma}}{m_W^2}\right) \\ & \times \mathrm{Re}\left[\mathrm{Tr}\left[(\mathbb{1}_4 + \gamma^5)\gamma^\nu \gamma^\mu \not{p}_3 \gamma^\sigma \gamma^\rho \not{p}_4\right]\right] \\ =& \frac{m_{\nu_i}^2 g_W^4 |U_{ei}|^4}{(2^2)(3^2)(t - m_{\nu_i}^2)(u - m_{\nu_i}^2) m_W^4} \\ & \times \left[2\left(p_3 \cdot p_4\right)\left(p_1 \cdot p_2\right)^2 + 4m_W^4 \left(p_3 \cdot p_4\right) - 4m_W^2 \left(p_2 \cdot p_3\right)\left(p_2 \cdot p_4\right)\right. \\ & \quad + 2\left(p_1 \cdot p_3\right)\left(\left(p_1 \cdot p_4\right)\left(p_2^2 - 2m_W^2\right) - \left(p_1 \cdot p_2\right)\left(p_2 \cdot p_4\right)\right) \\ & \quad \left. - 2\left(p_1 \cdot p_2\right)\left(p_1 \cdot p_4\right)\left(p_2 \cdot p_3\right) + 2p_1^2 \left(p_2 \cdot p_3\right)\left(p_2 \cdot p_4\right) - p_1^2 p_2^2 \left(p_3 \cdot p_4\right)\right] \end{aligned} \tag{4.14}$$

Then, in terms of Mandelstam variables,

$$\begin{aligned} 2Re\left[\langle\mathcal{M}_1^*\mathcal{M}_2\rangle\right] =& \frac{m_{\nu_i}^2 g_W^4 |U_{ei}|^4}{144(t-m_{\nu_i}^2)(u-m_{\nu_i}^2)m_W^4} \\ &\times \Big[(s-2m_e^2)\left((s-2m_W^2)^2+6m_W^4\right) - 4m_W^2\left(m_W^2+m_e^2-u\right)\left(m_W^2+m_e^2-t\right) \\ &\quad -\left(s-2m_W^2\right)\left(\left(m_W^2+m_e^2-t\right)^2+\left(m_W^2+m_e^2-u\right)^2\right)\Big] \end{aligned} \tag{4.15}$$

Adding all three components and remembering the relative negative sign between t and u-channel, we obtain the total averaged matrix element squared as

$$\left\langle|\mathcal{M}|^2\right\rangle = \left\langle|\mathcal{M}_1|^2\right\rangle + \left\langle|\mathcal{M}_2|^2\right\rangle - 2\mathrm{Re}\left[\langle\mathcal{M}_1^*\mathcal{M}_2\rangle\right] \tag{4.16}$$

where $\left\langle|\mathcal{M}_1|^2\right\rangle$ is in Eq. (4.9), $\left\langle|\mathcal{M}_2|^2\right\rangle$ in Eq. (4.12) and $2\mathrm{Re}\left[\langle\mathcal{M}_1^*\mathcal{M}_2^*\rangle\right]$ in Eq. (4.15). We can then define the 4-momenta in the centre of mass reference frame:

$$p_1 = (E_0, \vec{p}), \quad p_2 = (E_0, -\vec{p}), \quad p_3 = (E_0, \vec{q}), \quad p_1 = (E_0, -\vec{q}) \tag{4.17}$$

with

$$|\vec{p}| = \sqrt{E_0^2 - m_W^2}, \quad |\vec{q}| = \sqrt{E_0^2 - m_e^2}, \quad \vec{p}\cdot\vec{q} = |\vec{p}||\vec{q}|\cos\theta \tag{4.18}$$

This results in the following Mandelstam variables in terms of only the collision energy E_0 and the electron scattering scattering angle θ:

$$\begin{cases} s = 4E_0^2 \\ t = m_W^2 + m_e^2 - 2E_0^2 + 2\sqrt{E_0^2 - m_W^2}\sqrt{E_0^2 - m_e^2}\cos\theta \\ u = m_W^2 + m_e^2 - 2E_0^2 - 2\sqrt{E_0^2 - m_W^2}\sqrt{E_0^2 - m_e^2}\cos\theta \end{cases} \tag{4.19}$$

The differential cross-section for a 2 to 2 process in the centre of mass reference frame, using the above defined 4-momenta, is given [36] by

$$\frac{d\sigma}{d\phi d\cos\theta} = \frac{1}{64\pi^2 s}\frac{|\vec{q}|}{|\vec{p}|}\left\langle|\mathcal{M}|^2\right\rangle = \frac{1}{256\pi^2 E_0^2}\frac{\sqrt{E_0^2 - m_e^2}}{\sqrt{E_0^2 - m_W^2}}\left\langle|\mathcal{M}|^2\right\rangle \tag{4.20}$$

Evaluating this expression on Mathematica and comparing to the analogous lepton number conserving process $W^-W^+ \to e^-e^+$, which we left to calculate in the Appendix A, we obtain the plot in Figure 5 (left). Finally, integrating the differential cross-sections, we obtain the total cross-section in terms of the Neutrino mass depicted in Figure 5 (right). Both plots show a very distinct behaviour of the cross-section between both processes. $W^-W^- \to e^-e^-$ is symmetric in the solid angle due to the presence of the u-channel in addition to the t-channel, while $W^+W^- \to e^+e^-$ shows an asymmetry shifted towards smaller angles. Also, $W^-W^- \to e^-e^-$ is minimum when $\theta = \frac{\pi}{2}$ while $W^+W^- \to e^+e^-$ has its minima at $\theta = \pi$ or $\theta = 0$. Hence, both show an inverse dependency on $\cos\theta$. The dependency on the neutrino mass is another interesting, but not surprising, distinction. $W^+W^- \to e^+e^-$ has no dependency on m_ν as this term drops out of the trace due to the chirality projectors, leaving only a $\frac{1}{m_\nu^2}$ term in the propagator.

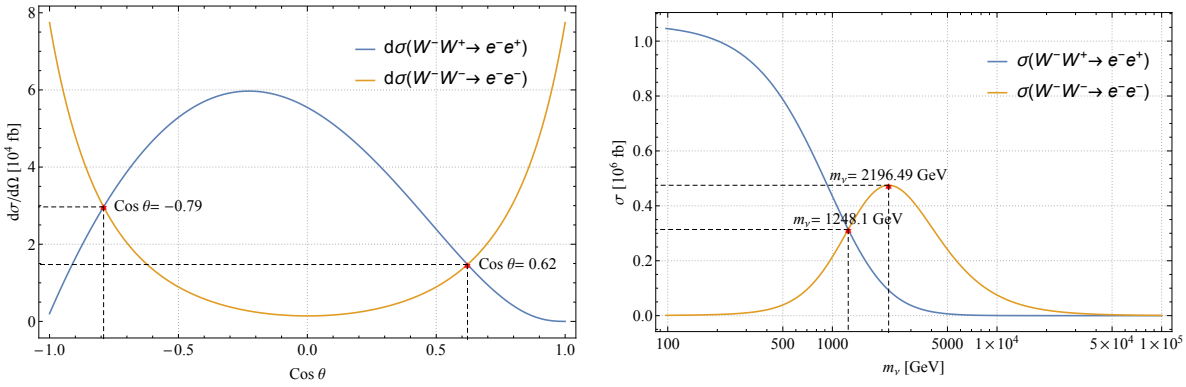

Figure 5: $W^-W^- \to e^-e^-$ (orange) and $W^-W^+ \to e^-e^+$ (blue). *Left:* Differential cross-section $d\sigma/d\Omega$ at $E_0 = 1$ TeV. *Right:* Total cross-section σ at $E_0 = 1$ TeV as a function of m_{ν_i}.

$W^-W^- \to e^-e^-$, on the other hand, has a non-vanishing dependency on m_ν in the trace, which causes the peak in the total cross-section. Again, we reiterate that this is not a realistic process and, as far as we know, will never be observable. Nonetheless, we extracted useful information from this exercise.

4.2 $0\nu\beta\beta\phi$ Leptonic Current with Scalar ϕ Emission

In Section 4.1 we have calculated a full matrix element with all indices contracted. From now on, we will not be considering the terms which connect to the leptonic current, namely, the W-bosons and the hadronic current. As mentioned in Section 3, the leptonic current is the only part that actually changes among our different $\beta\beta$ processes, thus, we will be calculating only this part of the total matrix element. Since the leptonic current is not contracted with the hadronic current, we will have an object depending on two indices (or four indices for the averaged current squared).

We shall now calculate the simplest Majoron-emitting $\beta\beta$ decay mode. To be as general as possible, we consider the vertex between the Majoron and the neutrinos to have the generic form

$$g^\phi \left(\alpha + \beta\gamma^5\right) \tag{4.21}$$

which contains both left and right-handed components. We start, again, with the t-channel diagram depicted in Figure 6 left, but this time the W-bosons are not included. Also, with five 4-momenta, the

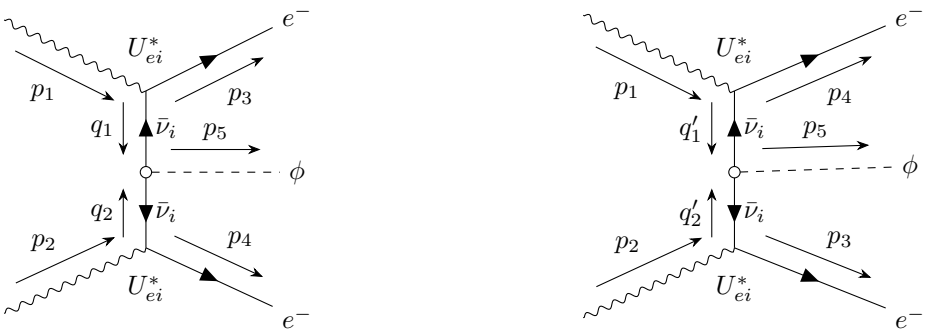

Figure 6: $0\nu\beta\beta\phi$ Feynman diagram. *Left:* t-channel with $q_1 = p_1 - p_3$, $q_2 = p_2 - p_4$. *Right:* u-channel with $q_1' = p_1 - p_4$, $q_2' = p_2 - p_3$.

Mandelstam variables are not applicable anymore. Following the Feynman rules, we obtain the current

$$
\begin{aligned}
J_1^{\mu\nu} &= \frac{g_\phi^* g_W^2 (U_{ei}^*)^2}{8(q_1^2 - m_{\nu_i}^2)(q_2^2 - m_{\nu_i}^2)} \\
&\quad \times \left[\bar{u}_e(p_3)\right]_f \left[\gamma^\mu(\mathbb{1}_4 - \gamma^5)\right]_{fe} \left[(\not{q}_1 + m_{\nu_i})\right]_{ed} \left[\left(\alpha + \beta\gamma^5\right)\hat{C}\right]_{cd} \left[(\not{q}_2 + m_{\nu_i})\right]_{bc} \left[\gamma^\nu(\mathbb{1}_4 - \gamma^5)\right]_{ab} \left[\bar{u}_e(p_4)\right]_a \\
&= \frac{-g_\phi^* g_W^2 (U_{ei}^*)^2}{8(q_1^2 - m_{\nu_i}^2)(q_2^2 - m_{\nu_i}^2)} \left[\bar{u}_e(p_3)\gamma^\mu \underbrace{(\mathbb{1}_4 - \gamma^5)(\not{q}_1 + m_{\nu_i})\left(\alpha + \beta\gamma^5\right)(\not{q}_2 - m_{\nu_i})(\mathbb{1}_4 - \gamma^5)}\gamma^\nu v_e(p_4)\right]
\end{aligned}
\tag{4.22}
$$

Expanding the underbraced block between γ^μ and γ^ν, we obtain four terms

$$
\begin{aligned}
&(\mathbb{1}_4 - \gamma^5)(\not{q}_1 + m_{\nu_i})\left(\alpha + \beta\gamma^5\right)(\not{q}_2 - m_{\nu_i})(\mathbb{1}_4 - \gamma^5) \\
&= \left[\not{q}_1(\mathbb{1}_4 + \gamma^5) + m_{\nu_i}(\mathbb{1}_4 - \gamma^5)\right]\left(\alpha + \beta\gamma^5\right)\left[(\mathbb{1}_4 + \gamma^5)\not{q}_2 - (\mathbb{1}_4 - \gamma^5)m_{\nu_i}\right] \\
&= \not{q}_1(\mathbb{1}_4 + \gamma^5)\left(\alpha + \beta\gamma^5\right)(\mathbb{1}_4 + \gamma^5)\not{q}_2 + m_{\nu_i}(\mathbb{1}_4 - \gamma^5)\left(\alpha + \beta\gamma^5\right)(\mathbb{1}_4 + \gamma^5)\not{q}_2 \\
&\quad - \not{q}_1(\mathbb{1}_4 + \gamma^5)\left(\alpha + \beta\gamma^5\right)(\mathbb{1}_4 - \gamma^5)m_{\nu_i} - m_{\nu_i}(\mathbb{1}_4 - \gamma^5)\left(\alpha + \beta\gamma^5\right)(\mathbb{1}_4 - \gamma^5)m_{\nu_i}
\end{aligned}
$$

For each of these terms we have the following results:

$$
\begin{aligned}
\not{q}_1(\mathbb{1}_4 + \gamma^5)\left(\alpha + \beta\gamma^5\right)(\mathbb{1}_4 + \gamma^5)\not{q}_2 &= \not{q}_1\left(\alpha + \alpha\gamma^5 + \beta\gamma^5 + \beta(\gamma^5)^2\right)(\mathbb{1}_4 + \gamma^5)\not{q}_2 \\
&= \not{q}_1\left(\alpha + \beta + (\alpha + \beta)\gamma^5 + (\alpha + \beta)\gamma^5 + (\alpha + \beta)(\gamma^5)^2\right)\not{q}_2 \\
&= 2(\alpha + \beta)\left(\mathbb{1}_4 - \gamma^5\right)\not{q}_1\not{q}_2
\end{aligned}
\tag{4.23}
$$

$$
\begin{aligned}
m_{\nu_i}(\mathbb{1}_4 - \gamma^5)\left(\alpha + \beta\gamma^5\right)(\mathbb{1}_4 + \gamma^5)\not{q}_2 &= m_{\nu_i}\left(\alpha - \alpha\gamma^5 + \beta\gamma^5 - \beta(\gamma^5)^2\right)(\mathbb{1}_4 + \gamma^5)\not{q}_2 \\
&= m_{\nu_i}\left(\alpha - \beta + (\alpha - \beta)\gamma^5 - (\alpha - \beta)\gamma^5 - (\alpha - \beta)(\gamma^5)^2\right)\not{q}_2 \\
&= 0
\end{aligned}
\tag{4.24}
$$

$$
\begin{aligned}
\not{q}_1(\mathbb{1}_4 + \gamma^5)\left(\alpha + \beta\gamma^5\right)(\mathbb{1}_4 - \gamma^5)m_{\nu_i} &= \not{q}_1\left(\alpha + \alpha\gamma^5 + \beta\gamma^5 + \beta(\gamma^5)^2\right)(\mathbb{1}_4 - \gamma^5)m_{\nu_i} \\
&= \not{q}_1\left(\alpha + \beta + (\alpha + \beta)\gamma^5 - (\alpha + \beta)\gamma^5 - (\alpha + \beta)(\gamma^5)^2\right)m_{\nu_i} \\
&= 0
\end{aligned}
\tag{4.25}
$$

$$
\begin{aligned}
m_{\nu_i}(\mathbb{1}_4 - \gamma^5)\left(\alpha + \beta\gamma^5\right)(\mathbb{1}_4 - \gamma^5)m_{\nu_i} &= \left(\alpha - \alpha\gamma^5 + \beta\gamma^5 - \beta(\gamma^5)^2\right)(\mathbb{1}_4 - \gamma^5)m_{\nu_i}^2 \\
&= \left(\alpha - \beta - (\alpha - \beta)\gamma^5 - (\alpha - \beta)\gamma^5 + (\alpha - \beta)(\gamma^5)^2\right)m_{\nu_i}^2 \\
&= 2(\alpha - \beta)\left(\mathbb{1}_4 - \gamma^5\right)m_{\nu_i}^2
\end{aligned}
\tag{4.26}
$$

Which largely simplifies the calculation by cancelling the crossed terms between $q_{1,2}$ and m_{ν_i}, hence

$$
(\mathbb{1}_4 - \gamma^5)(\not{q}_1 + m_{\nu_i})\left(\alpha + \beta\gamma^5\right)(\not{q}_2 - m_{\nu_i})(\mathbb{1}_4 - \gamma^5) = 2(\mathbb{1}_4 - \gamma^5)\left[(\alpha + \beta)\not{q}_1\not{q}_2 - (\alpha - \beta)m_{\nu_i}^2\right]
$$

Inserting this result back into the current, we obtain

$$
\mathcal{M}_1 = \frac{-g_\phi^* g_W^2 (U_{ei}^*)^2}{4(q_1^2 - m_{\nu_i}^2)(q_2^2 - m_{\nu_i}^2)}\bar{u}_e(p_3)\gamma^\mu(\mathbb{1}_4 - \gamma^5)\left[(\alpha + \beta)\not{q}_1\not{q}_2 + (\beta - \alpha)m_{\nu_i}^2\right]\gamma^\nu v_e(p_4)
\tag{4.27}
$$

We can now proceed with the trace technique as before. Defining the matrices Γ_1 and $\bar{\Gamma}_2$ by

$$\begin{aligned}\Gamma_1 &= (\mathbb{1}_4+\gamma^5)\gamma^\mu(\alpha+\beta)\not{q}_1\not{q}_2 + (\beta-\alpha)m_{\nu_i}^2)\gamma^\nu \\ \bar{\Gamma}_2 &= \gamma^0\left[(\mathbb{1}_4+\gamma^5)\gamma^\rho((\alpha+\beta)\not{q}_1\not{q}_2+(\beta-\alpha)m_{\nu_i}^2)\gamma^\sigma\right]^\dagger\gamma^0 \\ &= \gamma^0(\gamma^\sigma)^\dagger\left[(\alpha+\beta)\not{q}_2^\dagger\not{q}_1^\dagger+(\beta-\alpha)m_{\nu_i}^2\right](\gamma^\rho)^\dagger(\mathbb{1}_4+\gamma^5)\gamma^0 \\ &= \gamma^\sigma\left[(\alpha+\beta)\not{q}_2\not{q}_1+(\beta-\alpha)m_{\nu_i}^2\right]\gamma^\rho(\mathbb{1}_4-\gamma^5)\end{aligned} \tag{4.28}$$

Evidently, from the cyclic property of the trace, $\bar{\Gamma}_2(\not{p}_4 - m_e)\Gamma_1$ yields

$$(\mathbb{1}_4-\gamma^5)(\not{p}_3-m_e)(\mathbb{1}_4+\gamma^5) = 2\not{p}_3(\mathbb{1}_4+\gamma^5)$$

Also, by remembering that any term with an odd number of γ^μ vanishes, the second m_e term is eliminated, thus, we obtain the averaged leptonic current squared

$$\begin{aligned}\left\langle|J_1|^2\right\rangle =& \frac{|g_\phi|^2 g_W^4|U_{ei}|^4|\phi|^2}{2^5(q_1^2-m_{\nu_i}^2)^2(q_2^2-m_{\nu_i}^2)^2} \\ &\times \mathrm{Tr}\left[(\mathbb{1}_4+\gamma^5)\gamma^\mu\left[(\alpha+\beta)\not{q}_1\not{q}_2+(\beta-\alpha)m_{\nu_i}^2\right]\gamma^\nu\not{p}_4\gamma^\sigma\left[(\alpha+\beta)\not{q}_2\not{q}_1+(\beta-\alpha)m_{\nu_i}^2\right]\gamma^\rho\not{p}_3\right]\end{aligned} \tag{4.29}$$

Here we have dropped the indices on the left-hand side to simplify the notation. Splitting the trace using its linearity, we obtain 4 traces to calculate

$$\begin{aligned}\left\langle|J_1^{\mu\nu}|^2\right\rangle =& \frac{|g_\phi|^2 g_W^4|U_{ei}|^4}{32(q_1^2-m_{\nu_i}^2)^2(q_2^2-m_{\nu_i}^2)^2} \\ &\times\Big\{(\alpha+\beta)^2\mathrm{Tr}\left[(\mathbb{1}_4+\gamma^5)\gamma^\mu\not{q}_1\not{q}_2\gamma^\nu\not{p}_4\gamma^\sigma\not{q}_2\not{q}_1\gamma^\rho\not{p}_3\right]+m_{\nu_i}^4(\beta-\alpha)^2\mathrm{Tr}\left[(\mathbb{1}_4+\gamma^5)\gamma^\mu\gamma^\nu\not{p}_4\gamma^\sigma\gamma^\rho\not{p}_3\right] \\ &+m_{\nu_i}^2(\beta^2-\alpha^2)\left(\mathrm{Tr}\left[(\mathbb{1}_4+\gamma^5)\gamma^\mu\not{q}_1\not{q}_2\gamma^\nu\not{p}_4\gamma^\sigma\gamma^\rho\not{p}_3\right]+\mathrm{Tr}\left[(\mathbb{1}_4+\gamma^5)\gamma^\mu\gamma^\nu\not{p}_4\gamma^\sigma\not{q}_2\not{q}_1\gamma^\rho\not{p}_3\right]\right)\Big\}\end{aligned} \tag{4.30}$$

Without contracting all indices, these traces result in thousands of terms, hence, instead of evaluating them in this abstract scenario, we can check four interesting special cases:

$$\beta=\alpha\rightarrow\left\langle|J_1|^2\right\rangle = \frac{\alpha^2|g_\phi|^2 g_W^4|U_{ei}|^4}{8(q_1^2-m_{\nu_i}^2)^2(q_2^2-m_{\nu_i}^2)^2}\mathrm{Tr}\left[(\mathbb{1}_4+\gamma^5)\gamma^\mu\not{q}_1\not{q}_2\gamma^\nu\not{p}_4\gamma^\sigma\not{q}_2\not{q}_1\gamma^\rho\not{p}_3\right] \tag{4.31}$$

$$\beta=-\alpha\rightarrow\left\langle|J_1|^2\right\rangle = \frac{\alpha^2 m_{\nu_i}^4|g_\phi|^2 g_W^4|U_{ei}|^4}{8(q_1^2-m_{\nu_i}^2)^2(q_2^2-m_{\nu_i}^2)^2}\mathrm{Tr}\left[(\mathbb{1}_4+\gamma^5)\gamma^\mu\gamma^\nu\not{p}_4\gamma^\sigma\gamma^\rho\not{p}_3\right] \tag{4.32}$$

$$\begin{aligned}\alpha=0\rightarrow\left\langle|J_1|^2\right\rangle =& \frac{\beta^2|g_\phi|^2 g_W^4|U_{ei}|^4}{32(q_1^2-m_{\nu_i}^2)^2(q_2^2-m_{\nu_i}^2)^2} \\ &\times\Big\{\mathrm{Tr}\left[(\mathbb{1}_4+\gamma^5)\gamma^\mu\not{q}_1\not{q}_2\gamma^\nu\not{p}_4\gamma^\sigma\not{q}_2\not{q}_1\gamma^\rho\not{p}_3\right]+m_{\nu_i}^4\mathrm{Tr}\left[(\mathbb{1}_4+\gamma^5)\gamma^\mu\gamma^\nu\not{p}_4\gamma^\sigma\gamma^\rho\not{p}_3\right] \\ &+m_{\nu_i}^2\left(\mathrm{Tr}\left[(\mathbb{1}_4+\gamma^5)\gamma^\mu\not{q}_1\not{q}_2\gamma^\nu\not{p}_4\gamma^\sigma\gamma^\rho\not{p}_3\right]+\mathrm{Tr}\left[(\mathbb{1}_4+\gamma^5)\gamma^\mu\gamma^\nu\not{p}_4\gamma^\sigma\not{q}_2\not{q}_1\gamma^\rho\not{p}_3\right]\right)\Big\}\end{aligned} \tag{4.33}$$

$$\beta = 0 \to \langle |J_1|^2 \rangle = \frac{\alpha^2 |g_\phi|^2 g_W^4 |U_{ei}|^4}{32(q_1^2 - m_{\nu_i}^2)^2 (q_2^2 - m_{\nu_i}^2)^2} \times \Big\{ \mathrm{Tr}\left[(\mathbb{1}_4 + \gamma^5)\gamma^\mu \not{q}_1 \not{q}_2 \gamma^\nu \not{p}_4 \gamma^\sigma \not{q}_2 \not{q}_1 \gamma^\rho \not{p}_3\right] + m_{\nu_i}^4 \mathrm{Tr}\left[(\mathbb{1}_4 + \gamma^5)\gamma^\mu \gamma^\nu \not{p}_4 \gamma^\sigma \gamma^\rho \not{p}_3\right] - m_{\nu_i}^2 \left(\mathrm{Tr}\left[(\mathbb{1}_4 + \gamma^5)\gamma^\mu \not{q}_1 \not{q}_2 \gamma^\nu \not{p}_4 \gamma^\sigma \gamma^\rho \not{p}_3\right] + \mathrm{Tr}\left[(\mathbb{1}_4 + \gamma^5)\gamma^\mu \gamma^\nu \not{p}_4 \gamma^\sigma \not{q}_2 \not{q}_1 \gamma^\rho \not{p}_3\right]\right)\Big\} \tag{4.34}$$

For $\beta = \alpha$, the averaged matrix element squared has no explicit dependence on m_{ν_i}, while for $\beta = -\alpha$ it is dominated by $m_{\nu_i}^4$. As for $\alpha = 0$ and $\beta = 0$, each case yields an opposite interference term of order $m_{\nu_i}^2$. We can also rewrite the vertex factor in terms of r and l such that the chirality projection operators are explicitly separated:

$$\alpha + \beta\gamma^5 = lP_L + rP_R = \frac{r+l}{2}\mathbb{1}_4 + \frac{r-l}{2}\gamma^5 \quad \Rightarrow \quad \alpha = \frac{r+l}{2}, \quad \beta = \frac{r-l}{2} \tag{4.35}$$

The four cases above can be, respectively, understood as $l = 0$, $r = 0$, $l = -r$, $l = r$. That is, only right handed currents, only left handed currents, and two mixed currents with opposite interferences respectively. Therefore, we see that right-handed currents are proportional to the momenta of the internal neutrinos while left-handed currents are proportional to the neutrino mass.

Now, to compute the u-channel, the only change will be switching p_1 with p_2 in the matrix element, similarly as done for $W^-W^- \to e^-e^-$. Thus, the current resulting from the Feynman diagram in Figure 6 right is

$$J_2^{\mu\nu} = \frac{-g_\phi^* g_W^2 (U_{ei}^*)^2}{4({q_1'}^2 - m_{\nu_i}^2)({q_2'}^2 - m_{\nu_i}^2)} \bar{u}_e(p_3)\gamma^\nu(\mathbb{1}_4 - \gamma^5)\left[(\alpha+\beta)\not{q}_2'\not{q}_1' + (\beta-\alpha)m_{\nu_i}^2\right]\gamma^\mu v_e(p_4) \tag{4.36}$$

and the resulting averaged current squared is

$$\langle J_2^{\mu\nu}|^2 \rangle = \frac{|g_\phi|^2 g_W^4 |U_{ei}|^4}{32({q_1'}^2 - m_{\nu_i}^2)^2({q_2'}^2 - m_{\nu_i}^2)^2} \times \Big\{ (\alpha+\beta)^2 \mathrm{Tr}\left[(\mathbb{1}_4 + \gamma^5)\gamma^\nu \not{q}_2' \not{q}_1' \gamma^\mu \not{p}_4 \gamma^\rho \not{q}_1' \not{q}_2' \gamma^\sigma \not{p}_3\right] + m_{\nu_i}^4 (\beta-\alpha)^2 \mathrm{Tr}\left[(\mathbb{1}_4 + \gamma^5)\gamma^\nu \gamma^\mu \not{p}_4 \gamma^\rho \gamma^\sigma \not{p}_3\right] + m_{\nu_i}^2(\beta^2 - \alpha^2)\left(\mathrm{Tr}\left[(\mathbb{1}_4 + \gamma^5)\gamma^\nu \not{q}_2' \not{q}_1' \gamma^\mu \not{p}_4 \gamma^\rho \gamma^\sigma \not{p}_3\right] + \mathrm{Tr}\left[(\mathbb{1}_4 + \gamma^5)\gamma^\nu \gamma^\mu \not{p}_4 \gamma^\rho \not{q}_1' \not{q}_2' \gamma^\sigma \not{p}_3\right]\right)\Big\} \tag{4.37}$$

The total leptonic current is, therefore, by summing both the t- and u-channel,

$$J^{\mu\nu} = \frac{-g_\phi^* g_W^2 (U_{ei}^*)^2}{4} \times \left[\frac{\bar{u}_e(p_3)\gamma^\mu(\mathbb{1}_4 - \gamma^5)((\alpha+\beta)\not{q}_1\not{q}_2 + (\beta-\alpha)m_{\nu_i}^2)\gamma^\nu v_e(p_4)}{(q_1^2 - m_{\nu_i}^2)(q_2^2 - m_{\nu_i}^2)} - \frac{\bar{u}_e(p_3)\gamma^\nu(\mathbb{1}_4 - \gamma^5)((\alpha+\beta)\not{q}_2'\not{q}_1' + (\beta-\alpha)m_{\nu_i}^2)\gamma^\mu v_e(p_4)}{({q_1'}^2 - m_{\nu_i}^2)({q_2'}^2 - m_{\nu_i}^2)} \right] \tag{4.38}$$

As for the crossed term between t- and u-channels, we have simply

$$\langle J_1^* J_2 \rangle = \frac{|g_\phi|^2 g_W^4 |U_{ei}|^4}{32(q_1^2 - m_{\nu_i}^2)(q_2^2 - m_{\nu_i}^2)({q_1'}^2 - m_{\nu_i}^2)({q_2'}^2 - m_{\nu_i}^2)} \times \Big\{ (\alpha+\beta)^2 \mathrm{Tr}\left[(\mathbb{1}_4 + \gamma^5)\gamma^\mu \not{q}_1 \not{q}_2 \gamma^\nu \not{p}_4 \gamma^\rho \not{q}_1' \not{q}_2' \gamma^\sigma \not{p}_3\right] + m_{\nu_i}^4 (\beta-\alpha)^2 \mathrm{Tr}\left[(\mathbb{1}_4 + \gamma^5)\gamma^\mu \gamma^\nu \not{p}_4 \gamma^\rho \gamma^\sigma \not{p}_3\right] + m_{\nu_i}^2(\beta^2 - \alpha^2)\left(\mathrm{Tr}\left[(\mathbb{1}_4 + \gamma^5)\gamma^\mu \not{q}_1 \not{q}_2 \gamma^\nu \not{p}_4 \gamma^\rho \gamma^\sigma \not{p}_3\right] + \mathrm{Tr}\left[(\mathbb{1}_4 + \gamma^5)\gamma^\mu \gamma^\nu \not{p}_4 \gamma^\rho \not{q}_1' \not{q}_2' \gamma^\sigma \not{p}_3\right]\right)\Big\} \tag{4.39}$$

Although daunting, this expression is the most general form possible for $0\nu\beta\beta\phi$. With the small

neutrino mass, we can neglect it without much loss of generality and consider only the terms proportional to the 4-momenta of the internal neutrinos. Doing so is equivalent to setting $\beta = \alpha$ or, in other words, considering only right-handed currents. Even though we are not calculating these traces explicitly and the 4-momenta p_1 and p_2 are actually internal momenta that would be determined by the 4-momenta of the hadronic current, we can, heuristically, set the outgoing 4-momenta as

$$p_3 = (E_3, \vec{p}_3)\,,\ p_4 = (E_4, \vec{p}_4)\,,\ p_5 = (E_5, \vec{p}_5) \tag{4.40}$$

We then call φ' the angle from $\vec{p}_3$ to $\vec{p}_4$, and φ the angle from $\vec{p}_4$ to $\vec{p}_5$. However, these angles are fixed by the condition $\vec{p}_3 + \vec{p}_4 + \vec{p}_5 = 0$, hence

$$\begin{array}{ll} (1) & \vec{p}_3\cdot\vec{p}_3 + \vec{p}_4\cdot\vec{p}_3 + \vec{p}_5\cdot\vec{p}_3 = 0 \\ (2) & \vec{p}_3\cdot\vec{p}_4 + \vec{p}_4\cdot\vec{p}_4 + \vec{p}_5\cdot\vec{p}_4 = 0 \Rightarrow \\ (3) & \vec{p}_3\cdot\vec{p}_5 + \vec{p}_4\cdot\vec{p}_5 + \vec{p}_5\cdot\vec{p}_5 = 0 \end{array} \left\{ \begin{array}{l} |\vec{p}_3| + |\vec{p}_4|\cos(\varphi') + |\vec{p}_5|\cos(\varphi'+\varphi) = 0 \\ |\vec{p}_3|\cos(\varphi') + |\vec{p}_4| + |\vec{p}_5|\cos(\varphi) = 0 \\ |\vec{p}_3|\cos(\varphi'+\varphi) + |\vec{p}_4|\cos(\varphi) + |\vec{p}_5| = 0 \end{array} \right. \tag{4.41}$$

Where we have used that the angle from $\vec{p}_3$ to $\vec{p}_5$ is simply the sum of the angles from $\vec{p}_3$ to $\vec{p}_4$ and $\vec{p}_4$ to $\vec{p}_5$. From (2) we have

$$\cos(\varphi) = -\frac{|\vec{p}_4| + |\vec{p}_3|\cos(\varphi')}{|\vec{p}_5|} \tag{4.42}$$

Putting it in (3) and calculating $|\vec{p}_3| \times (1) = |\vec{p}_5| \times (3)$, we obtain

$$|\vec{p}_3|^2 + |\vec{p}_3||\vec{p}_4|\cos(\varphi') = -|\vec{p}_4|^2 - |\vec{p}_3||\vec{p}_4|\cos(\varphi') + |\vec{p}_5|^2 \quad \Rightarrow \quad \cos(\varphi') = \frac{|\vec{p}_5|^2 - |\vec{p}_3|^2 - |\vec{p}_4|^2}{2|\vec{p}_3||\vec{p}_4|} \tag{4.43}$$

which, results in

$$\begin{gathered} \varphi' = \cos^{-1}\left(\frac{|\vec{p}_5|^2 - |\vec{p}_4|^2 - |\vec{p}_3|^2}{2|\vec{p}_3||\vec{p}_4|}\right), \quad \varphi = \cos^{-1}\left(\frac{|\vec{p}_3|^2 - |\vec{p}_4|^2 - |\vec{p}_5|^2}{2|\vec{p}_4||\vec{p}_5|}\right), \\ \varphi + \varphi' = \cos^{-1}\left(\frac{|\vec{p}_3|^2 + |\vec{p}_5|^2 - |\vec{p}_4|^2}{2|\vec{p}_3||\vec{p}_5|}\right) \end{gathered} \tag{4.44}$$

From these angles we can see 3 interesting special cases:

1. $m_e,\ m_\phi << E_3,\ E_4,\ E_5 \ \Rightarrow\ \varphi \approx \cos^{-1}\left(\frac{E_3^2 - E_4^2 - E_5^2}{2E_4E_5}\right),\ \varphi' \approx \cos^{-1}\left(\frac{E_5^2 - E_4^2 - E_3^2}{2E_3E_4}\right)$
2. $E_3 \approx E_4 \ \Rightarrow\ \cos(\varphi') \approx \left(\frac{1}{2}\frac{|\vec{p}_5|^2}{|\vec{p}_3|^2} - 1\right) = \cos(2\varphi),\ \cos(\varphi) \approx \left(-\frac{1}{2}\frac{|\vec{p}_5|}{|\vec{p}_3|}\right)$
3. $|\vec{p}_5| << |\vec{p}_3|,\ |\vec{p}_4| \ \Rightarrow\ \varphi' \to \pi,\ \varphi \to \frac{\pi}{2}$

Although all 3 cases are interesting limits as they greatly simplify the calculations, the third result yields both a similar angular dependency to that of $0\nu\beta\beta$, as the electrons would be flying approximately in opposite directions, and a direct measure of m_ϕ as almost all the missing energy would have to be due to the Majoron mass.

For a real process, in principle, it would not be difficult to write p_1 and p_2 in terms of the 4-momenta of the hadronic current and obtain all the relations between the hadronic 4-momenta, p_3, p_4 and p_5 in a similar fashion as done in this example. Also, we would have to consider the scattering to be happening in

3 dimensions, which would produce extra angles that we have purposely neglected in this brief illustration. In fact, the momentum conservation would allow the two incoming momenta to be in a different plane to the three outgoing momenta and we would have to use spherical trigonometry. This is similar to what we will do in Section 5.3. Nonetheless, we have now obtained the leptonic current for both neutrinoless processes and understood the role that the Majoron, right-handed currents and the neutrino mass play. What is left for us to do is calculate their respective phase spaces and show how each process depend on the Q-Value and the Majoron mass m_ϕ.

4.3 Neutrinoless Phase Space and Decay Rates

To calculate the phase space for $0\nu\beta\beta$, we could proceed with the exact differential decay rate for the $0^+ \to 0^+$ transition as given by [21], which reads

$$\begin{aligned} d\Gamma(0^+ \to 0^+) &= \frac{(Gg_a)^4 m_e^7}{2(2\pi R)^2} \left[A_0 + \cos(\theta) B_0\right] d\Omega_0 \\ d\Omega_0 &= m_e^{-5} |\vec{p}_{e_1}||\vec{p}_{e_2}| \epsilon_{e_1}\epsilon_{e_2} \delta(\epsilon_{e_1} + \epsilon_{e_2} + E_f - M_i) d\epsilon_{e_1} d\epsilon_{e_2} d\cos(\theta) \end{aligned} \tag{4.45}$$

where $\cos(\theta) = (\vec{p}_{e_1} \cdot \vec{p}_{e_2})$, $\vec{p}_j$ and ϵ_j are the momentum and energy of the emitted electrons, E_F the energy of the daughter nucleus, M_i the mass of the parent nucleus, m_e the electron mass, R the nuclear radius, A_0 and B_0 a combination of kinematic factors arising from the nuclear matrix element, G the Fermi constant and g_a the axial coupling constant. This is a quite general expression, however, since the phase space for neutrinoless $\beta\beta$ decay processes will always have terms of the form $A + B(\hat{p}_1 \cdot \hat{p}_2)$, we choose to use the decay rate given by [30], which reads

$$\Gamma_{0\nu\beta\beta} \approx \frac{|\mathcal{M}_{0\nu\beta\beta}|^2}{2M} \int \frac{d^3\vec{P}}{2(2\pi)^3 M} \frac{d^3\vec{p}_{e_1}}{2(2\pi)^3\epsilon_{e_1}} \frac{d^3\vec{p}_{e_2}}{2(2\pi)^3\epsilon_{e_2}} (p_{e_1} \cdot p_{e_2}) (2\pi)^4 \delta^{(4)}(P - p_{e_1} - p_{e_2} - \tilde{P}) a(\epsilon_{e_1}, \epsilon_{e_2}) \tag{4.46}$$

In this approximation, $\mathcal{M}_{0\nu\beta\beta}$ is assumed to depend only on the 4-momenta of the hadronic current, while the 4-momenta of the leptonic current is carried only by the scalar products inside the integral. This is achieved by using a Fierz transformation, as mentioned in Section 3.4. The notation remains the same, but this time we have the masses and 4-momenta of the daughter and parent nuclei respectively denoted by P, M and $\tilde{P}, \tilde{M}$, and the form factor $a(\epsilon_{e_1}, \epsilon_{e_2})$, which describes the effect of the Coulomb potential on the emitted electrons discussed in Section 3.4. We shall now proceed with solving Eq. (4.46) in detail. First we integrate over $\vec{P}$, resulting in

$$\Gamma_{0\nu\beta\beta} \approx \frac{|\mathcal{M}_{0\nu\beta\beta}|^2}{(2\pi)^5 16 M^2} \int \frac{d^3\vec{p}_{e_1}}{\epsilon_{e_1}} \frac{d^3\vec{p}_{e_2}}{\epsilon_{e_2}} (\epsilon_{e_1}\epsilon_{e_2} - |\vec{p}_{e_1}||\vec{p}_{e_2}| \cos(\theta)) \delta(Q + 2m_e - \epsilon_{e_1} - \epsilon_{e_2}) a(\epsilon_{e_1}, \epsilon_{e_2}) \tag{4.47}$$

It's important to note, in this step, that the definition of the Q-value used is the kinetic energy difference between final and initial states. That is, $Q = \tilde{M} - M - 2m_e = \epsilon_{e_1} + \epsilon_{e_2} - 2m_e$, being $M \approx \tilde{M}$. The best way to proceed from now on is to change the 3-momentum to polar coordinates, as given by

$$d^3\vec{p}_j \to |\vec{p}_j|^2 \; d|\vec{p}_j| \; d\phi \; d\cos\theta \tag{4.48}$$

Integrating over ϕ and $\cos(\theta)$, we find that the term proportional to $\cos(\theta)$) cancels identically since the integral $\int_{-1}^{1}\cos(\theta)d\cos(\theta)$ is odd. The parity properties of the solid angle integrals will used without ceremonies throughout all phase space calculations. Putting it all together, we have

$$\Gamma_{0\nu\beta\beta} \approx \frac{(4\pi)^2}{(2\pi)^5 16M^2}\left|\mathcal{M}_{0\nu\beta\beta}\right|^2 \int |\vec{p}_{e_1}|^2 d|\vec{p}_{e_1}||\vec{p}_{e_2}|^2 d|\vec{p}_{e_2}|\delta(Q+2m_e-\epsilon_{e_1}-\epsilon_{e_2})a(\epsilon_{e_1},\epsilon_{e_2}) \tag{4.49}$$

Now, for the last change of variables, we can write $|\vec{p}_j|d|\vec{p_j}| = \epsilon_j d\epsilon_j$, resulting in

$$\Gamma_{0\nu\beta\beta} \approx \frac{(4\pi)^2}{(2\pi)^5 16M^2}\left|\mathcal{M}_{0\nu\beta\beta}\right|^2 \int |\vec{p}_{e_1}|\epsilon_{e_1} d\epsilon_{e_1}|\vec{p}_{e_2}|\epsilon_{e_2} d\epsilon_{e_2}\delta(Q+2m_e-\epsilon_{e_1}-\epsilon_{e_2})a(\epsilon_{e_1},\epsilon_{e_2}) \tag{4.50}$$

There are many approximations that can be made to go even further in this calculation but, for now, we will repeat the same process and calculate the phase space of $0\nu\beta\beta\phi$ [30].

$$\begin{aligned}\Gamma_{0\nu\beta\beta\phi} \approx \frac{\left|\mathcal{M}_{0\nu\beta\beta\phi}\right|^2}{2M}\int \frac{d^3\vec{P}}{2(2\pi)^3 M}\frac{d^3\vec{p}_{e_1}}{2(2\pi)^3\epsilon_{e_1}}\frac{d^3\vec{p}_{e_2}}{2(2\pi)^3\epsilon_{e_2}}\frac{d^3\vec{p}_{\phi}}{2(2\pi)^3\epsilon_{\phi}} \\ \times\left[(p_{e_1}\cdot p_{e_2})(2\pi)^4\delta^{(4)}(P-p_{e_1}-p_{e_2}-p_{\phi}-\tilde{P})a(\epsilon_{e_1},\epsilon_{e_2})\right]\end{aligned} \tag{4.51}$$

The first steps are identical, but we integrate first over the variables of the Majoron rather than over those of the electrons. This results in

$$\begin{aligned}\Gamma_{0\nu\beta\beta\phi} &\approx \frac{(4\pi)^3\left|\mathcal{M}_{0\nu\beta\beta\phi}\right|^2}{(2\pi)^8 32M^2}\int |\vec{p}_{e_1}|\epsilon_{e_1}d\epsilon_{e_1}|\vec{p}_{e_2}|\epsilon_{e_2}d\epsilon_{e_2}|\vec{p}_{\phi}|d\epsilon_{\phi}\delta(Q+2m_e-\epsilon_{e_1}-\epsilon_{e_2}-\epsilon_{\phi})a(\epsilon_{e_1},\epsilon_{e_2}) \\ &= \frac{\left|\mathcal{M}_{0\nu\beta\beta\phi}\right|^2}{4(2\pi)^5 M^2}\int |\vec{p}_{e_1}|\epsilon_{e_1}d\epsilon_{e_1}|\vec{p}_{e_2}|\epsilon_{e_2}d\epsilon_{e_2}\sqrt{(Q+2m_e-\epsilon_{e_1}-\epsilon_{e_2})^2-m_{\phi}^2}\,a(\epsilon_{e_1},\epsilon_{e_2})\end{aligned} \tag{4.52}$$

Although calculating this decay rate seems simple, we have one more integration to do as we have one extra final particle. It is also important to notice that the Form factor $a(\epsilon_{e_1},\epsilon_{e_2})$ does not depend on the Majoron. It is only due to the electromagnetic potential, and thus affects only electromagnetically charged particles. To deal with this term, we can now consider a few interesting approximations that will also be applied to all other $\beta\beta$ processes in the work. As argued by [30], for electron momenta $|\vec{p}_i| > m_e$, the form factor can be expressed as $a(\epsilon_{e_1},\epsilon_{e_2}) = F_0(\epsilon_{e_1})F_0(\epsilon_{e_2})$, where F_0 is the Fermi factor for $k=0$. This is a realistic assumption for the energies involved in $\beta\beta$ decay. The next thing we can do is the so-called non-relativistic approximation, in which the Fermi factor Eq. 3.24 can be written as [21]

$$F_0^{NR}(\epsilon) = \frac{2\pi y}{1-e^{-2\pi y}}, \quad y = \frac{\alpha Z\epsilon}{|\vec{p}|} \tag{4.53}$$

Again, $\beta\beta$ decays emit non-relativistic electrons, making this approximation quite reasonable. To be able to obtain an analytical expression for the decay rate, we can take the Primakoff-Rosen approximation

$$F_0^{NR}(\epsilon) \approx \frac{2\pi y}{1-e^{-2\pi\alpha Z}} \tag{4.54}$$

without loss of generality for the energies considered. Putting this resulting form factor back into 4.52, we obtain

$$\Gamma_{0\nu\beta\beta\phi} \approx \left(\frac{2\pi\alpha Z}{1-e^{-2\pi\alpha Z}}\right)^2 \frac{|\mathcal{M}_{0\nu\beta\beta\phi}|^2}{4(2\pi)^5 M^2} \int \epsilon_{e_1}^2 d\epsilon_{e_1} \epsilon_{e_2}^2 d\epsilon_{e_2} \sqrt{(Q+2m_e-\epsilon_{e_1}-\epsilon_{e_2})^2 - m_\phi^2} \tag{4.55}$$

Although feasible, this integral is rather complicated. We will be solving it exactly in Section 4.4, but for now, if we take the limit $m_\phi \to 0$ it becomes trivial and we can see how it depends on the Q-value. Integrating over ϵ_2 and subsequently over ϵ_1, we obtain

$$\begin{aligned}
\Gamma_{0\nu\beta\beta\phi} &\approx \left(\frac{2\pi\alpha Z}{1-e^{-2\pi\alpha Z}}\right)^2 \frac{|\mathcal{M}_{0\nu\beta\beta\phi}|^2}{4(2\pi)^5 M^2} \int_{m_e}^{Q+m_e} d\epsilon_{e_1} \epsilon_{e_1}^2 \int_{m_e}^{Q+2m_e-\epsilon_{e_1}} d\epsilon_{e_2} \epsilon_{e_2}^2 \left(Q+2m_e-\epsilon_{e_1}-\epsilon_{e_2}\right) \\
&= \left(\frac{2\pi\alpha Z}{1-e^{-2\pi\alpha Z}}\right)^2 \frac{|\mathcal{M}_{0\nu\beta\beta\phi}|^2}{4(2\pi)^5 M^2} \int_{m_e}^{Q+m_e} d\epsilon_{e_1} \frac{\epsilon_{e_1}^2}{12} \left[\left(11m_e^2 + 6m_e(Q-e_1) + (Q-e_1)^2\right)(m_e+Q-e_1)^2\right] \\
&= \left(\frac{\alpha Z}{1-e^{-2\pi\alpha Z}}\right)^2 \frac{1}{(2\pi)^3} \frac{|\mathcal{M}_{0\nu\beta\beta\phi}|^2}{5040M^2} \left[210m_e^4Q^3 + 210m_e^3Q^4 + 84m_e^2Q^5 + 14m_eQ^6 + Q^7\right]
\end{aligned} \tag{4.56}$$

For $m_\phi > 0$ MeV the expression is much more complicated, but the order in Q is the same, hence, $0\nu\beta\beta\phi$ is of the order of Q^7. Finally, doing the same calculation for $(0\nu\beta\beta)$ and comparing the results, we obtain

$$\begin{aligned}
\Gamma_{0\nu\beta\beta} &\approx \left(\frac{2\pi\alpha Z}{1-e^{-2\pi\alpha Z}}\right)^2 \frac{|\mathcal{M}_{0\nu\beta\beta}|^2}{4(2\pi)^3 M^2} \int_{m_e}^{Q+m_e} \epsilon_{e_1}^2 d\epsilon_{e_1} \int_{m_e}^{Q+m_e-\epsilon_{e_1}} \epsilon_{e_2}^2 d\epsilon_{e_2} \delta(Q+2m_e-\epsilon_{e_1}-\epsilon_{e_2}) \\
&= \left(\frac{2\pi\alpha Z}{1-e^{-2\pi\alpha Z}}\right)^2 \frac{|\mathcal{M}_{0\nu\beta\beta}|^2}{4(2\pi)^3 M^2} \int_{m_e}^{Q+m_e} \epsilon_{e_1}^2 d\epsilon_{e_1} (Q+2m_e-\epsilon_{e_1})^2 \\
&= \left(\frac{\alpha Z}{1-e^{-2\pi\alpha Z}}\right)^2 \frac{1}{(2\pi)} \frac{|\mathcal{M}_{0\nu\beta\beta}|^2}{120M^2} \left[120m_e^4Q + 60m_e^3Q^2 + 40m_e^2Q^3 + 10m_eQ^4 + Q^5\right]
\end{aligned} \tag{4.57}$$

As expected, the phase space for the Majoron emitting mode scales by two additional powers in Q compared to the mode without Majoron emission. This is due to the extra particle in the final state and will serve as to counter balance the change in the matrix element, which will have one extra propagator for the second internal neutrino. Therefore, as the Q dependence of the phase space increases by 2, the Q dependence of the matrix element squared reduces by 2, conserving the dimension of the decay rate.

We now have the phase space and the resulting decay rates of the selected neutrinoless processes. From an experimental point of view, however, what we can measure is the energy distribution of the emitted electrons. Most experiments are not able to separate both electrons and end up measuring the energy spectrum of the two emitted electrons together. Very few experiments, such as NEMO-3 [37] and Super-Kamiokande [14], are able to measure the emitted electrons individually. With that in mind, we will now use the results we have obtained to provide such energy distributions.

4.4 Neutrinoless Energy Distribution

In this section, we will not worry about constants affecting the total decay rate and focus only on the shape of the distributions. We will begin by analysing the 2 dimensional distribution as a function of both electron energies before integrating it to analyse how the total energy shared by the electrons behaves. The simplest phase space among all selected processes is that of $0\nu\beta\beta$ as it contains a Dirac delta function.

This is evident from an energy conservation standpoint since there are no extra particles to share the energy with the electrons, meaning that the total energy of the two electrons must add up to $Q + 2m_e$. From Eq. (4.57), we have

$$\left[\frac{d\Gamma}{d\epsilon_{e_1} d\epsilon_{e_2}}\right]_{0\nu\beta\beta} \propto \epsilon_{e_1}^2 \epsilon_{e_2}^2 \delta(Q + 2m_e - \epsilon_{e_1} - \epsilon_{e_2}) \tag{4.58}$$

We can understand it as being a parabola defined solely by ϵ_{e_1}. As for the total energy of the electrons, we can change the variables to

$$\epsilon = \epsilon_{e_1} + \epsilon_{e_2}, \quad \Delta\epsilon = \epsilon_{e_1} - \epsilon_{e_2} \tag{4.59}$$

and integrate over $\Delta\epsilon$. Doing so, we obtain

$$\begin{aligned}\left[\frac{d\Gamma}{d\epsilon}\right]_{0\nu\beta\beta} &\propto -\frac{1}{2}\int_{\epsilon-2m_e}^{2m_e-\epsilon} \left(\frac{\epsilon+\Delta\epsilon}{2}\right)^2 \left(\frac{\epsilon-\Delta\epsilon}{2}\right)^2 \delta(Q + 2m_e - \epsilon) d(\Delta\epsilon) \\ &= \left(\frac{\epsilon^5}{30} - \frac{2\epsilon^2 m_e^3}{3} + \epsilon m_e^4 - \frac{2m_e^5}{5}\right) \delta(Q + 2m_e - \epsilon)\end{aligned} \tag{4.60}$$

which is clearly still displays a Dirac delta constraining the total energy of the electrons to $Q + 2m_e$, as expected. As a matter of fact, this integral over $d(\Delta\epsilon)$ will be present in all energy distributions and will be used without ceremony. Now, for $0\nu\beta\beta\phi$, we can actually visualise the energy distribution. From Eq. (4.56) we have

$$\left[\frac{d\Gamma}{d\epsilon_{e_1} d\epsilon_{e_2}}\right]_{0\nu\beta\beta\phi} \propto \epsilon_{e_1}^2 \epsilon_{e_2}^2 \sqrt{(Q + 2m_e - \epsilon_{e_1} - \epsilon_{e_2})^2 - m_\phi^2} \tag{4.61}$$

The Majoron mass is now present as a free parameter which can assume any value from 0 to Q. For a convenient Q-value of 3MeV ($\sim$ Q-value of ^{100}Mo) and $m_\phi = 1$MeV, the 2D energy distribution is depicted in Figure 7 (left), where the axes represent the kinetic energy of each electron. Notice that those are limited to a maximum value of $Q - m_\phi$, rather than Q. Nonetheless, we see that the distribution reaches a maximum value for large electron energies, such that a massive Majoron would tend to have a low momentum. This adds to the discussion we had about the electron scattering angle that we had in Section 4.2. The limit in which m_ϕ dominates and the two electrons fly in opposite directions seem to be favoured. We can see this same phenomenon in the distribution of the total energy of the electrons. Using again the variable substitution defined by Eq. (4.59), we obtain

$$\left[\frac{d\Gamma}{d\epsilon}\right]_{0\nu\beta\beta\phi} \propto \left(\frac{\epsilon^5}{30} - \frac{2\epsilon^2 m_e^3}{3} + \epsilon m_e^4 - \frac{2m_e^5}{5}\right) \sqrt{(Q + 2m_e - \epsilon)^2 - m_\phi^2} \tag{4.62}$$

This gives us the energy distribution depicted in Figure 7 (right) for different choices of m_ϕ. As expected, the decay rate is suppressed by m_ϕ has a maximum shifted towards a higher kinetic energy. Moreover, this is the opposite behaviour of the neutrino emitting processes, as will be shown later in Section 5.4. Even though we do not detect either the Majoron or the neutrinos directly, such a big difference in the energy distributions would be of substantial help to experimentally identify what decay mode is taking place.

In Section 4.3 we have only considered the limit $m_\phi \to 0$ of the $0\nu\beta\beta\phi$ decay rate as to obtain its Q-value dependency more easily. Now, we want to use its full analytic form so that we can normalise

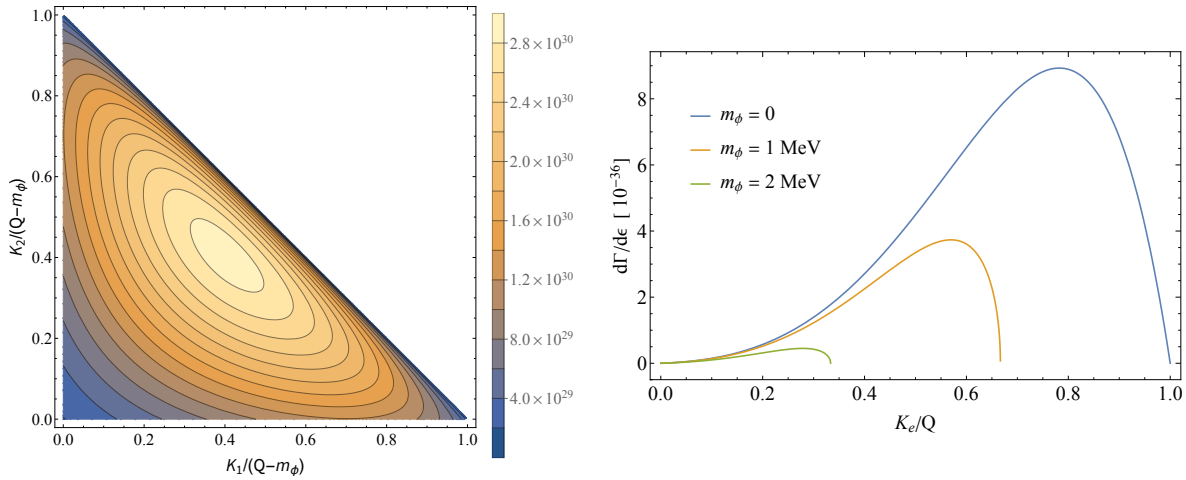

Figure 7: *Left:* $0\nu\beta\beta\phi$ 2-dimensional electron kinetic energy distribution at $Q = 3$ MeV and $m_\phi = 1$ MeV. *Right:* $0\nu\beta\beta\phi$ total electron kinetic energy distribution at $Q = 3$ MeV for 3 values of m_ϕ.

the energy distribution for different values of m_ϕ and have a fair comparison with the standard $2\nu\beta\beta$ distribution. As Eq. (4.62) is quite cumbersome to solve by hand, we rely on Mathematica to integrate.

$$\begin{aligned}\Gamma_{0\nu\beta\beta} \propto &\left[128m_\phi^6 + 1779m_\phi^4Q^2 + 1518m_\phi^2Q^4 + 40Q^6 + 8400m_e^4(2m_\phi^2 + Q^2) + 4200m_e^3(13m_\phi^2Q + 2Q^3)\right.\\ &\left.+560m_e^2(16m_\phi^4 + 83m_\phi^2Q^2 + 6Q^4) + 70m_e(113m_\phi^4Q + 194m_\phi^2Q^3 + 8Q^5)\right]\frac{\sqrt{Q^2-m_\phi^2}}{50400}\\ &+\frac{m_\phi^2}{960}\left[240m_e^4Q + 5m_\phi^4Q + 20m_\phi^2Q^3 + 8Q^5 + 120m_e^3(m_\phi^2 + 4Q^2) + 80m_e^2(3m_\phi^2Q + 4Q^3)\right.\\ &\left.+10m_e(m_\phi^4 + 12m_\phi^2Q^2 + 8Q^4)\right]\left[\log\left(\frac{Q}{\sqrt{Q^2-m_\phi^2}} - 1\right) - \log\left(1 + \frac{Q}{\sqrt{Q^2-m_\phi^2}}\right)\right]\end{aligned} \tag{4.63}$$

Although intimidating, this expression results in the neat downward curve plotted in Figure 8 (left). As for Figure 8 (right), we show a comparison between the normalised energy distribution of $0\nu\beta\beta\phi$ and that of $2\nu\beta\beta$, calculated in Appendix B, for 3 values of m_ϕ. It is evident that the curves will never approach each other as they show very distinct behaviours and the Majoron mass caps the maximum kinetic energy of the electrons.

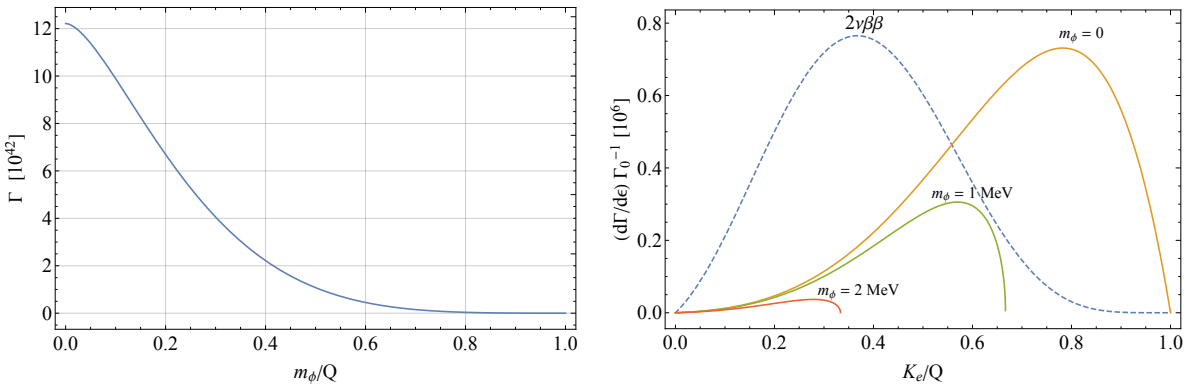

Figure 8: *Left:* $0\nu\beta\beta\phi$ total decay rate as a function of m_ϕ at $Q = 3$ MeV. *Right:* Comparison between normalised $2\nu\beta\beta$ and $0\nu\beta\beta\phi$ total electron kinetic energy distributions at $Q = 3$ MeV for 3 values of m_ϕ.

5 $2\nu_\phi\beta\beta$ with Virtual Scalar ϕ Exchange

In this section we present a very intriguing process which has not yet been thoroughly studied in the literature. Said process is, arguably, the simplest Majoron-induced neutrino-emitting double beta decay. It consists of a standard $2\nu\beta\beta$ decay in which the two emitted neutrinos are actually connected by a virtual scalar Majoron to two virtual neutrinos arising from the W-boson vertices. For this reason, we label it as $2\nu_\phi\beta\beta$.

What is most attractive about this process is that it is composed of two components: The first is what we call the s-channel and will label as $2\nu^s_\phi\beta\beta$. In this process, the Majoron has a vertex which couples with the two virtual neutrinos and another vertex from which the two emitted electrons are produced. Depicted in Figure 9, this is analogous to an s-channel pair annihilation and production and, as we will show, can only occur if neutrinos are Majorana neutrinos. The second is what we call the t+u-channel and will label as $2\nu^{t+u}_\phi\beta\beta$. In this process, the Majoron has one vertex for each pair of virtual and real neutrinos. Depicted in Figures 10 ahd 11 this is analogous to a t+u-channel scattering and can occur regardless of the nature of the neutrinos.

Due to the fundamental difference between $2\nu^s_\phi\beta\beta$ and $2\nu^{t+u}_\phi\beta\beta$, we will deal with each current in a different section. The phase space, on the other hand, depends on the same particles and, in principle, one would have to consider all processes when calculating the decay rate for Majorana neutrinos. We will not be as general.We will only be calculating the full decay rate for $2\nu^s_\phi\beta\beta$, as partly done by [30], and then the decay rate of one of the many terms of the $2\nu^{t+u}_\phi\beta\beta$. We will show how the remaining terms can be promptly obtained from the symmetry properties of the matrix element and are not needed for our qualitative discussion. Lastly, the energy distributions resulting from this analysis are key to understanding how $2\nu_\phi\beta\beta$ compares to $0\nu\beta\beta$ and, most importantly, $2\nu\beta\beta$. We will close this section by showing how and when the energy spectrum of $2\nu_\phi\beta\beta$ is closer to that of $2\nu\beta\beta$.

5.1 s-Channel Leptonic Current

Having calculated the leptonic current for $0\nu\beta\beta\phi$ in Section 4.2, obtaining the leptonic current of $2\nu^s_\phi\beta\beta$, here labeled $J^{\mu\nu}_{2\nu^s_\phi\beta\beta}$, becomes trivial. You may have noticed that the diagrams in Figure 9 are, to some extent, a $0\nu\beta\beta\phi$ in which the emitted Majoron subsequently decays into two neutrinos. Hence, the leptonic current can be acquired by connecting the matrix element $\mathcal{M}_{\phi\bar\nu\bar\nu}$ of the process $\phi \to \bar\nu\bar\nu$ to

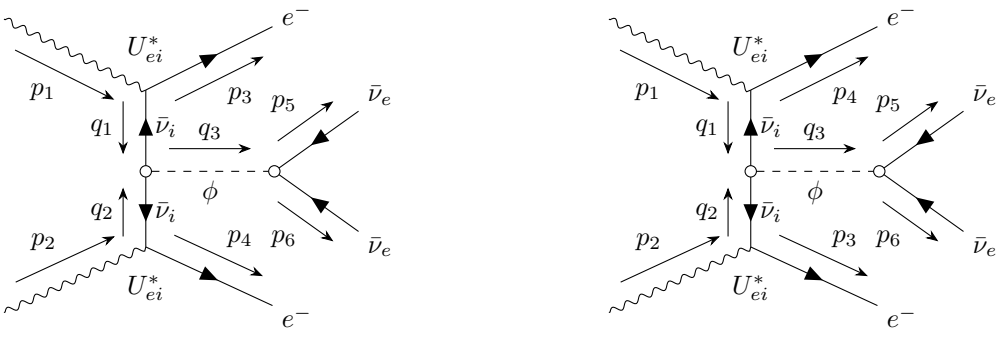

Figure 9: $2\nu^s_\phi\beta\beta$ Feynman diagrams. *Left* s1-channel. *Right* s2-channel.

the leptonic current $J^{\mu\nu}_{0\nu\beta\beta\phi}$, calculated in Section 4.2, via the Majoron propagator, which is simply the propagator of a scalar particle up to a first order correction of $i\Gamma_\phi m_\phi$. The permutation of the electrons is already accounted for in $J_{0\nu\beta\beta}$ and is the only symmetry present since the two neutrinos are coming from the same vertex. Moreover, $J^{\mu\nu}_{2\nu^s_\phi\beta\beta}$ inherits the lepton number violating vertices from $J^{\mu\nu}_{0\nu\beta\beta\phi}$ and cannot occur for Dirac neutrinos. Following the Feynman rules for Majorana particles, we obtain

$$\mathcal{M}^{\mu\nu}_{\phi\bar{\nu}\bar{\nu}} = g_\phi \left[v_{\nu_e}(p_6)\right]_\alpha \left[\hat{C}^{-1}\left(\alpha+\beta\gamma^5\right)\right]_{\alpha\beta} \left[v_{\nu_e}(p_5)\right]_\beta = g_\phi v^T_{\nu_e}(p_6)\hat{C}^{-1}\left(\alpha+\beta\gamma^5\right) v_{\nu_e}(p_5) \tag{5.1}$$

Using the identities in Eq. (3.19), the transposed spinor becomes

$$v^T_{\nu_e}\hat{C}^{-1} = \left(\hat{C}^T v_{\nu_e}\right)^T = -\left(\hat{C} v_{\nu_e}\right)^T = -\left(\bar{u}^T_{\nu_e}\right)^T = -\bar{u}_{\nu_e}$$

which yields

$$\mathcal{M}_{\phi\bar{\nu}\bar{\nu}} = -g_\phi \bar{u}_{\nu_e}(p_6)\left(\alpha+\beta\gamma^5\right) v_{\nu_e}(p_5) \tag{5.2}$$

The resulting leptonic current is, therefore

$$\begin{aligned} J^{\mu\nu}_{2\nu^s_\phi\beta\beta} =& \frac{|g_\phi|^2 g_W^2 (U^*_{ei})^2}{4\left(q_3^2 - m_\phi^2 + i m_\phi \Gamma_\phi\right)} \left[\bar{u}_{\nu_e}(p_6)\left(\alpha+\beta\gamma^5\right) v_{\nu_e}(p_5)\right] \\ &\times \left[\frac{\bar{u}_e(p_3)\gamma^\mu(\mathbb{1}_4-\gamma^5)((\alpha+\beta)\not{q}_1\not{q}_2 + (\beta-\alpha)m^2_{\nu_i})\gamma^\nu v_e(p_4)}{(q_1^2 - m^2_{\nu_i})(q_2^2 - m^2_{\nu_i})}\right. \\ &\left. - \frac{\bar{u}_e(p_3)\gamma^\mu(\mathbb{1}_4-\gamma^5)((\alpha+\beta)\not{q}'_2\not{q}'_1 + (\beta-\alpha)m^2_{\nu_i})\gamma^\nu v_e(p_4)}{({q'_1}^2 - m^2_{\nu_i})({q'_2}^2 - m^2_{\nu_i})}\right] \end{aligned} \tag{5.3}$$

where the Majoron 4-momentum satisfies $q_3 = q_1 - q_2 = q'_1 + q'_2 = p_5 + p_6$. The averaged current squared $\left\langle \left| J_{2\nu^s_\phi\beta\beta} \right| \right\rangle$ follows promptly by multiplying the averaged current squared obtained in Section 4.2 by $\left\langle |\mathcal{M}_{\phi\bar{\nu}\bar{\nu}}|^2 \right\rangle / \left(\left(q_3^2 - m_\phi^2\right)^2 + \Gamma_\phi^2 m_\phi^2\right)$. The latter is obtained by using Casimir's trick on Eq. (5.1), giving

$$\left\langle |\mathcal{M}_{\phi\bar{\nu}\bar{\nu}}|^2 \right\rangle = \frac{|g_\phi|^2}{4} \mathrm{Tr}\left[\left(\alpha+\beta\gamma^5\right)\left(\not{p}_5 - m_{\nu_e}\right)\left(\alpha-\beta\gamma^5\right)\left(\not{p}_6 + m_{\nu_e}\right)\right] \tag{5.4}$$

Expanding the terms within the trace and using $\mathrm{Tr}[\gamma^\mu] = 0$, $\mathrm{Tr}[\gamma^5\gamma^\mu] = 0$ and $\mathrm{Tr}[\gamma^5\gamma^\mu\gamma^\nu] = 0$, only 2 terms remain, resulting in

$$\left\langle |\mathcal{M}_{\phi\bar{\nu}\bar{\nu}}|^2 \right\rangle = \frac{|g_\phi|^2}{4} \mathrm{Tr}\left[\left(\alpha^2+\beta^2\right)\not{p}_5\not{p}_6 - \left(\alpha^2-\beta^2\right)m^2_{\nu_e}\right] = |g_\phi|^2\left[\left(\alpha^2+\beta^2\right)p_5\cdot p_6 - \left(\alpha^2-\beta^2\right)m^2_{\nu_e}\right] \tag{5.5}$$

$\mathcal{M}_{\phi\bar{\nu}\bar{\nu}}$ will be useful again in Section 5.3, where we will have to calculate the decay rate Γ_ϕ explicitly. We will not by as lucky with the phase space calculation for this process as we were with the current since, as we will see, the phase space of $0\nu\beta\beta\phi$ is not adaptable to conform with this process.

5.2 t+u-Channel Leptonic Current

The t+u-channel is a very distinct process to the s-channel. To begin with, no Majorana neutrino is required as there is no antineutrino pair annihilation in the Majoron vertices. In fact, if we replace the

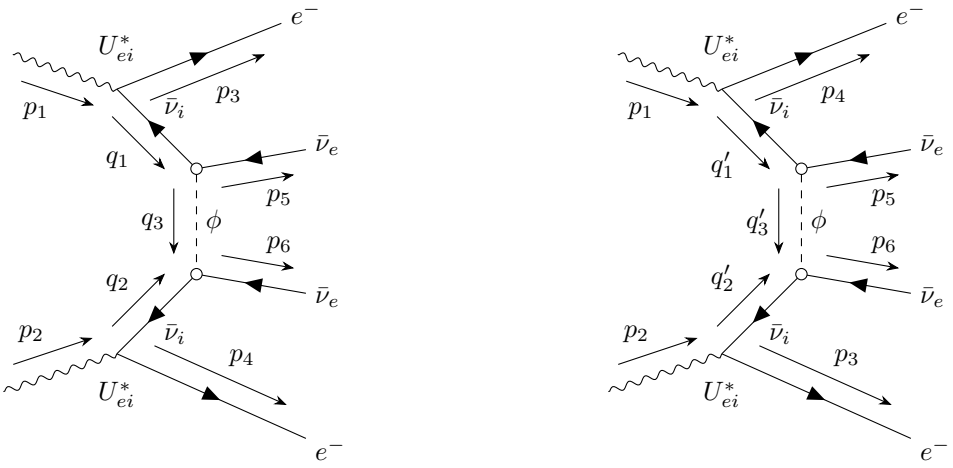

Figure 10: $2\nu^t_\phi\beta\beta$ Feynman diagrams. *Left:* t1-channel with $q_3 = p_1 - p_3 - p_5 = p_6 + p_4 - p_2$. *Right:* t2-channel with $q'_3 = p_1 - p_4 - p_5 = p_6 + p_3 - p_2$.

Majoron by a Z-boson, this becomes an allowed process in the Standard Model. It is not relevant, though, as it is heavily suppressed by the large mass of the Z-boson. In our model the Majoron mass is assumed small enough so that we can have a substantial contribution to $\beta\beta$ decay.

The nomenclatures may become a little confusing as we now have t and u-channels for both the electrons and neutrinos. We will keep the t and u labels for the neutrinos and use 1 and 2 for the electrons to avoid confusion. Also, q'_i always refers to the electron u-channel (2) while q_i refers to the t-channel (1). Lastly, the Majoron momentum will be different in each of the four diagrams, therefore, in addition to the primed notation, we will add a tilde to momenta referring to the neutrino u-channel.

We begin with the t1-channel. The diagram in Figure 10 (left) yields

$$j^{\mu\nu}_{t1} = \frac{|g_\phi|^2 g_W^4 (U^*_{ei})^2}{8(q_1^2 - m^2_{\nu_i})(q_2^2 - m^2_{\nu_i})(q_3^2 - m^2_\phi)} \left[\bar{u}_e(p_3)\gamma^\mu(\mathbb{1}_4 - \gamma^5)(\not{q}_1 + m_{\nu_i})(\alpha + \beta\gamma^5)v_{\nu_e}(p_5)\right] \times \left[\bar{u}_e(p_4)\gamma^\nu(\mathbb{1}_4 - \gamma^5)(\not{q}_2 + m_{\nu_i})(\alpha + \beta\gamma^5)v_{\nu_e}(p_6)\right] \tag{5.6}$$

We neglect the higher order correction $im_\phi\Gamma_\phi$ in the Majoron propagator since it is too small when compared to the internal momentum transfer, as we will show in Section 5.3.2.Using $\{\gamma^\mu, \gamma^5\} = 0$, the terms squeezed between projectors simplify to

$$(\mathbb{1}_4 - \gamma^5)(\not{q}_i + m_{\nu_i})(\alpha + \beta\gamma^5) = (\mathbb{1}_4 - \gamma^5)\left[(\alpha + \beta)\not{q}_i + (\alpha - \beta)m_{\nu_i}\right]$$

Plugging this result back in the current, we obtain a similar result to that of $2\nu^s_\phi\beta\beta$, in which the neutrino mass depends on $(\alpha - \beta)$ while the internal momenta depends on $(\alpha + \beta)$.

$$j^{\mu\nu}_{t1} = \frac{|g_\phi|^2 g_W^4 (U^*_{ei})^2}{8(q_1^2 - m^2_{\nu_i})(q_2^2 - m^2_{\nu_i})(q_3^2 - m^2_\phi)} \left[\bar{u}_e(p_3)(\mathbb{1}_4 + \gamma^5)\gamma^\mu\left[(\alpha + \beta)\not{q}_1 + (\alpha - \beta)m_{\nu_i}\right]v_{\nu_e}(p_5)\right] \times \left[\bar{u}_e(p_4)(\mathbb{1}_4 + \gamma^5)\gamma^\nu\left[(\alpha + \beta)\not{q}_2 + (\alpha - \beta)m_{\nu_i}\right]v_{\nu_e}(p_6)\right] \tag{5.7}$$

Taking advantage of the symmetry when swapping $p_3 \leftrightarrow p_4$, the current for the t2-channel, depicted in

Figure 10 (right), follows immediately

$$j_{t2}^{\mu\nu} = \frac{|g_\phi|^2 g_W^2 (U_{ei}^*)^2}{8(q_1'^2 - m_{\nu_i}^2)(q_2'^2 - m_{\nu_i}^2)(q_3'^2 - m_\phi^2)} \left[\bar{u}_e(p_4)(\mathbb{1}_4 + \gamma^5)\gamma^\mu \left[(\alpha+\beta)\not{q}_1' + (\alpha-\beta)m_{\nu_i}\right] v_{\nu_e}(p_5)\right] \times \left[\bar{u}_e(p_3)(\mathbb{1}_4 + \gamma^5)\gamma^\nu \left[(\alpha+\beta)\not{q}_2' + (\alpha-\beta)m_{\nu_i}\right] v_{\nu_e}(p_6)\right] \tag{5.8}$$

Now, for the averaged current squared, we will make use of the following definition:

$$\Gamma(q_k) = (\alpha+\beta)\not{q}_k + (\alpha-\beta)m_{\nu_i} \tag{5.9}$$

This definition will not be used for anything other than keeping the calculations concise in this section, hence, it is nothing more than a shorthand and has no profound mathematical relevance. Following Casimir's trick, we take the first term in square brackets in Eq. (5.7), multiply it by its dagger (complex conjugate transposed) and then take the trace of the product. This gives

$$\begin{aligned}&\mathrm{Tr}\left[\left(\bar{v}_{\nu_e}(p_5)\Gamma(q_1)\gamma^\rho(\mathbb{1}_4 - \gamma^5)u_e(p_3)\right)\left(\bar{u}_e(p_3)(\mathbb{1}_4 - \gamma^5)\gamma^\mu\Gamma(q_1)v_{\nu_e}(p_5)\right)\right]\\ =&2\mathrm{Tr}\left[\left((\alpha+\beta)\not{q}_1 + (\alpha-\beta)m_{\nu_i}\right)(\mathbb{1}_4+\gamma^5)\gamma^\rho\not{p}_3\gamma^\mu\left((\alpha+\beta)\not{q}_1 + (\alpha-\beta)m_{\nu_i}\right)(\not{p}_5 - m_{\nu_e})\right]\end{aligned}$$

Recalling that the trace of any odd number of γ^μ is zero, we can get rid of 3 terms in the trace, leaving us with

$$2\mathrm{Tr}\left[(\mathbb{1}_4+\gamma^5)\gamma^\rho\not{p}_3\gamma^\mu\left((\alpha+\beta)^2\not{q}_1\not{p}_5\not{q}_1 + (\alpha-\beta)^2 m_{\nu_i}^2\not{p}_5 - 2(\alpha^2-\beta^2)m_{\nu_i}^2\not{q}_1\right)\right]$$

Where we have used the cyclic property of the trace and assumed $m_{\nu_e} \approx m_{\nu_i}$ as these masses are of the same tiny order even though ν_e is not a mass eigenstate. By symmetry, the second term in square brackets has the exact same form, therefore, the first averaged current squared is

$$\begin{aligned}\left\langle|j_{t1}|^2\right\rangle =& \frac{|g_\phi|^4 g_W^4 |U_{ei}|^4}{256(q_1^2 - m_{\nu_i}^2)^2(q_2^2 - m_{\nu_i}^2)^2(q_3^2 - m_\phi^2)^2}\\ &\times \mathrm{Tr}\left[(\mathbb{1}_4+\gamma^5)\gamma^\rho\not{p}_3\gamma^\mu\left((\alpha+\beta)^2\not{q}_1\not{p}_5\not{q}_1 + (\alpha-\beta)^2 m_{\nu_i}^2\not{p}_5 - 2(\alpha^2-\beta^2)m_{\nu_i}^2\not{q}_1\right)\right]\\ &\times \mathrm{Tr}\left[(\mathbb{1}_4+\gamma^5)\gamma^\sigma\not{p}_4\gamma^\nu\left((\alpha+\beta)^2\not{q}_2\not{p}_6\not{q}_2 + (\alpha-\beta)^2 m_{\nu_i}^2\not{p}_6 - 2(\alpha^2-\beta^2)m_{\nu_i}^2\not{q}_2\right)\right]\end{aligned} \tag{5.10}$$

Swapping $p_3 \leftrightarrow p_4$ the second averaged matrix element squared follows

$$\begin{aligned}\left\langle|j_{t2}|^2\right\rangle =& \frac{|g_\phi|^4 g_W^4 |U_{ei}|^4}{256(q_1'^2 - m_{\nu_i}^2)^2(q_2'^2 - m_{\nu_i}^2)^2(q_3'^2 - m_\phi^2)^2}\\ &\times \mathrm{Tr}\left[(\mathbb{1}_4+\gamma^5)\gamma^\rho\not{p}_4\gamma^\mu\left((\alpha+\beta)^2\not{q}_1'\not{p}_5\not{q}_1' + (\alpha-\beta)^2 m_{\nu_i}^2\not{p}_5 - 2(\alpha^2-\beta^2)m_{\nu_i}^2\not{q}_1'\right)\right]\\ &\times \mathrm{Tr}\left[(\mathbb{1}_4+\gamma^5)\gamma^\sigma\not{p}_3\gamma^\nu\left((\alpha+\beta)^2\not{q}_2'\not{p}_6\not{q}_2' + (\alpha-\beta)^2 m_{\nu_i}^2\not{p}_6 - 2(\alpha^2-\beta^2)m_{\nu_i}^2\not{q}_2'\right)\right]\end{aligned} \tag{5.11}$$

We are now left with calculating the crossed term. Arranging the spinor blocks of $j_{t1}^\dagger j_{t2}$ in the correct order we obtain, without further ado, the following trace

$$4\mathrm{Tr}\left[\Gamma(q_1)\gamma^\rho\not{p}_3\underbrace{(\mathbb{1}_4+\gamma^5)\gamma^\nu\Gamma(q_2')(\not{p}_6 - m_{\nu_e})\Gamma(q_2)\gamma^\sigma(\mathbb{1}_4-\gamma^5)}\not{p}_4\gamma^\mu\Gamma(q_1')(\not{p}_5 - m_{\nu_e})\right] \tag{5.12}$$

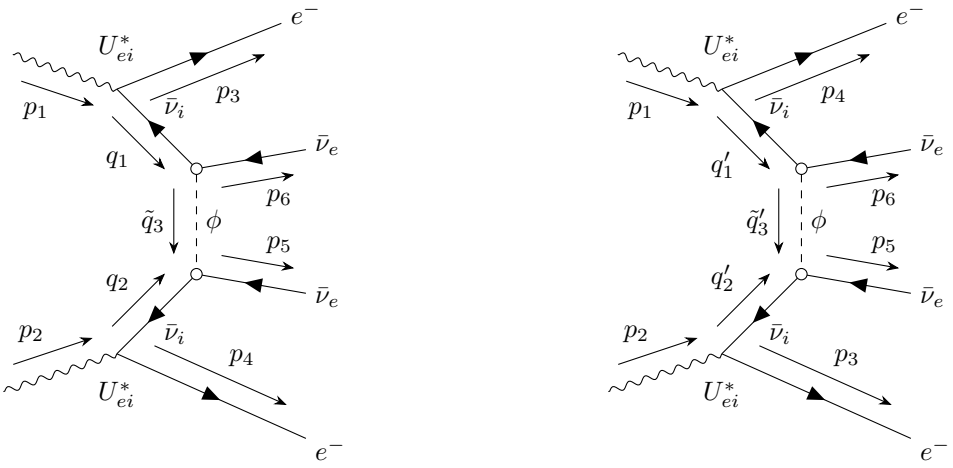

Figure 11: $2\nu^u_\phi\beta\beta$ Feynman diagrams. *Left:* $u1$-channel with $q_3 = p_1 - p_3 - p_6 = p_5 + p_4 - p_2$. *Right:* $u2$-channel with $q'_3 = p_1 - p_4 - p_6 = p_5 + p_3 - p_2$.

The underbraced term can be expanded, as done for $\left\langle |j_{t1}|^2 \right\rangle$, giving

$$\begin{aligned}
&(\mathbb{1}_4 - \gamma^5)\Gamma(q'_2)(\not{p}_6 - m_{\nu_e})\Gamma(q_2)(\mathbb{1}_4 + \gamma^5) \\
=&2(\mathbb{1}_4 - \gamma^5)\left[(\alpha+\beta)^2 \not{q}'_2 \not{p}_6 \not{q}_2 + (\alpha-\beta)^2 m^2_{\nu_i} \not{p}_6 - (\alpha^2-\beta^2) m^2_{\nu_i}(\not{q}_2 + \not{q}'_2)\right]
\end{aligned}$$

Notice that this term contains only odd combinations of γ^μ. Yet, we have another term to expand, namely, $\Gamma(q'_1)(\not{p}_5 - m_{\nu_e})\Gamma(q_1)$. However, since the rest of the terms contain only odd combinations of γ^μ, we can neglect all terms with an even combination of γ^μ, thus

$$\Gamma(q'_1)(\not{p}_5 - m_{\nu_e})\Gamma(q_1) \to (\alpha+\beta)^2 \not{q}'_1 \not{p}_5 \not{q}_1 + (\alpha-\beta)^2 m^2_{\nu_i} \not{p}_5 - (\alpha^2-\beta^2) m^2_{\nu_i}(\not{q}'_1 + \not{q}_1)$$

Plugging these results back into the trace, we obtain the crossed term

$$\begin{aligned}
\left\langle j^\dagger_{t1} j_{t2} \right\rangle =& \frac{|g_\phi|^4 g_W^4 |U_{ei}|^4}{128(q_1^2 - m^2_{\nu_i})(q_2^2 - m^2_{\nu_i})(q_3^2 - m^2_\phi)(q_1'^2 - m^2_{\nu_i})(q_2'^2 - m^2_{\nu_i})(q_3'^2 - m^2_\phi)} \\
&\times \mathrm{Tr}\left[(\mathbb{1}_4 + \gamma^5)\gamma^\rho \not{p}_3 \gamma^\nu \left((\alpha+\beta)^2 \not{q}'_2 \not{p}_6 \not{q}_2 + (\alpha-\beta)^2 m^2_{\nu_i} \not{p}_6 - (\alpha^2-\beta^2) m^2_{\nu_i}(\not{q}_2 + \not{q}'_2)\right)\right. \\
&\left.\gamma^\sigma \not{p}_4 \gamma^\mu \left((\alpha+\beta)^2 \not{q}'_1 \not{p}_5 \not{q}_1 + (\alpha-\beta)^2 m^2_{\nu_i} \not{p}_5 - (\alpha^2-\beta^2) m^2_{\nu_i}(\not{q}'_1 + \not{q}_1)\right)\right]
\end{aligned} \tag{5.13}$$

The u-channel, represented by the diagrams in Figure 11, immediately follows by swapping $p_5 \leftrightarrow p_6$ in the results obtained so far for the t-channel. Even though the internal momenta of the neutrinos are the same as the equivalent t-channel processes, the Majoron internal momentum is different for each diagram. The currents are given by

$$\begin{aligned}
j^{\mu\nu}_{u1} = \frac{|g_\phi|^2 g_W^2 (U^*_{ei})^2}{8(q_1^2 - m^2_{\nu_i})(q_2^2 - m^2_{\nu_i})(\tilde{q}_3^2 - m^2_\phi)} &\left[\bar{u}_e(p_3)(\mathbb{1}_4 + \gamma^5)\gamma^\mu \left[(\alpha+\beta)\not{q}_1 + (\alpha-\beta) m_{\nu_i}\right] v_{\nu_e}(p_6)\right] \\
&\times \left[\bar{u}_e(p_4)(\mathbb{1}_4 + \gamma^5)\gamma^\nu \left[(\alpha+\beta)\not{q}_2 + (\alpha-\beta) m_{\nu_i}\right] v_{\nu_e}(p_5)\right]
\end{aligned} \tag{5.14}$$

$$j_{u2}^{\mu\nu} = \frac{|g_\phi|^2 g_W^2 (U_{ei}^*)^2}{8(q_1'^2 - m_{\nu_i}^2)(q_2'^2 - m_{\nu_i}^2)(\tilde{q}_3'^2 - m_\phi^2)} \left[\bar{u}_e(p_4)(\mathbb{1}_4 + \gamma^5)\gamma^\mu \left[(\alpha+\beta)\not{q}_1' + (\alpha-\beta)m_{\nu_i}\right] v_{\nu_e}(p_6)\right] \times \left[\bar{u}_e(p_3)(\mathbb{1}_4 + \gamma^5)\gamma^\nu \left[(\alpha+\beta)\not{q}_2' + (\alpha-\beta)m_{\nu_i}\right] v_{\nu_e}(p_5)\right] \tag{5.15}$$

The averaged current squared terms are, respectively

$$\begin{aligned}\left\langle |j_{u1}|^2 \right\rangle =& \frac{|g_\phi|^4 g_W^4 |U_{ei}|^4}{256(q_1^2 - m_{\nu_i}^2)^2(q_2^2 - m_{\nu_i}^2)^2(\tilde{q}_3^2 - m_\phi^2)^2} \\ &\times \mathrm{Tr}\left[(\mathbb{1}_4 + \gamma^5)\gamma^\rho \not{p}_3 \gamma^\mu \left((\alpha+\beta)^2 \not{q}_1 \not{p}_6 \not{q}_1 + (\alpha-\beta)^2 m_{\nu_i}^2 \not{p}_6 - 2(\alpha^2-\beta^2)m_{\nu_i}^2 \not{q}_1\right)\right] \\ &\times \mathrm{Tr}\left[(\mathbb{1}_4 + \gamma^5)\gamma^\sigma \not{p}_4 \gamma^\nu \left((\alpha+\beta)^2 \not{q}_2 \not{p}_5 \not{q}_2 + (\alpha-\beta)^2 m_{\nu_i}^2 \not{p}_5 - 2(\alpha^2-\beta^2)m_{\nu_i}^2 \not{q}_2\right)\right]\end{aligned} \tag{5.16}$$

$$\begin{aligned}\left\langle |j_{u2}|^2 \right\rangle =& \frac{|g_\phi|^4 g_W^4 |U_{ei}|^4}{256(q_1'^2 - m_{\nu_i}^2)^2(q_2'^2 - m_{\nu_i}^2)^2(\tilde{q}_3'^2 - m_\phi^2)^2} \\ &\times \mathrm{Tr}\left[(\mathbb{1}_4 + \gamma^5)\gamma^\rho \not{p}_4 \gamma^\mu \left((\alpha+\beta)^2 \not{q}_1' \not{p}_6 \not{q}_1' + (\alpha-\beta)^2 m_{\nu_i}^2 \not{p}_6 - 2(\alpha^2-\beta^2)m_{\nu_i}^2 \not{q}_1'\right)\right] \\ &\times \mathrm{Tr}\left[(\mathbb{1}_4 + \gamma^5)\gamma^\sigma \not{p}_3 \gamma^\nu \left((\alpha+\beta)^2 \not{q}_2' \not{p}_5 \not{q}_2' + (\alpha-\beta)^2 m_{\nu_i}^2 \not{p}_5 - 2(\alpha^2-\beta^2)m_{\nu_i}^2 \not{q}_2'\right)\right]\end{aligned} \tag{5.17}$$

$$\begin{aligned}\left\langle j_{u1}^\dagger j_{u2} \right\rangle =& \frac{|g_\phi|^4 g_W^4 |U_{ei}|^4}{128(q_1^2 - m_{\nu_i}^2)(q_2^2 - m_{\nu_i}^2)(\tilde{q}_3^2 - m_\phi^2)(q_1'^2 - m_{\nu_i}^2)(q_2'^2 - m_{\nu_i}^2)(\tilde{q}_3'^2 - m_\phi^2)} \\ &\times \mathrm{Tr}\Big[(\mathbb{1}_4 + \gamma^5)\gamma^\rho \not{p}_3 \gamma^\nu \left((\alpha+\beta)^2 \not{q}_2' \not{p}_5 \not{q}_2 + (\alpha-\beta)^2 m_{\nu_i}^2 \not{p}_5 - (\alpha^2-\beta^2)m_{\nu_i}^2 (\not{q}_2 + \not{q}_2')\right) \\ &\gamma^\sigma \not{p}_4 \gamma^\mu \left((\alpha+\beta)^2 \not{q}_1' \not{p}_6 \not{q}_1 + (\alpha-\beta)^2 m_{\nu_i}^2 \not{p}_6 - (\alpha^2-\beta^2)m_{\nu_i}^2 (\not{q}_1' + \not{q}_1)\right)\Big]\end{aligned} \tag{5.18}$$

which are perfectly symmetric to those of the t-channel.

The u-channel results came for free from the t-channel calculations, but now we are left with yet more crossed terms to calculate: We must also consider the crossed terms between each t-channel and u-channel. These are much simpler to calculate once we have understood how the t-channel calculations were done, but we still cannot simply swap momenta as there were some cancellations in the non-crossed terms that will not be present now. Let us start by considering $\left\langle j_{t1}^\dagger j_{u1} \right\rangle$. Arranging the spinor blocks in the correct order, we obtain the trace

$$4\mathrm{Tr}\left[\Gamma(q_1)\gamma^\rho \not{p}_3 (\mathbb{1}_4 + \gamma^5)\gamma^\mu \Gamma(q_1)(\not{p}_6 - m_{\nu_e})\Gamma(q_2)\gamma^\sigma(\mathbb{1}_4 - \gamma^5)\not{p}_4 \gamma^\nu \Gamma(q_2)(\not{p}_5 - m_{\nu_e})\right]$$

If we compare it to the trace obtained in Eq. (5.13), we see that they are both the same if we swap $q_2' \to q_1, q_1' \to q_2$ and $\mu \leftrightarrow \nu$. Doing so, we obtain

$$\begin{aligned}\left\langle j_{t1}^\dagger j_{u1} \right\rangle =& \frac{|g_\phi|^4 g_W^4 |U_{ei}|^4}{128(q_1^2 - m_{\nu_i}^2)^2(q_2^2 - m_{\nu_i}^2)^2(q_3^2 - m_\phi^2)(\tilde{q}_3^2 - m_\phi^2)} \\ &\times \mathrm{Tr}\Big[(\mathbb{1}_4 + \gamma^5)\gamma^\rho \not{p}_3 \gamma^\mu \left((\alpha+\beta)^2 \not{q}_1 \not{p}_6 \not{q}_2 + (\alpha-\beta)^2 m_{\nu_i}^2 \not{p}_6 - (\alpha^2-\beta^2)m_{\nu_i}^2 (\not{q}_2 + \not{q}_1)\right) \\ &\gamma^\sigma \not{p}_4 \gamma^\nu \left((\alpha+\beta)^2 \not{q}_2 \not{p}_5 \not{q}_1 + (\alpha-\beta)^2 m_{\nu_i}^2 \not{p}_5 - (\alpha^2-\beta^2)m_{\nu_i}^2 (\not{q}_2 + \not{q}_1)\right)\Big]\end{aligned} \tag{5.19}$$

The $\left\langle j_{t2}^{\dagger} j_{u2} \right\rangle$ term follows identically by swapping $p_3 \leftrightarrow p_4$, $q_1 \to q_1'$ and $q_2 \to q_2'$, thus,

$$\begin{aligned}\left\langle j_{t2}^{\dagger} j_{u2} \right\rangle =& \frac{|g_\phi|^4 g_W^4 |U_{ei}|^4}{128(q_1'^2 - m_{\nu_i}^2)^2(q_2'^2 - m_{\nu_i}^2)^2(q_3'^2 - m_\phi^2)(\tilde{q}_3'^2 - m_\phi^2)} \\ & \times \mathrm{Tr}\left[(\mathbb{1}_4 + \gamma^5)\gamma^\rho \not{p}_4 \gamma^\mu \left((\alpha+\beta)^2 \not{q}_1' \not{p}_6 \not{q}_2' + (\alpha-\beta)^2 m_{\nu_i}^2 \not{p}_6 - (\alpha^2-\beta^2) m_{\nu_i}^2 (\not{q}_2' + \not{q}_1')\right)\right. \\ & \left. \gamma^\sigma \not{p}_3 \gamma^\nu \left((\alpha+\beta)^2 \not{q}_2' \not{p}_5 \not{q}_1' + (\alpha-\beta)^2 m_{\nu_i}^2 \not{p}_5 - (\alpha^2-\beta^2) m_{\nu_i}^2 (\not{q}_2' + \not{q}_1')\right)\right]\end{aligned} \tag{5.20}$$

As for the remaining terms, they follow a similar calculation to that of Eq. (5.10). Starting by $\left\langle j_{t1}^{\dagger} j_{u2} \right\rangle$, we have the two traces

$$4\mathrm{Tr}\left[\Gamma(\not{q}_1)(\mathbb{1}_4 + \gamma^5)\gamma^\rho \not{p}_3 \gamma^\nu \Gamma(\not{q}_2')(\not{p}_5 - m_{\nu_e})\right] \mathrm{Tr}\left[\Gamma(\not{q}_2)(\mathbb{1}_4 + \gamma^5)\gamma^\sigma \not{p}_4 \gamma^\mu \Gamma(\not{q}_1')(\not{p}_6 - m_{\nu_e})\right]$$

The only differences from that of Eq. (5.10) are having two distinct internal momenta in each trace and swapping $\mu \leftrightarrow \nu$, therefore

$$\begin{aligned}\left\langle j_{t1}^{\dagger} j_{u2} \right\rangle =& \frac{|g_\phi|^4 g_W^4 |U_{ei}|^4}{256(q_1^2 - m_{\nu_i}^2)(q_2^2 - m_{\nu_i}^2)(q_3^2 - m_\phi^2)(q_1'^2 - m_{\nu_i}^2)(q_2'^2 - m_{\nu_i}^2)(\tilde{q}_3'^2 - m_\phi^2)} \\ & \times \mathrm{Tr}\left[(\mathbb{1}_4 + \gamma^5)\gamma^\rho \not{p}_3 \gamma^\nu \left((\alpha+\beta)^2 \not{q}_2' \not{p}_5 \not{q}_1 + (\alpha-\beta)^2 m_{\nu_i}^2 \not{p}_5 - (\alpha^2-\beta^2) m_{\nu_i}^2 (\not{q}_1 + \not{q}_2')\right)\right] \\ & \times \mathrm{Tr}\left[(\mathbb{1}_4 + \gamma^5)\gamma^\sigma \not{p}_4 \gamma^\mu \left((\alpha+\beta)^2 \not{q}_1' \not{p}_6 \not{q}_2 + (\alpha-\beta)^2 m_{\nu_i}^2 \not{p}_6 - (\alpha^2-\beta^2) m_{\nu_i}^2 (\not{q}_2 + \not{q}_1')\right)\right]\end{aligned} \tag{5.21}$$

By swapping $p_3 \leftrightarrow p_4$, $q_1 \leftrightarrow q_2'$ and $q_2 \leftrightarrow q_1'$, we obtain the last term

$$\begin{aligned}\left\langle j_{t2}^{\dagger} j_{u1} \right\rangle =& \frac{|g_\phi|^4 g_W^4 |U_{ei}|^4}{256(q_1'^2 - m_{\nu_i}^2)(q_2'^2 - m_{\nu_i}^2)(q_3'^2 - m_\phi^2)(q_1^2 - m_{\nu_i}^2)(q_2^2 - m_{\nu_i}^2)(\tilde{q}_3^2 - m_\phi^2)} \\ & \times \mathrm{Tr}\left[(\mathbb{1}_4 + \gamma^5)\gamma^\sigma \not{p}_3 \gamma^\mu \left((\alpha+\beta)^2 \not{q}_1 \not{p}_6 \not{q}_2' + (\alpha-\beta)^2 m_{\nu_i}^2 \not{p}_6 - (\alpha^2-\beta^2) m_{\nu_i}^2 (\not{q}_1 + \not{q}_2')\right)\right] \\ & \times \mathrm{Tr}\left[(\mathbb{1}_4 + \gamma^5)\gamma^\rho \not{p}_4 \gamma^\nu \left((\alpha+\beta)^2 \not{q}_2 \not{p}_5 \not{q}_1' + (\alpha-\beta)^2 m_{\nu_i}^2 \not{p}_5 - (\alpha^2-\beta^2) m_{\nu_i}^2 (\not{q}_2 + \not{q}_1')\right)\right]\end{aligned} \tag{5.22}$$

The full leptonic current is then defined by

$$J_{(t+u)}^{\mu\nu} = j_{(t1)}^{\mu\nu} - j_{(t2)}^{\mu\nu} - j_{(u1)}^{\mu\nu} + j_{(u2)}^{\mu\nu} \tag{5.23}$$

where we have taken into account the relative minus sign gained by swapping two fermions. The averaged leptonic current squared is

$$\begin{aligned}\left\langle |J_{(t+u)}|^2 \right\rangle =& \left\langle |j_{t1}|^2 \right\rangle + \left\langle |j_{t2}|^2 \right\rangle + \left\langle |j_{u1}|^2 \right\rangle + \left\langle |j_{u2}|^2 \right\rangle - 2\mathrm{Re}\left[j_{t1}^{\dagger} j_{t2}\right] - 2\mathrm{Re}\left[j_{u1}^{\dagger} j_{u2}\right] \\ & - 2\mathrm{Re}\left[j_{t1}^{\dagger} j_{u1}\right] + 2\mathrm{Re}\left[j_{t1}^{\dagger} j_{u2}\right] + 2\mathrm{Re}\left[j_{t2}^{\dagger} j_{u1}\right] - 2\mathrm{Re}\left[j_{t2}^{\dagger} j_{u2}\right]\end{aligned} \tag{5.24}$$

You might be wondering why we have not considered the crossed terms involving the s-channel. As we have mentioned before, the s-channel is only possible for Majorana neutrinos while the t+u-channel is possible in any case. Therefore, we choose to keep the processes independent.

5.3 Phase Space and Decay Rates

All calculations so far have assumed the most general coupling between the neutrinos and the Majoron given in Eq. (4.21). In practice, the terms containing the neutrino mass have an insignificant contribution that can be neglected when other terms are considered. Of course, this is not the case if $\alpha + \beta = 0$ and only terms containing the neutrino mass would survive. Nonetheless, we will neglect the neutrino mass. The exotic $\beta\beta$ modes are suppressed by α, β and m_ν, hence they are very small unless α and β are very large.

5.3.1 s-Channel

We shall begin the calculation by the s-channel. The decay rate is given, again, by [30] and reads

$$\begin{aligned}\Gamma^s_{2\nu_\phi\beta\beta} \approx & \frac{1}{2M}\left|\mathcal{M}_{0\nu\beta\beta\phi}\right|^2 \int \frac{d^3\vec{P}}{2(2\pi)^3 M}\frac{d^3\vec{p}_{e_1}}{2(2\pi)^3\epsilon_{e_1}}\frac{d^3\vec{p}_{e_2}}{2(2\pi)^3\epsilon_{e_2}}\frac{d^3\vec{p}_{\nu_1}}{2(2\pi)^3\epsilon_{\nu_1}}\frac{d^3\vec{p}_{\nu_2}}{2(2\pi)^3\epsilon_{\nu_2}}(p_{e_1}\cdot p_{e_2}) \\ & \times \frac{\left|\mathcal{M}_{\phi\bar{\nu}\bar{\nu}}\right|^2}{\left(\left(p_{\nu_1}+p_{\nu_2}\right)^2 - m_\phi^2\right)^2 + m_\phi^2\Gamma_\phi^2}(2\pi)^4\delta^{(4)}(P - p_{e_1} - p_{e_2} + p_{\nu_1} + p_{\nu_2} - \tilde{P})a(\epsilon_{e_1},\epsilon_{e_2})\end{aligned} \tag{5.25}$$

In this expression, we have two nuclear matrix elements. This comes from the decomposition of $2\nu^s_\phi\beta\beta$ decay as a $0\nu\beta\beta\phi$ decay followed by a $\phi \to \bar{\nu}\bar{\nu}$ decay we have done in Section 5.1. Here, $\mathcal{M}_{0\nu\beta\beta\phi}$ carries the nuclear part of the decay while the leptonic part is carried by $\mathcal{M}_{\phi\bar{\nu}\bar{\nu}}$, the Majoron propagator and $(p_{e_1}\cdot_{e_2})$. This separation between leptonic and nuclear parts is made possible, again, by doing a Fierz Transformation. Moreover, the decay rate Γ_ϕ of the Majoron appears explicitly. It is calculated via the decay rate formula for a two body decay in the centre-of-mass reference frame, as given in [36]. To do so, we use the averaged matrix element squared $\langle|\mathcal{M}_{\phi\bar{\nu}\bar{\nu}}|\rangle$ obtained in Eq. (5.5), since the Majoron is assumed to couple only to neutrinos. This results in

$$\Gamma_\phi = \frac{|\vec{p}_{\nu_1}|}{32\pi^2 m_\phi^2}\int |g_\phi|^2\left[\left(\alpha^2+\beta^2\right)p_{\nu_1}\cdot p_{\nu_2} - \left(\alpha^2-\beta^2\right)m^2_{\nu_e}\right]d\Omega \tag{5.26}$$

where Ω is the solid angle of the scattering. By using 4-momentum conservation, $\vec{p}_{\nu_1}\cdot\vec{p}_{\nu_2} = -|\vec{p}_{\nu_1}|^2$, $m_\phi = 2\epsilon_{\nu_1}$ and $|\vec{p}_{\nu_1}| = \sqrt{\frac{m_\phi^2 - 4m^2_{\nu_e}}{4}}$, thus

$$\begin{aligned}\Gamma_\phi =& \frac{|g_\phi|^2}{16\pi m_\phi^2}\sqrt{\frac{m_\phi^2-4m^2_{\nu_e}}{4}}\left[\left(\alpha^2+\beta^2\right)\left(m_\phi^2 - 2m^2_{\nu_e}\right) - 2\left(\alpha^2-\beta^2\right)m^2_{\nu_e}\right] \\ =& \frac{|g_\phi|^2}{32\pi m_\phi^2}\sqrt{m_\phi^2-4m^2_{\nu_e}}\left[\left(\alpha^2+\beta^2\right)m_\phi^2 - 4\alpha^2 m^2_{\nu_e}\right]\end{aligned} \tag{5.27}$$

and, taking the limit $m_\phi >> m_\nu$

$$\Gamma_\phi \approx \frac{|g_\phi|^2 m_\phi}{32\pi}\left(\alpha^2+\beta^2\right) \tag{5.28}$$

Now, back to $\Gamma^s_{2\nu_\phi\beta\beta}$, we will need to do a few changes of variables. We integrate Eq. (5.25) over $\vec{P}$ and use Eq. (4.48) again for all coordinates. Integrating over the solid angle of the two electrons adds a factor of $(4\pi)^2$. The solid angle of the neutrinos can be written in spherical coordinates under the assumption that both neutrinos are in the same place. This yields two free azymuthal angles, one free polar angle

and the angle between the two neutrinos, which we call θ. Integrating over the azimuthal angle of each neutrino and the free polar angle adds a factor of $2(2\pi)^2$. The only remaining angle, upon which the denominator depends, is the angle θ between the two neutrinos. We are now left with

$$\begin{aligned}\Gamma^s_{2\nu_\phi\beta\beta} \approx & |g_\phi|^2 \frac{\left|\mathcal{M}_{0\nu\beta\beta\phi}\right|^2}{8(2\pi)^7 M^2} \int |\vec{p}_{e_1}|\epsilon_{e_1} d\epsilon_{e_1} |\vec{p}_{e_2}|\epsilon_{e_2} d\epsilon_{e_2} a(\epsilon_{e_1},\epsilon_{e_2}) \delta(Q+2m_e-\epsilon_{e_1}-\epsilon_{e_2}-\epsilon_{\nu_1}-\epsilon_{\nu_2}) \\ & \times \frac{\left[\left(\alpha^2+\beta^2\right)\left(\epsilon_{\nu_1}\epsilon_{\nu_2}-|\vec{p}_{\nu_1}||\vec{p}_{\nu_2}|\cos\theta\right)-\left(\alpha^2-\beta^2\right)m^2_{\nu_e}\right]}{\left(2m^2_{\nu_e}+2\epsilon_{\nu_1}\epsilon_{\nu_2}-2|\vec{p}_{\nu_1}||\vec{p}_{\nu_2}|\cos\theta-m^2_\phi\right)^2+m^2_\phi\Gamma^2_\phi} |\vec{p}_{\nu_1}| d\epsilon_{\nu_1} |\vec{p}_{\nu_2}| d\epsilon_{\nu_2} d\cos\theta\end{aligned} \tag{5.29}$$

We can not go any further without changing variables. Since we do not actually observe the two neutrinos, but the sum of their energies as a total missing energy, we can write each neutrino's energy as a projection of this total missing energy ϵ,

$$\epsilon_{\nu_1} = \epsilon\sin^2\xi,\ \ \epsilon_{\nu_2} = \epsilon\cos^2\xi \quad \Rightarrow \quad \epsilon_{\nu_1}+\epsilon_{\nu_2}=\epsilon,\ \ \epsilon_{\nu_1}\epsilon_{\nu_2} = \epsilon^2\sin^2\xi\cos^2\xi = \frac{\epsilon^2\sin^2(2\xi)}{4} \tag{5.30}$$

The Jacobian determinant for such a transformation is given by

$$d\epsilon_{\nu_1} d\epsilon_{\nu_2} = \epsilon\sin(2\xi) d\epsilon d\xi \tag{5.31}$$

It is important to note, however, that since both energies are always positive, we must limit the angle ξ to $0 \le \xi \le \frac{\pi}{2}$, otherwise we would be counting the same value twice and the coordinate change would not be bijective. Also, we finally assume $m_{\nu_e} \approx 0$ and the decay rate becomes

$$\begin{aligned}\Gamma^s_{2\nu_\phi\beta\beta} \approx & |g_\phi|^2 \frac{\left|\mathcal{M}_{0\nu\beta\beta\phi}\right|^2}{8(2\pi)^7 M^2} \int |\vec{p}_{e_1}|\epsilon_{e_1} d\epsilon_{e_1} |\vec{p}_{e_2}|\epsilon_{e_2} d\epsilon_{e_2} a(\epsilon_{e_1},\epsilon_{e_2}) \delta(Q+2m_e-\epsilon_{e_1}-\epsilon_{e_2}-\epsilon) \\ & \times \frac{\left(\alpha^2+\beta^2\right)\frac{\sin^2(2\xi)-\sin^2(2\xi)\cos\theta}{2}}{\left(\frac{\epsilon^2}{m^2_\phi}\frac{\sin^2(2\xi)-\sin^2(2\xi)\cos\theta}{2}-1\right)^2+\frac{\Gamma^2_\phi}{m^2_\phi}} \frac{\epsilon^5\sin^3(2\xi)}{8m^4_\phi} d\cos\theta d\epsilon d\xi\end{aligned} \tag{5.32}$$

We are getting closer to the final result, but there is one more change of variables we have to do to get this integral in a suitable form. We define new variables x and y such that

$$\begin{aligned} 1-x^2 &= \frac{\sin^2(2\xi)-\sin^2(2\xi)\cos\theta}{2} \\ 1-y^2 &= \frac{\sin^2(2\xi)+\sin^2(2\xi)\cos\theta}{2} \end{aligned} \Rightarrow \begin{cases} x = \sqrt{1-\sin^2(2\xi)\sin^2(\theta/2)} \\ y = \sqrt{1-\sin^2(2\xi)\cos^2(\theta/2)} \end{cases} \tag{5.33}$$

Inverting the expressions to isolate ξ and θ, we obtain

$$\xi = \frac{\arcsin\sqrt{2-x^2-y^2}}{2}, \quad \theta = 2\arcsin\sqrt{\frac{1-x^2}{2-x^2-y^2}} = 2\arccos\sqrt{\frac{1-y^2}{2-x^2-y^2}}$$

and the Jacobian determinant for this transformation is given by

$$|\mathbf{J}|(x,y) = \frac{xy}{\sqrt{1-x^2}\sqrt{1-y^2}\sqrt{x^2+y^2-2}\sqrt{1-x^2-y^2}}$$

Combining all this information, we can write

$$\begin{aligned}\sin^3(2\xi)d\cos\theta d\xi &= -\frac{xy(2-x^2+y^2)^{\frac{3}{2}}\sin\left(2\arcsin\sqrt{\frac{1-x^2}{2-x^2+y^2}}\right)}{\sqrt{1-x^2}\sqrt{1-y^2}\sqrt{x^2+y^2-2}\sqrt{1-x^2-y^2}}dxdy \\ &= -\frac{2xy(2-x^2+y^2)^{\frac{3}{2}}\sqrt{\frac{1-x^2}{2-x^2+y^2}}\sqrt{\frac{1-y^2}{2-x^2+y^2}}}{\sqrt{1-x^2}\sqrt{1-y^2}\sqrt{x^2+y^2-2}\sqrt{1-x^2-y^2}}dxdy \\ &= -\frac{2ixy}{\sqrt{1-x^2-y^2}}dxdy\end{aligned}$$

The only dependency of the decay rate in y is in the expression we have just obtained. Therefore, we can integrate it and get rid of the y variable. Our definition of the coordinates gives $1 \leq x^2+y^2 \leq 2$, which implies $\sqrt{1-x^2} \leq y \leq \sqrt{2-x^2}$, hence

$$\int_{\sqrt{1-x^2}}^{\sqrt{2-x^2}} \frac{2ixy}{\sqrt{1-x^2-y^2}}dy = -2ix\left(\sqrt{1-x^2-\sqrt{2-x^2}^2}-\sqrt{1-x^2-\sqrt{1-x^2}^2}\right) = -2ix\sqrt{-1} = 2x$$

The resulting decay rate is

$$\begin{aligned}\Gamma^s_{2\nu_\phi\beta\beta} \approx & |g_\phi|^2 \frac{|\mathcal{M}_{0\nu\beta\beta\phi}|^2}{32(2\pi)^7 M^2}\int_0^{Q+2m_e-\epsilon_{e_1}-\epsilon_{e_2}} |\vec{p}_{e_1}|\epsilon_{e_1}d\epsilon_{e_1}|\vec{p}_{e_2}|\epsilon_{e_2}d\epsilon_{e_2}a(\epsilon_{e_1},\epsilon_{e_2})\delta(Q+2m_e-\epsilon_{e_1}-\epsilon_{e_2}-\epsilon) \\ & \times \frac{\epsilon^5}{m_\phi^4}\int_0^1 \frac{\left(\alpha^2+\beta^2\right)x\left(1-x^2\right)}{\left(\frac{\epsilon^2}{m_\phi^2}\left(1-x^2\right)-1\right)^2+\frac{\Gamma_\phi^2}{m_\phi^2}}dxd\epsilon \end{aligned} \tag{5.34}$$

There is, however, an important remark we have to make: If we consider both emitted neutrinos to be identical particles, we must not integrate $\cos\theta$ from -1 to 1 as there is an extra symmetry in the exchange of one neutrino with the other. In this case, our integration limits would be -1 and 0. As per the definition of our change of variables, limiting θ to $\frac{\pi}{2}$ results in setting the upper limit for x to 1/2, hence, integrating it from 0 to $\frac{1}{2}$. Nonetheless, We will continue with the calculation without limiting θ. The integral in x is rather complicated, but we can approximate it by expanding the integrand in $\frac{\epsilon}{m_\phi}$. This can only be done if $\epsilon << m_\phi$, which is not always true. This is an arbitrary decision we are making for the sake of simplicity since, for now, we are only interested in the Q-value dependency of this process. In fact, we will be revisiting this calculation later in Section 5.4 where we will integrate it analytically to obtain the energy distributions. The expansion yields, up to first order

$$\int_0^1 \frac{x\left(1-x^2\right)}{\left(\frac{\epsilon^2}{m_\phi^2}\left(1-x^2\right)-1\right)^2+\frac{\Gamma_\phi^2}{m_\phi^2}}dx \approx \int_0^1 \frac{x-x^3}{\frac{\Gamma_\phi^2}{m_\phi^2}+1}dx + \mathcal{O}\left(\frac{\epsilon^2}{m_\phi^2}\right) = \frac{1}{4\left(\frac{\Gamma_\phi^2}{m_\phi^2}+1\right)} + \mathcal{O}\left(\frac{\epsilon^2}{m_\phi^2}\right)$$

By considering, without any loss of generality, $\Gamma_\phi << m_\phi$, dropping higher order terms of the expansion, and integrating over ϵ, the decay rate results in

$$\Gamma^s_{2\nu_\phi\beta\beta} \approx \frac{\left(\alpha^2+\beta^2\right)|g_\phi|^2}{128(2\pi)^7 M^2}|\mathcal{M}_{0\nu\beta\beta\phi}|^2 \int |\vec{p}_{e_1}|\epsilon_{e_1}|\vec{p}_{e_2}|\epsilon_{e_2}a(\epsilon_{e_1},\epsilon_{e_2})\frac{(Q+2m_e-\epsilon_{e_1}-\epsilon_{e_2})^5}{m_\phi^4}d\epsilon_{e_1}d\epsilon_{e_2} \tag{5.35}$$

The last thing we will be doing now is the integral over the two electrons. As done previously, we take the non-relativistic and the Primakoff-Rosen approximations in Eq. (4.53) and Eq. (4.54). Also, we use

Eq. (5.28) to absorb some prefactors into Γ_ϕ. This yields

$$\Gamma^s_{2\nu_\phi\beta\beta} = \frac{\Gamma_\phi}{8(2\pi)^4 M^2 m_\phi^5}\left(\frac{|\mathcal{M}_{0\nu\beta\beta\phi}|}{1-e^{-2\pi\alpha Z}}\right)^2 \int_{m_e}^{Q+m_e}\int_{m_e}^{Q+2m_e-\epsilon_2} \epsilon_{e_1}^2\epsilon_{e_2}^2(Q+2m_e-\epsilon_{e_1}-\epsilon_{e_2})^5 d\epsilon_{e_1}d\epsilon_{e_2} \quad (5.36)$$

The integrals evaluate as

$$\begin{aligned}
&\int_{m_e}^{Q+m_e}\int_{m_e}^{Q+2m_e-\epsilon_2} \epsilon_{e_1}^2\epsilon_{e_2}^2(Q+2m_e-\epsilon_{e_1}-\epsilon_{e_2})^5 d\epsilon_{e_1}d\epsilon_{e_2} \\
&= \int_{m_e}^{Q+m_e} \frac{\epsilon_{e_2}^2}{168}(Q+m_e-\epsilon_{e_2})^6(Q^2+10Qm_e+37m_e^2-2Q\epsilon_{e_2}-10m_e\epsilon_{e_2}+\epsilon_{e_2}^2)d\epsilon_2 \\
&= \frac{Q^{11}+22Q^{10}m_e+220Q^9m_e^2+990Q^8m_e^3+1980Q^7m_e^4}{83160}
\end{aligned}$$

giving our final result

$$\Gamma^s_{2\nu_\phi\beta\beta} \approx \frac{\Gamma^\phi}{(2\pi)^4 M^2 m_\phi^5}\left(\frac{|\mathcal{M}_{0\nu\beta\beta\phi}|}{1-e^{-2\pi\alpha Z}}\right)^2 \frac{Q^{11}+22Q^{10}m_e+220Q^9m_e^2+990Q^8m_e^3+1980Q^7m_e^4}{83160} \quad (5.37)$$

The Q-value dependency is to the 11^{th} power, 4 powers larger than that of $0\nu\beta\beta\phi$. We will now show that the t+u-channel also scales as Q^{11}, as one would naturally expect.

5.3.2 t+u-Channel

The t+u-channel phase space has a few additional layers of complexity. To begin with, we do not have a matrix element which is composed of a neutrinoless decay plus the Majoron decaying to the neutrinos. Instead, we have something closer to the standard double beta decay, with the neutrinos and electrons coupled in the same vertex. Also, we have different terms which couples both electrons and neutrinos differently among each other. With that in mind, we will not be calculating the phase space for the total matrix element squared, but rather only for the $t1$-channel depicted in Figure 10 (left) and obtained in Eq. (5.10). The remaining channels are permutations and, after calculating the former, the rest would follow trivially by swapping 4-momenta. Moreover, we do not have a clear predefined decomposition of the matrix element as we have in the s-channel. we can define

$$|\mathcal{M}^{t1}_{2\nu_\phi\beta\beta}|^2 = \frac{|\mathcal{M}^{t1}_{0\nu_\phi\beta\beta}|^2}{(q_\phi^2-m_\phi^2)^2}(p_{e_1}\cdot p_{\nu_1})(p_{e_2}\cdot p_{\nu_2}) \quad (5.38)$$

where the term $\mathcal{M}^{t1}_{0\nu_\phi\beta\beta}$ is obtained by separating the nuclear from the leptonic part of $\mathcal{M}^{t1}_{2\nu\beta\beta}$ via a Fierz transformation. Thus, $\mathcal{M}^{t1}_{0\nu_\phi\beta\beta}$ contains only the nuclear part of the process while the leptonic part is carried by $(p_{e_1}\cdot p_{\nu_1})(p_{e_2}\cdot p_{\nu_2})/(q_\phi^2-m_\phi^2)^2$. We have then the decay rate for the $t1$-channel given by

$$\begin{aligned}
\Gamma^{t1}_{2\nu_\phi\beta\beta} \approx &\frac{|g_\phi|^2}{64(2\pi)^{11}M^2}\left|\mathcal{M}^{t1}_{0\nu_\phi\beta\beta}\right|^2 \int \frac{d^3\vec{p}_{e_1}}{\epsilon_{e_1}}\frac{d^3\vec{p}_{e_2}}{\epsilon_{e_2}}\frac{d^3\vec{p}_{\nu_1}}{\epsilon_{\nu_1}}\frac{d^3\vec{p}_{\nu_2}}{\epsilon_{\nu_2}} a(\epsilon_{e_1},\epsilon_{e_2}) \\
&\times \frac{(p_{e_1}\cdot p_{\nu_1})(p_{e_2}\cdot p_{\nu_2})}{\left((p_1-p_{e_1}-p_{\nu_1})^2-m_\phi^2\right)^2}\delta(Q+2m_e-\epsilon_{e_1}-\epsilon_{e_2}-\epsilon_{\nu_1}-\epsilon_{\nu_2})
\end{aligned} \quad (5.39)$$

We immediately notice that there is a huge complication in this expression as it depends explicitly on the momentum of the virtual W-boson, namely p_1. Strictly speaking, the 4-momentum of the virtual W-boson (p_1) would be integrated in the nuclear part of the matrix element before joining the phase space. We will come back to this matter in due course, but now, let us start by integrating the terms which are independent of the denominator. Using Eq. (4.48), taking $m_{\nu_e} = 0$ and integrating over the solid angles of $\vec{p}_{e_2}$ and $\vec{p}_{\nu_2}$, as those are currently the only free parameters, we obtain

$$\begin{aligned}&\int \frac{d^3\vec{p}_{e_2}}{\epsilon_{e_2}} \frac{d^3\vec{p}_{\nu_2}}{\epsilon_{\nu_2}} a(\epsilon_{e_1}, \epsilon_{e_2})(p_{e_2} \cdot p_{\nu_2}) \delta(Q + 2m_e - \epsilon_{e_1} - \epsilon_{e_2} - \epsilon_{\nu_1} - \epsilon_{\nu_2}) \\ =&16\pi^2 \left(\frac{2\pi}{1 - e^{-2\pi\alpha Z}}\right)^2 \int \frac{\epsilon_{e_1}}{|\vec{p_{e_1}}|} \epsilon_{e_2}^2 d\epsilon_{e_2} \epsilon_{\nu_2}^2 d\epsilon_{\nu_2} \delta(Q + 2m_e - \epsilon_{e_1} - \epsilon_{e_2} - \epsilon_{\nu_1} - \epsilon_{\nu_2})\end{aligned} \tag{5.40}$$

This we then integrate over ϵ_{ν_2} to eliminate the delta function and finally over ϵ_{e_2}:

$$\begin{aligned}&16\pi^2 \left(\frac{2\pi}{1 - e^{-2\pi\alpha Z}}\right)^2 \int_{m_e}^{Q+2m_e-\epsilon_{e_1}-\epsilon_{\nu_1}} \frac{\epsilon_{e_1}}{|\vec{p_{e_1}}|} \epsilon_{e_2}^2 \left(Q + 2m_e - \epsilon_{e_1} - \epsilon_{e_2} - \epsilon_{\nu_1}\right)^2 d\epsilon_{e_2} \\ =&16\pi^2 \left(\frac{2\pi}{1 - e^{-2\pi\alpha Z}}\right)^2 \frac{\epsilon_{e_1}}{|\vec{p_{e_1}}|} \frac{1}{30} (Q + m_e - \epsilon_{e_1} - \epsilon_{\nu_1})^3 \left(16m^2 + 7m(Q - \epsilon_{e_1} - \epsilon_{\nu_1}) - (Q - \epsilon_{e_1} - \epsilon_{\nu_1})^2\right)\end{aligned} \tag{5.41}$$

Plugging this result back in the decay rate we have, without further ado

$$\begin{aligned}\Gamma^{t1}_{2\nu_\phi\beta\beta} \approx &|g_\phi|^2 \frac{\left|\mathcal{M}^{t1}_{0\nu\beta\beta\phi}\right|^2}{480(2\pi)^9 M^2} \left(\frac{2\pi}{1 - e^{-2\pi\alpha Z}}\right)^2 \int \left[16m_e^2 + 7m_e(Q - \epsilon_{e_1} - \epsilon_{\nu_1}) - (Q - \epsilon_{e_1} - \epsilon_{\nu_1})^2\right] \epsilon_{\nu_1} \epsilon_{e_1} \\ &\times (Q + m_e - \epsilon_{e_1} - \epsilon_{\nu_1})^3 \frac{\epsilon_{e_1}\epsilon_{\nu_1} - |\vec{p}_{e_1}|\epsilon_{\nu_1} \cos(\delta)}{\left((p_1 - p_{e_1} - p_{\nu_1})^2 - m_\phi^2\right)^2} d\epsilon_{e_1} d\cos\alpha \; d\phi_1 d\epsilon_{\nu_1} d\cos\beta \; d\phi_2\end{aligned} \tag{5.42}$$

We can see p_1 as the momentum transfer between the two incoming neutrons and outgoing protons, which have a relative 3-momentum $|\vec{P}_N|$ of the order of 100 MeV according to the closure approximation [21] discussed in Section 3.4. The total energy of the neutrons is then their mass m_N plus the kinetic energy term. However, the mass term cannot be transferred through the leptonic current since the proton and neutron have approximately the same mass. Thus, p_1 can then be separated into temporal (ϵ_1) and spatial ($\vec{p}_1$) components. $|\vec{p}_1|$ will be the 100 MeV from the relative 3-momenta of the nucleons, while the total energy ϵ_1 is given by the kinetic energy term only. Considering the order of magnitude of the energies involved, we can use the non-relativistic approximation and write $\epsilon_1 \approx \frac{|\vec{p}_1|^2}{2m_N} \approx 5$ MeV. These considerations made, we can drop the quantities in the denominator of the integrand which are too small. We have already done that for the higher order correction $im_\phi\Gamma_\phi$ in the Majoron propagator in Section 5.2 in anticipation to this step. Writing explicitly the momenta squared, we have

$$(p_1 - p_{e_1} - p_{\nu_1})^2 = p_1^2 + p_{e_1}^2 + p_{\nu_1}^2 - 2(p_1 \cdot p_{e_1}) - 2(p_1 \cdot p_{\nu_1}) + 2(p_{e_1} \cdot p_{\nu_1})$$

We now separate temporal and spatial components, and pull $|\vec{p}_1|^2$ out of the expression:

$$\begin{aligned}&\epsilon_1^2 - |\vec{p}_1|^2 + m_e^2 - 2\left(\epsilon_1\epsilon_{e_1} - |\vec{p}_1||\vec{p}_{e_1}|\cos\alpha\right) - 2\left(\epsilon_1\epsilon_{e_1} - |\vec{p}_1|\epsilon_{\nu_1}\cos\beta\right) + 2\left(\epsilon_{e_1}\epsilon_{\nu_1} - |\vec{p}_{e_1}|\epsilon_{\nu_1}\cos\delta\right) \\ =&|\vec{p}_1|^2 \left[\frac{\epsilon_1^2}{|\vec{p}_1|^2} + 2\frac{\epsilon_{e_1}\epsilon_{\nu_1} - \epsilon_1\epsilon_{e_1} - \epsilon_1\epsilon_{\nu_1}}{|\vec{p}_1|^2} + \frac{m_e^2}{|\vec{p}_1|^2} - 1 + 2\frac{|\vec{p}_{e_1}|}{|\vec{p}_1|}\cos\alpha + 2\frac{\epsilon_{\nu_1}}{|\vec{p}_1|}\cos\beta - 2\frac{|\vec{p}_{e_1}|}{|\vec{p}_1|}\frac{\epsilon_{\nu_1}}{|\vec{p}_1|}\cos\delta\right]\end{aligned}$$

Where α, β and δ are respectively the angles between $\vec{p}_1$ and $\vec{p}_{e_1}$, $\vec{p}_1$ and $\vec{p}_{\nu_1}$, and $\vec{p}_{e_1}$ and $\vec{p}_{\nu_1}$. Now we see two terms which we know are negligible: $\frac{m_e}{|\vec{p}_1|}$ and $\frac{\epsilon_1}{|\vec{p}_1|}$. Neglecting these terms, we are left with

$$(p_1 - p_{e_1} - p_{\nu_1})^2 \approx 2|\vec{p}_1|^2 \left[\frac{|\vec{p}_{e_1}|}{|\vec{p}_1|} \cos\alpha + \frac{\epsilon_{\nu_1}}{|\vec{p}_1|} \cos\beta + \frac{|\vec{p}_{e_1}|}{|\vec{p}_1|} \frac{\epsilon_{\nu_1}}{|\vec{p}_1|} (1 - \cos\delta) - \frac{1}{2} \right]$$

By defining two new variables as

$$x = \frac{|\vec{p}_{e_1}|}{|\vec{p}_1|}, \quad y = \frac{\epsilon_{\nu_1}}{|\vec{p}_1|} \tag{5.43}$$

we can write the terms in the integrand which depend on the energies as

$$\begin{aligned} &\epsilon_{e_1}\epsilon_{\nu_1} \frac{\epsilon_{e_1}\epsilon_{\nu_1} - |\vec{p}_{e_1}|\epsilon_{\nu_1}\cos\delta}{\left(2|\vec{p}_1|^2 \left(x\cos\alpha + y\cos\beta + xy(1-\cos\delta) - \frac{1}{2}\right) - m_\phi^2\right)^2} \\ \approx &\frac{x^2y^2\left(1-\cos\left(\delta\right)\right)}{\left(2\left(x\cos\alpha + y\cos\beta + xy(1-\cos\delta) - \frac{1}{2}\right) - \frac{m_\phi^2}{|\vec{p}_1|^2}\right)^2} \end{aligned} \tag{5.44}$$

where we have neglected $\frac{m_\phi^2\Gamma_\phi^2}{|\vec{p}_1|^4}$ as $m_\phi^2\Gamma_\phi^2$ is a tiny number by itself and goes to zero when divided by $|\vec{p}_1|^4$. What we do now is a 3rd order expansion around x and y, which yield the 3 terms

$$1^{st}: \quad \frac{|\vec{p}_1|^4 x^2 y^2 (1-\cos\delta)}{\left(m_\phi^2 + |\vec{p}_1|^2\right)^2} \tag{5.45}$$

$$2^{nd}: \quad \frac{4|\vec{p}_1|^6 x^2 y^2 (1-\cos\delta)\left(x\cos\alpha + y\cos\beta\right)}{\left(m_\phi^2 + |\vec{p}_1|^2\right)^3} \tag{5.46}$$

$$3^{rd}: \quad \frac{4|\vec{p}_1|^6 x^3 y^3 (1-\cos\delta)\left((1-\cos\delta)\left(m_\phi^2 + |\vec{p}_1|^2\right) - 6|\vec{p}_1|^2\cos\alpha\cos\beta\right)}{\left(m_\phi^2 + |\vec{p}_1|^2\right)^4} \tag{5.47}$$

With this expansion, we simplify considerably the integral. However, you might have noticed that we have 3 angles coming from the 3 scalar products. Luckily for us, the 3 angles are not independent. Similarly to how we can calculate the great circle distance between two points on Earth by using latitude and longitude coordinates, we can obtain the angle δ between the electron and the neutrino by using their longitude and co-latitude. In our case, $\vec{p}_1$ is acting as the north pole as it can be fixed at an arbitrary axis in our coordinate system since it is not being integrated. The formula for the angle δ is then given by [38]

$$\cos\delta = \cos\alpha\cos\beta + \sin\alpha\sin\beta\cos\left(\phi_1 - \phi_2\right) \tag{5.48}$$

The first two terms in the expansion depend linearly on $\cos\delta$, but for the third we have the term $(1-\cos\delta)^2$, which results in

$$\cos^2\alpha\cos^2\beta\cos^2(\phi_1-\phi_2) + 2\cos\alpha\cos\beta(\sin\alpha\sin\beta - 1)\cos(\phi_1-\phi_2) + (\sin\alpha\sin\beta - 1)^2$$

Hence, upon integration, we will be dealing with the two terms

$$\int_0^{2\pi}\int_0^{2\pi}\cos(\phi_1-\phi_2)d\phi_1 d\phi_2=0,\qquad \int_0^{2\pi}\int_0^{2\pi}\cos^2(\phi_1-\phi_2)d\phi_1 d\phi_2=2\pi^2$$

which yield

$$\int_0^{2\pi}(1-\cos\delta)^2 d\phi_1 d\phi_2=2\pi^2\cos^2\alpha\cos^2\beta+4\pi^2(\sin\alpha\sin\beta-1)^2$$

Integrating the 3 terms in Eqs. 5.45 to 5.47 by ϕ_1 and ϕ_2 by using the calculations above, they reduce to

$$1^{st}:\ \frac{4\pi^2\epsilon_{e_1}^2\epsilon_{\nu_1}^2\left(1-\sqrt{1-\cos^2\alpha}\sqrt{1-\cos^2\beta}\right)}{\left(m_\phi^2-|\vec{p}_1|^2\right)^2} \tag{5.49}$$

$$2^{nd}:\ \frac{16\pi^2\epsilon_{e_1}^2\epsilon_{\nu_1}^2\left(1-\sqrt{1-\cos^2\alpha}\sqrt{1-\cos^2\beta}\right)\left(|\vec{p}_1|\epsilon_{e_1}\cos\alpha+|\vec{p}_1|\epsilon_{\nu_1}\cos\beta\right)}{\left(m_\phi^2+|\vec{p}_1|^2\right)^3} \tag{5.50}$$

$$\begin{aligned}3^{rd}:\ &\frac{8\pi^2\epsilon_{e_1}^3\epsilon_{\nu_1}^3\cos^2\alpha\cos^2\beta}{\left(m_\phi^2+|\vec{p}_1|^2\right)^3}+\frac{16\pi^2\epsilon_{e_1}^3\epsilon_{\nu_1}^3\left(\sqrt{1-\cos^2\alpha}\sqrt{1-\cos^2\beta}-1\right)^2}{\left(m_\phi^2+|\vec{p}_1|^2\right)^3}\\&-\frac{96\pi^2\epsilon_{e_1}^3\epsilon_{\nu_1}^3|\vec{p}_1|^2\left(1-\sqrt{1-\cos^2\alpha}\sqrt{1-\cos^2\beta}\right)\cos\alpha\cos\beta}{\left(m_\phi^2+|\vec{p}_1|^2\right)^4}\end{aligned} \tag{5.51}$$

We are now back to familiar ground in which the integration is only over cosines. The terms that we have to deal with now are of the form

$$\int_{-1}^{1}\sqrt{1-x^2}dx=\frac{\pi}{2},\quad \int_{-1}^{1}\sqrt{1-x^2}xdx=0$$

The second term and the last part of the third term of the expansion drop out upon integrating the cosines. As for the remaining integral,

$$\int_{-1}^{1}\int_{-1}^{1}\left(x^2y^2-2\sqrt{1-x^2}\sqrt{1-y^2}-x^2-y^2+2\right)dxdy=\frac{52}{9}-\frac{\pi^2}{2} \tag{5.52}$$

Hence, the remaining terms are

$$1^{st}:\ \frac{\pi^2\left(16-\pi^2\right)\epsilon_{e_1}^2\epsilon_{\nu_1}^2}{\left(m_\phi^2+|\vec{p}_1|^2\right)^2},\quad 3^{rd}:=\frac{8\pi^2\epsilon_{e_1}^3\epsilon_{\nu_1}^3\left(12-\pi^2\right)}{\left(m_\phi^2+|\vec{p}_1|^2\right)^3} \tag{5.53}$$

Putting these back into the decay rate equation gives

$$\begin{aligned}\Gamma^{t1}_{2\nu_\phi\beta\beta}\approx&|g_\phi|^2\frac{\left|\mathcal{M}^{t1}_{0\nu\beta\beta\phi}\right|^2}{480(2\pi)^9M^2}\left(\frac{2\pi}{1-e^{-2\pi\alpha Z}}\right)^2\int\left[16m^2+7m(Q-\epsilon_{e_1}-\epsilon_{\nu_1})-(Q-\epsilon_{e_1}-\epsilon_{\nu_1})^2\right]\\&\times(Q+m_e-\epsilon_{e_1}-\epsilon_{\nu_1})^3\left[\frac{\pi^2\left(16-\pi^2\right)\epsilon_{e_1}^2\epsilon_{\nu_1}^2}{\left(|\vec{p}_1|^2+m_\phi^2\right)^2}+\frac{8\pi^2(12-\pi^2)\epsilon_{e_1}^3\epsilon_{\nu_1}^3}{\left(|\vec{p}_1|^2+m_\phi^2\right)^3}\right]d\epsilon_{e_1}d\epsilon_{\nu_1}\end{aligned} \tag{5.54}$$

Notice that this time we have an integral over one electron and one neutrino, as opposed to the s-channel in which we had the remaining integral over two electrons. The term in Eq. (5.54) proportional to $\epsilon_{e_1}^2\epsilon_{\nu_1}^2$ yields

$$\begin{aligned}
&\int_{m_e}^{Q+m_e}\int_0^{Q+2m_e-\epsilon_{e_1}}(Q+m_e-\epsilon_{e_1}-\epsilon_{\nu_1})^3\left[16m^2+7m(Q-\epsilon_{e_1}-\epsilon_{\nu_1})-(Q-\epsilon_{e_1}-\epsilon_{\nu_1})^2\right]\epsilon_{e_1}^2\epsilon_{\nu_1}^2 d\epsilon_{\nu_1}d\epsilon_{e_1}\\
&=\int_{m_e}^{Q+m_e}\frac{\epsilon_{e_1}^2}{168}\left[-(Q-x)^8+16m_e(Q-x)^7+112m_e^2(Q-\epsilon_{e_1})^6+392m_e^3(Q-\epsilon_{e_1})^5+770m_e^4(Q-\epsilon_{e_1})^4\right.\\
&\qquad\left.+896m_e^5(Q-\epsilon_{e_1})^3+336m_e^6(Q-\epsilon_{e_1})^2+768m_e^7(\epsilon_{e_1}-Q)-864m_e^8\right]d\epsilon_{e_1}\\
&=\frac{Q}{83160}\left[Q^{10}+22m_eQ^9+220m_e^2Q^8+990m_e^3Q^7+1980m_e^4Q^6-4620m_e^6Q^4\right.\\
&\qquad\left.-41250m_e^7Q^3-148665m_e^8Q^2-198495m_e^9Q-89595m_e^{10}\right]
\end{aligned}$$

And the term in Eq. (5.54) proportional to $\epsilon_{e_1}^3\epsilon_{\nu_1}^3$ yields

$$\begin{aligned}
&\int_{m_e}^{Q+m_e}\int_0^{Q+2m_e-\epsilon_{e_1}}(Q+m_e-\epsilon_{e_1}-\epsilon_{\nu_1})^3\left[16m^2+7m(Q-\epsilon_{e_1}-\epsilon_{\nu_1})-(Q-\epsilon_{e_1}-\epsilon_{\nu_1})^2\right]\epsilon_{e_1}^3\epsilon_{\nu_1}^3 d\epsilon_{\nu_1}d\epsilon_{e_1}\\
&=\int_{m_e}^{Q+m_e}\epsilon_{e_1}^3\left[\frac{(Q-\epsilon_{e_1})^9}{504}+\frac{m_e(Q-\epsilon_{e_1})^8}{28}+\frac{2m_e^2(Q-\epsilon_{e_1})^7}{7}+\frac{7m_e^3(Q-\epsilon_{e_1})^6}{6}+\frac{11m_e^4(Q-\epsilon_{e_1})^5}{4}\right.\\
&\qquad\left.+4m_e^5(Q-\epsilon_{e_1})^4+2m_e^6(Q-\epsilon_{e_1})^3-\frac{48m_e^7(Q-\epsilon_{e_1})^2}{7}-\frac{108m_e^8(Q-\epsilon_{e_1})}{7}-\frac{608m_e^9}{63}\right]d\epsilon_{e_1}\\
&=\frac{(Q+m_e)^5}{1441440}\left[Q^8+21m_eQ^7+197m_e^2Q^6+797m_e^3Q^5+980m_e^4Q^4\right.\\
&\qquad\left.-2076m_e^5Q^3-25556m_e^6Q^2-79942m_e^7Q-489254m_e^8\right]
\end{aligned}$$

Combining these results with Eq. (5.54), we obtain the total decay rate for the $t1$-channel

$$\begin{aligned}
\Gamma^{t1}_{2\nu_\phi\beta\beta}\approx&\frac{|g_\phi|^2}{26611200(2\pi)^6M^2}\left(\frac{\left|\mathcal{M}^{t1}_{0\nu\beta\beta\phi}\right|}{1-e^{-2\pi\alpha Z}}\right)^2\\
&\times\left[\frac{\left(16-\pi^2\right)Q}{6\left(|\vec{p}_1|^2+m_\phi^2\right)^2}\left[Q^{10}+22m_eQ^9+220m_e^2Q^8+990m_e^3Q^7+1980m_e^4Q^6-4620m_e^6Q^4\right.\right.\\
&\qquad\left.-41250m_e^7Q^3-14865m_e^8Q^2-198495m_e^9Q-89595m_e^{10}\right]\\
&\quad\left.+\frac{\left(12-\pi^2\right)(Q+m_e)^5}{13\left(|\vec{p}_1|^2+m_\phi^2\right)^3}\left[Q^8+21m_eQ^7+197m_e^2Q^6+797m_e^3Q^5+980m_e^4Q^4\right.\right.\\
&\qquad\left.\left.-2076m_e^5Q^3-25556m_e^6Q^2-79942m_e^7Q-489254m_e^8\right]\right]
\end{aligned}\tag{5.55}$$

The Q-value dependency is of the order of Q^{11}, similarly to the s-channel. The remaining terms of the t+u-channel can be obtained in the exact same way, though not used in this work. We will keep using only the $t1$-channel for the energy distributions and show how it compares to the s-channel, to the standard $2\nu\beta\beta$, and what the addition of the missing terms would incur.

5.4 Energy Distribution

The energy distribution of neutrino-emitting processes is substantially harder to obtain as we must also integrate over the neutrinos' energies and solid angles. We will start with the s-channel and ignore constants as we care only about the shape of the function.

5.4.1 s-Channel

From Eq. (5.29) we have

$$\left[\frac{d\Gamma}{d\epsilon_{e_1} d\epsilon_{e_2}}\right]^s_{2\nu_\phi\beta\beta} \propto \epsilon_{e_1}^2 \epsilon_{e_2}^2 \int \delta(Q + 2m_e - \epsilon_{e_1} - \epsilon_{e_2} - \epsilon_\nu) \left[\frac{\epsilon_\nu^5}{m_\phi^4} \int_0^1 \frac{x\left(1-x^2\right)}{\left(\frac{\epsilon_\nu^2}{m_\phi^2}\left(1-x^2\right)-1\right)^2 + \frac{\Gamma_\phi^2}{m_\phi^2}} dx\right] d\epsilon_\nu \tag{5.56}$$

In Section 5.3 we have chosen a heuristic approach to treat this integral just to have an overview on the dependency of this process on the Q-value. Now we want to solve it analytically. This is a fairly complicated integral, so we rely on Mathematica to solve it. The term in square brackets evaluates to

$$\frac{\epsilon_\nu}{2}\frac{m_\phi}{\Gamma_\phi}\left[\arctan\left(\frac{\Gamma_\phi m_\phi}{m_\phi^2 - \epsilon_\nu^2}\right) - \arctan\left(\frac{\Gamma_\phi}{m_\phi}\right)\right] + \frac{\epsilon_\nu}{4}\left[\ln\left(\Gamma_\phi^2 m_\phi^2 + \left(m_\phi^2 - \epsilon_\nu^2\right)^2\right) - \ln\left(\Gamma_\phi^2 m_\phi^2 + m_\phi^4\right)\right]$$

As a side note, if we were to take the limit $\Gamma_\phi \to 0$, as done in Section 5.3, we would obtain

$$\frac{\epsilon_\nu}{4}\left(\frac{2\epsilon_\nu^2}{m_\phi^2 - \epsilon_\nu^2} + \log\left((m_\phi^2 - \epsilon_\nu^2)^2\right) - \log\left(m_\phi^4\right)\right)$$

which is not indeterminate, as one could fear due to the presence of a Γ_ϕ^{-1} term. Putting the full expression back into Eq. (5.56), we get

$$\begin{aligned}\left[\frac{d\Gamma}{d\epsilon_{e_1} d\epsilon_{e_2}}\right]^s_{2\nu_\phi\beta\beta} \propto & \epsilon_{e_1}^2 \epsilon_{e_2}^2 \frac{Q + 2m_e - \epsilon_{e_1} - \epsilon_{e_2}}{2} \\ & \times \left[\frac{m_\phi}{\Gamma_\phi}\left(\arctan\left(\frac{\Gamma_\phi m_\phi}{m_\phi^2 - (Q + 2m_e - \epsilon_{e_1} - \epsilon_{e_2})^2}\right) - \arctan\left(\frac{\Gamma_\phi}{m_\phi}\right)\right)\right. \\ & \left. + \frac{1}{2}\ln\left(\Gamma_\phi^2 m_\phi^2 + \left(m_\phi^2 - (Q + 2m_e - \epsilon_{e_1} - \epsilon_{e_2})^2\right)^2\right) - \frac{1}{2}\ln\left(\Gamma_\phi^2 m_\phi^2 + m_\phi^4\right)\right]\end{aligned} \tag{5.57}$$

The 2-dimensional energy distribution for this process is shown in Figure 12 with an arbitrary choice of $m_\phi = 4$ MeV and $\Gamma_\phi = 10^{-3} m_\phi$. These values were chosen because the Majoron coupling with neutrinos is expected to be small and the decay rate is greater for a m_ϕ closer to the Q-value. Also, the m_ϕ must be greater than Q, otherwise the process would be dominated by $0\nu\beta\beta\phi$. Contrary to the energy distribution of the neutrinoless processes, depicted in Figure 7, this process has an energy distribution shifted towards lower electron energies. We now want to see how the energy distribution in terms of the total energy of the electrons. We use the variable substitution in Eq. (4.59) and the integration in $d(\Delta\epsilon)$ in Eq. (4.60) to obtain

$$\begin{aligned}\left[\frac{d\Gamma}{d\epsilon}\right]^s_{2\nu_\phi\beta\beta} \propto & \left(\frac{\epsilon^5}{120} - \frac{\epsilon^2 m_e^3}{6} + \frac{\epsilon m_e^4}{4} - \frac{m_e^5}{10}\right)(Q + 2m_e - \epsilon) \\ & \times \left[\frac{2m_\phi}{\Gamma_\phi}\left(\arctan\left(\frac{\Gamma_\phi m_\phi}{m_\phi^2 - (Q + 2m_e - \epsilon)^2}\right) - \arctan\left(\frac{\Gamma_\phi}{m_\phi}\right)\right)\right. \\ & \left. + \ln\left(\Gamma_\phi^2 m_\phi^2 + \left(m_\phi^2 - (Q + 2m_e - \epsilon)^2\right)^2\right) - \ln\left(\Gamma_\phi^2 m_\phi^2 + m_\phi^4\right)\right]\end{aligned} \tag{5.58}$$

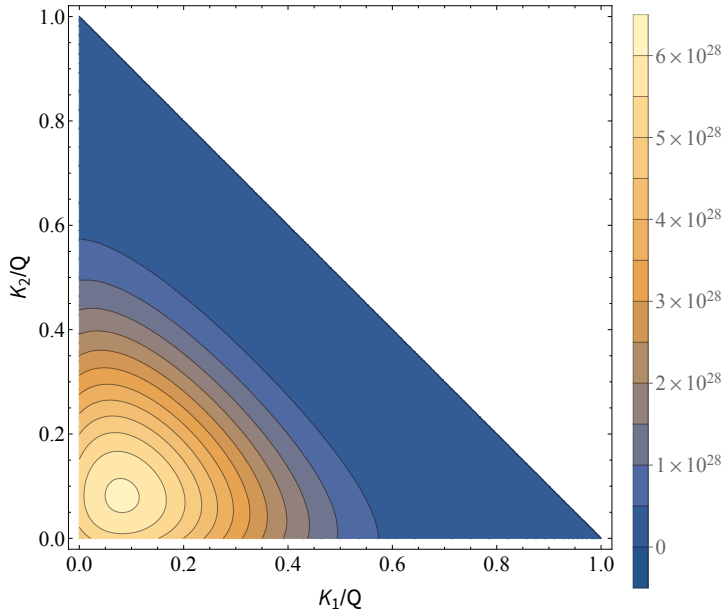

Figure 12: $2\nu^s_\phi\beta\beta$ 2-dimensional electron kinetic energy K_1, K_2 distribution at $Q = 3$ MeV for $m_\phi = 4$ MeV and $\Gamma_\phi = 10^{-3}m_\phi$.

As a result, we have two interesting graphs. Figure 13 (left) shows us how the decay rate is heavily suppressed by m_ϕ. Also, though hardly noticeable, increasing m_ϕ shifts the distribution towards higher energies. Figure 13 (right) shows how small the dependency of the decay rate actually is on Γ_ϕ. To have a considerable effect on the decay rate, we need a Γ_ϕ close to 1, which would mean a coupling as strong as that of the strong interaction. It is also possible to notice a small shift to the right for greater Γ_ϕ values.

Unfortunately, Eq. (5.58) cannot be integrated analytically. Resorting to numerical integration, we obtain the total decay rate as a function of m_ϕ for fixed $Q = 3$ MeV and $\Gamma_\phi = 10^{-3}m_\phi$ as shown in Figure 14 (left). Doing the same for a fixed $Q = 3$ MeV and $m_\phi = 4$ MeV, we obtain the total decay rate as a function of Γ_ϕ, as shown in Figure 14 (right). In Figure 14 (left) we see the same strong suppression of $\Gamma_{2\nu^s_\phi\beta\beta}$ that we saw in Figure 13 (left). The x-axis in Figure 14 (right) is in logarithm scale to make explicit how the function is barely affected by $\Gamma_\phi < 0.1$. As we do not expect the coupling to be too

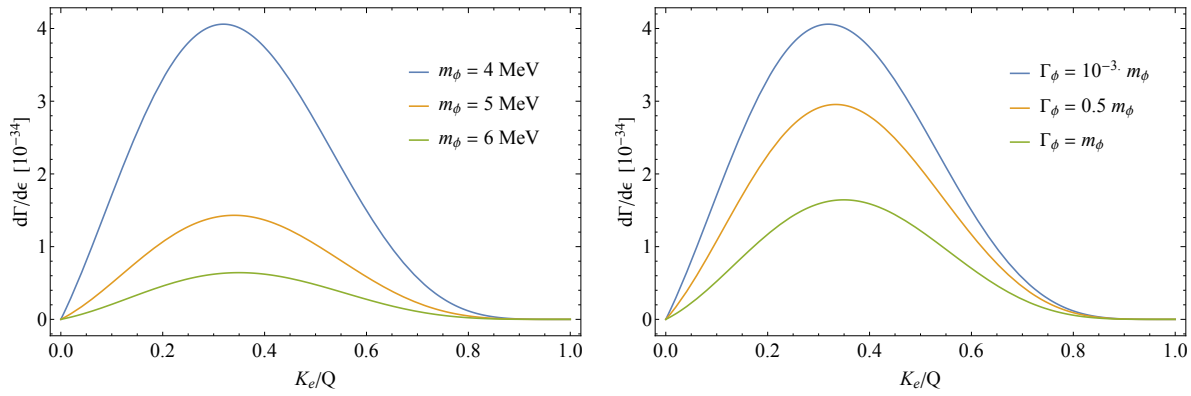

Figure 13: $2\nu^s_\phi\beta\beta$ total electron kinetic energy K_e distribution at $Q = 3$ MeV. *Left:* $\Gamma_\phi = 10^{-3}m_\phi$ for 3 values of m_ϕ. *Right:* $m_\phi = 4$ MeV for 3 values of Γ_ϕ.

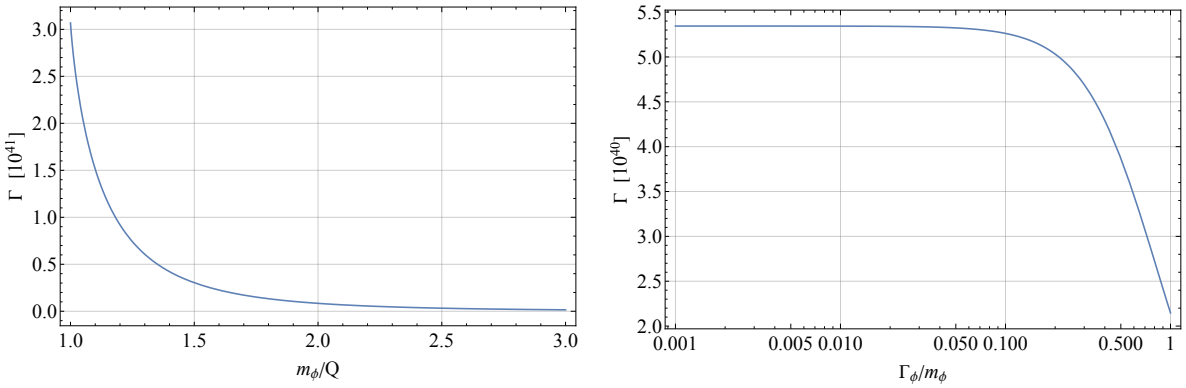

Figure 14: $2\nu^s_\phi\beta\beta$ total decay rate at $Q = 3$ MeV as a function of m_ϕ for and $\Gamma_\phi = 10^{-3}m_\phi$ (left) and as a function of Γ_ϕ for $m_\phi = 4$ MeV (right).

strong, we can safely take the limit $\Gamma_\phi \to 0$.

Both neutrino emitting processes ($2\nu\beta\beta$ and $2\nu_\phi\beta\beta$) yield analogous spectra, not to mention having identical signatures. The graph in Figure 15 shows the normalised energy distribution of both $2\nu\beta\beta$ and $2\nu^s_\phi\beta\beta$ for 2 values of m_ϕ. The normalisation is done by dividing the distributions by their integrals ($\frac{1}{\Gamma}\frac{d\Gamma}{d\epsilon}$) so that the total area under the curve is 1. The two values for m_ϕ were chosen to better demonstrate how the $2\nu^s_\phi\beta\beta$ energy distribution approaches that of $2\nu\beta\beta$ for larger m_ϕ, although even for small m_ϕ they are not very distant from each other. In fact, if we define a deviation

$$\mathrm{dev}(\epsilon, m_\phi, \Gamma_\phi) = \frac{\left[\frac{1}{\Gamma}\frac{d\Gamma}{d\epsilon}\right]^s_{2\nu_\phi\beta\beta} - \left[\frac{1}{\Gamma}\frac{d\Gamma}{d\epsilon}\right]_{2\nu\beta\beta}}{\left[\frac{1}{\Gamma}\frac{d\Gamma}{d\epsilon}\right]_{2\nu\beta\beta}} \tag{5.59}$$

we can visualise how the energy distributions move closer and away from each other. For the three values of m_ϕ, we have the deviation plotted in Figure 16 (left). The curves for all 3 values of m_ϕ seem to intercept at the same point short before crossing the x-axis. If we choose to vary m_ϕ rather than the kinetic energy, we can plot the maximum value of the deviation in the energy interval (from 0 to Q) as a function of m_ϕ. This yields the graph in Figure 16 (right). We see clearly that for larger m_ϕ the

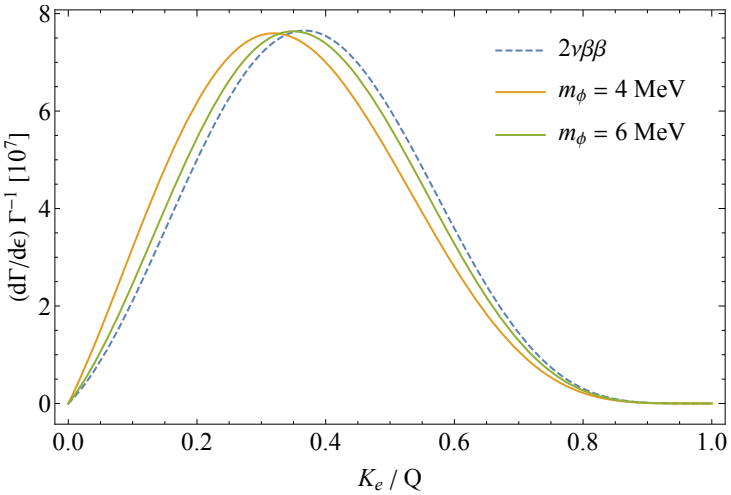

Figure 15: Comparison between $2\nu\beta\beta$ and $2\nu^s_\phi\beta\beta$ total electron kinetic energy K_e distributions at $Q = 3$ MeV for $m_\phi = 4$ MeV and 6 MeV. $\Gamma_\phi = 10^{-3}m_\phi$.

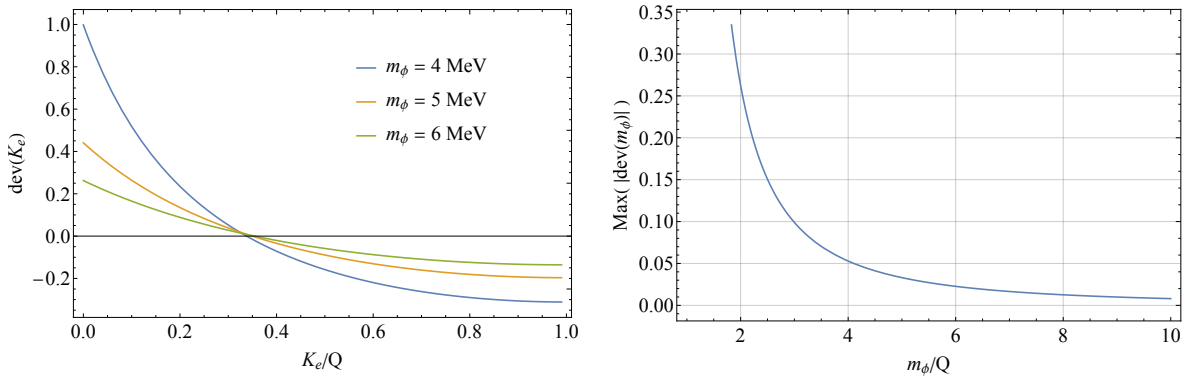

Figure 16: *Left:* $2\nu^s_\phi\beta\beta$ deviation from $2\nu\beta\beta$ at $Q = 3$ MeV for 3 values of m_ϕ; $\Gamma_\phi = 10^{-3}m_\phi$. *Right:* Maximum value of the deviation between $2\nu\beta\beta$ and $2\nu^s_\phi\beta\beta$ at $Q = 3$ MeV and $\Gamma_\phi = 10^{-3}m_\phi$ as a function of m_ϕ.

two curves approach and become practically indistinguishable. For small m_ϕ, on the other hand, the deviation grows very fast and the curves are separated.

5.4.2 t+u-Channel

The t1-channel is fairly easy to calculate once we have taken the expansion for $|\vec{p}_1| >> \epsilon_1$. From Eq. (5.54) we have the partial decay rate in terms of ϵ_{e_1} ad ϵ_{ν_1}, however, we need to obtain it as a function of the 2 electron energies. For that, we first have to undo the integral over ϵ_{e_2} in Eq. (5.41). Doing so results in

$$\left[\frac{d\Gamma}{d\epsilon_{e_1}d\epsilon_{e_2}}\right]^{t1}_{2\nu_\phi\beta\beta} \propto \int \epsilon_{e_2}^2(Q+2m_e-\epsilon_{e_1}-\epsilon_{e_2}-\epsilon_{\nu_1})^2\left[\frac{(16-\pi^2)\,\epsilon_{e_1}^2\epsilon_{\nu_1}^2}{\left(|\vec{p}_1|+m_\phi^2\right)^2}+\frac{8(12-\pi^2)\epsilon_{e_1}^3\epsilon_{\nu_1}^3}{\left(|\vec{p}_1|^2+m_\phi^2\right)^3}\right]d\epsilon_{\nu_1} \tag{5.60}$$

We now have only to integrate over ϵ_{ν_1}. Calculating the 2 polynomial integrals

$$\begin{cases} \int_0^{Q+2m_e-\epsilon_{e_1}-\epsilon_{e_2}}(Q+2m_e-\epsilon_{e_1}-\epsilon_{e_2}-\epsilon_{\nu_1})^2\epsilon_{\nu_1}^2\,d\epsilon_{\nu_1} = \frac{1}{30}(Q+2m_e-\epsilon_{e_1}-\epsilon_{e_2})^5 \\ \int_0^{Q+2m_e-\epsilon_{e_1}-\epsilon_{e_2}}(Q+2m_e-\epsilon_{e_1}-\epsilon_{e_2}-\epsilon_{\nu_1})^2\epsilon_{\nu_1}^3\,d\epsilon_{\nu_1} = \frac{1}{60}(Q+2m_e-\epsilon_{e_1}-\epsilon_{e_2})^6 \end{cases}$$

and plugging them back into Eq. (5.60) yields

$$\begin{aligned}\left[\frac{d\Gamma}{d\epsilon_{e_1}d\epsilon_{e_2}}\right]^{t1}_{2\nu_\phi\beta\beta} \propto& \frac{1}{30}(Q+2m_e-\epsilon_{e_1}-\epsilon_{e_2})^5\epsilon_{e_1}^2\epsilon_{e_2}^2 \\ &\times\left[(Q+2m-\epsilon_{e_1}-\epsilon_{e_2})\frac{4(12-\pi^2)\epsilon_{e_1}}{\left(|\vec{p}_1|^2+m_\phi^2\right)^3}+\frac{(16-\pi^2)}{\left(|\vec{p}_1|^2+m_\phi^2\right)^2}\right]\end{aligned} \tag{5.61}$$

The first characteristic of this equation that we promptly notice is that it is asymmetric with respect to the two electrons. In fact, Figure 17 shows this 2D energy distribution for the same $m_\phi = 4$ MeV and $Q = 3$ MeV chosen for the s-channel, but this time with an extra $|\vec{p}_1| = 100$ MeV factor and no Γ_ϕ dependency. The asymmetry is heavily suppressed by the magnitude of $|\vec{p}_1|$ added to that of m_ϕ in the denominator and is barely noticeable in the plot. The peak is located at the point $(0.127638, 0.127556)$,

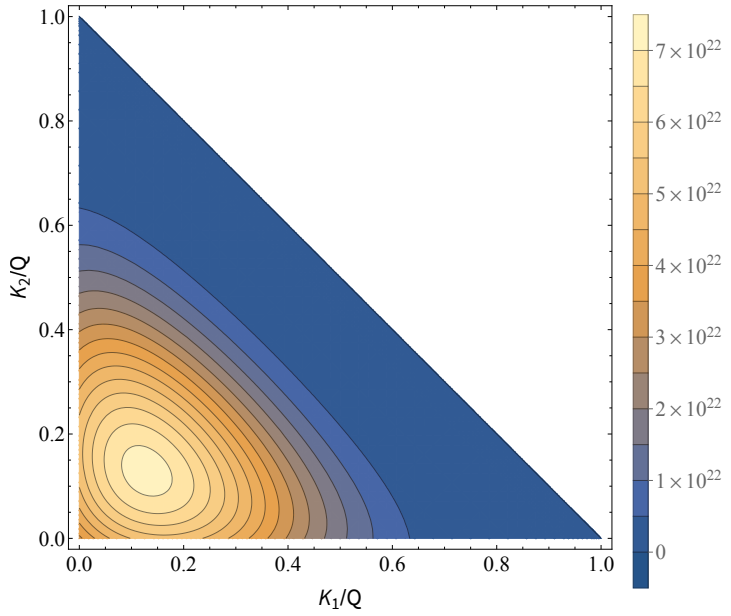

Figure 17: $2\nu_\phi^{t1}\beta\beta$ 2-dimensional electron kinetic energy K_{e_1}, K_{e_2} distribution at $Q = 3$ Mev, $m_\phi = 4$ MeV and $|\vec{p}_1| = 100$ MeV.

which represents an asymmetry of less than 0.1%. Other than that, we see a figure almost identical to Figure 12. As for the energy distribution in terms of the total energy of the electrons, the asymmetry is eliminated by the integration over $\Delta\epsilon$. We have, again, two polynomial terms to integrate. The first is the usual integral from Eq. (4.60), the second is

$$-\frac{1}{2}\int_{\epsilon-2m_e}^{2m_e-\epsilon}\left(\frac{\epsilon+\Delta\epsilon}{2}\right)^3\left(\frac{\epsilon-\Delta\epsilon}{2}\right)^2 d(\Delta\epsilon) = \frac{\epsilon}{60}\left(\epsilon^5 - 20m_e^3\epsilon^2 + 30m_e^4\epsilon - 12m_e^5\right)$$

resulting in the partial decay rate

$$\begin{aligned}\left[\frac{d\Gamma}{d\epsilon}\right]^{t1}_{2\nu_\phi\beta\beta} \propto & \frac{1}{900}(Q+2m_e-\epsilon)^5\left(\epsilon^5 - 20m_e^3\epsilon^2 + 30m_e^4\epsilon - 12m_e^5\right) \\ & \times\left[(Q+2m-\epsilon)\frac{2(12-\pi^2)\epsilon}{\left(|\vec{p}_1|^2+m_\phi^2\right)^3} + \frac{\left(16-\pi^2\right)}{\left(|\vec{p}_1|^2+m_\phi^2\right)^2}\right]\end{aligned} \tag{5.62}$$

Before we proceed to analyse its behaviour, let us have a brief digression on why we saw that asymmetry in the first place. As opposed to the s-channel, we have broken the t+u-channel into 4 processes, namely t1, t2, u1 and u2. Each of these processes compose the final t+u-channel and bring a different but symmetric dependency on the neutrinos and electrons. Here, we have calculated the decay rate only for the particular process t1, which carries only e_1 and ν_1. Should we include the remaining processes, t1 would be compensated by the dependency on e_2 and ν_2 present on those. This said, we may now come back to the energy distribution of the t1-channel, which is shown in Figure 18 (left) for different choices of m_ϕ. Here we have chosen larger variations for the value of m_ϕ than done for the s-channel to account to the large value of $|\vec{p}_1|$ that would make a variation of only 1 MeV unnoticeable. Although barely noticeable, the distribution has a tiny shift towards larger energies for larger m_ϕ due to the term of order 3 in the denominator. The most pronounced feature of this distribution, however, is the

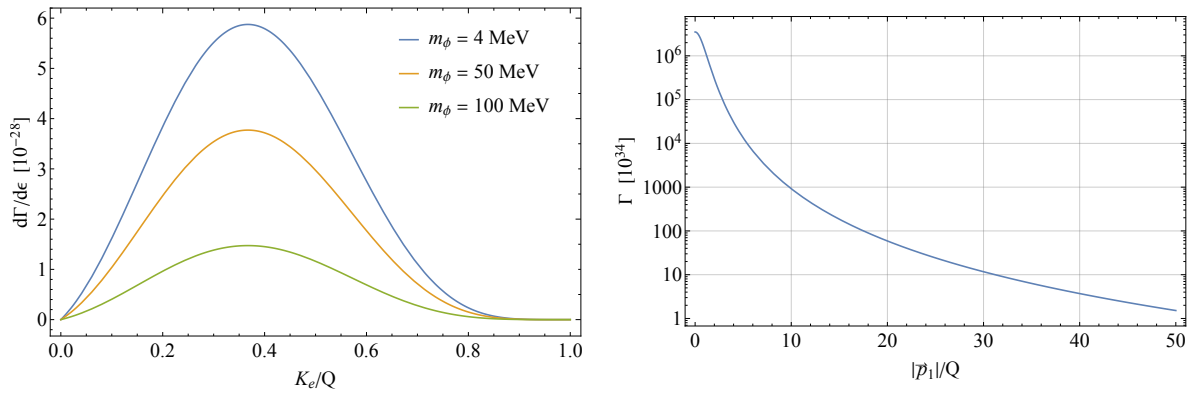

Figure 18: *Left:* $2\nu^{t1}_{\phi}\beta\beta$ total electron kinetic energy K_e distribution at $Q = 3$ MeV and $|\vec{p}_1| = 100$ MeV for 3 values of m_ϕ. *Right:* $2\nu^{t1}_{\phi}\beta\beta$ decay rate as a function of $|\vec{p}_1|$ at $Q = 3$ MeV and $m_\phi = 4$ MeV.

heavy suppression promoted by $|\vec{p}_1|$ in the denominator. Of course we cannot go to low values of $|\vec{p}_1|$ as this would go against our first assumption that $|\vec{p}_1|$ is a large number compared to the other energies involved. Hence, the order of magnitude of $|\vec{p}_1|$ is of paramount importance to this process and ends up overshadowing m_ϕ. The total decay rate obtained in Eq. (5.55) shows, in Figure 18 (right), how big the contribution of $|\vec{p}_1|$ is. The y-axis is now in logarithmic scale to better display the slope, which decreases too fast for a linear scale. It is, however, not realistic to look at values lower than 10Q for $Q = 3$ MeV and the expansion we have made stops being valid. Due to this large value of $|\vec{p}_1|$, the normalised energy distribution is in an almost perfect overlap with that of $2\nu\beta\beta$ for any value of m_ϕ. Indeed, we cannot distinguish them if plotted together. Instead, we define the same deviation for the t1-channel as done for the s-channel in Eq. (5.59), however, it is now a function of $|\vec{p}_1|$ rather than Γ_ϕ. Plotting the deviation for 3 realistic values of $|\vec{p}_1|$ and $m_\phi = 3$ MeV results in the parabolic curves shown in Figure 19 (left). When comparing to the s-channel, we see that the t-channel has a deviation of order 10^{-4} compared to that of the s-channel. The shape of the curve is also different, but this is not so relevant as it is purely the result of how much the shapes are overlapped point by point. What is useful is how the maximum of the deviation varies as a function of m_ϕ as shown in Figure 19 (right). Again, we see a different shape to that obtained for of the s-channel. Of course both processes have a different dependency on m_ϕ, nonetheless Figure 19 (right) is mostly the result of an illusion caused by the magnitude of $|\vec{p}_1|$. Indeed, if plotting

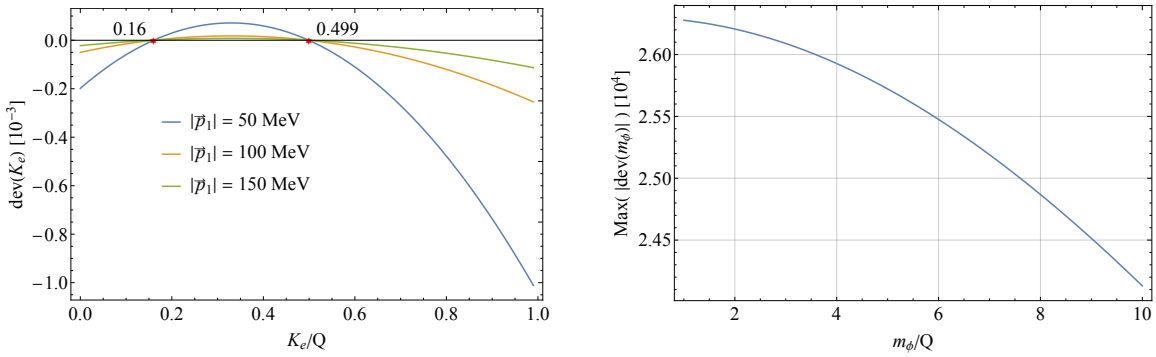

Figure 19: *Left:* $2\nu^{t1}_{\phi}\beta\beta$ deviation from $2\nu\beta\beta$ at $Q = 3$ MeV and $m_\phi = 4$ MeV for 3 values of $|\vec{p}_1|$. *Right:* Maximum value of the relative error between $2\nu\beta\beta$ and $2\nu^{s}_{\phi}\beta\beta$ at $Q = 3$ MeV and $|\vec{p}_1| = 100$ MeV as a function of m_ϕ.

the same curve as a function of $|\vec{p}_1|$ rather than m_ϕ, one would observe a plot almost identical to that in Figure 16 (right). Notwithstanding, for a large enough m_ϕ, the normalised energy distribution of all neutrino emitting processes approach and overlap. This is a explicit of the Majoron coupling approaching an effective operator that couples 4 particles without a propagating virtual particle, such that we only see 2 neutrinos entering and 2 neutrinos leaving the vertex.

6 Conclusion

In this work we have scrutinized some of the most promising exotic $\beta\beta$ decay modes: the standard neutrinoless double beta ($0\nu\beta\beta$) decay, the simplest Majoron emitting neutrinoless double beta ($0\nu\beta\beta\phi$) decay, and the two variations of the simplest Majoron triggered double beta ($2\nu_\phi\beta\beta$) decay. Both neutrinoless modes have been well investigated in the literature, thus, we chose to have a more heuristic approach. As for $2\nu_\phi\beta\beta$ decay, it had never been thoroughly studied before and we present calculations of the leptonic amplitudes and decay distributions as a starting point for further investigations.

Firstly, we studied the leptonic part of $0\nu\beta\beta$ decay as if it was a $W^-W^- \to e^-e^-$ collision and compared it to the lepton number conserving process $W^+W^- \to e^+e^-$. While the latter depends on the momentum of the virtual neutrino, we have shown that the former is proportional to the neutrino mass. This behaviour is due to the chirality mismatch in the W-boson vertices and causes the process to be greatly suppressed by the smallness of the neutrino mass.

Then, for the leptonic part of $0\nu\beta\beta\phi$ decay, we have considered the most general $\nu - \phi$ coupling, which considers both left and right-handed currents. We have shown that such a process favours emitting electrons with a large share of the decay's kinetic energy release, resulting in an almost antiparallel electron scattering and a low energy Majoron. This is very distinct to the neutirno emitting processes, in which the spectra favours electrons with a smaller share of the decay's kinetic energy release.

Finally, the $2\nu_\phi\beta\beta$ decay was separated into s and t+u-channels. The former being only possible for Majorana neutrinos. Both channels result in very distinct leptonic currents, but a similar phase space and energy distribution. The $2\nu^s_\phi\beta\beta$ mode has the advantage of having the m_ϕ as the only suppression while the $2\nu^{t+u}_\phi\beta\beta$ mode is heavily suppressed by the 4-momentum of the internal W-boson. We have shown that a larger m_ϕ also shifts the energy distribution towards larger electron energies. This behaviour is opposite to that of $0\nu\beta\beta\phi$ decay and, for a large enough m_ϕ, makes the normalised energy distribution of $2\nu_\phi\beta\beta$ decay indistinguishable from that of $2\nu\beta\beta$ decay. Due to the large average value of the internal momentum flow, the $2\nu^{t+u}_\phi\beta\beta$ mode normalised energy spectrum always overlaps with that of $2\nu\beta\beta$ decay.

These results show that, while the neutrinoless processes can be easily distinguished from $2\nu\beta\beta$ decay, $2\nu_\phi\beta\beta$ decay yields a practically identical spectrum to it under the right conditions. Using realistic values for the Q-value and m_ϕ, we have shown that these required conditions are, in fact, easily achievable. Of course the extra suppression from m_ϕ makes the half life of $2\nu_\phi\beta\beta$ very long, nonetheless, this process provides an outstanding contribution to $\beta\beta$ decay. We have offered a generic model coupling both left and right-handed currents which can be refined to more specific scenarios. Using this kind of processes, one can search for exotic scalar particles coupling to neutrinos. A wonderful consequence of finding such weakly interacting particles would be obtaining a straightforward candidate to dark matter.

A $W^+W^- \to e^+e^-$ Matrix Element

Following the standard Feynman rules, the $W^+W^- \to e^+e^-$ matrix element is

$$\mathcal{M} = \frac{g_W^2 |U_{ei}|^2 \epsilon_\mu(p_1)\epsilon_\nu(p_2)}{8m_W^2(q^2 - m_{\nu_i}^2)} \left[\bar{u}_e(p_3)(\mathbb{1}_4 + \gamma^5)\gamma^\mu\right] (\not{q} + m_{\nu_i}) \left[\gamma^\nu(\mathbb{1}_4 - \gamma^5)v_e(p_4)\right] \tag{A.1}$$

We can clearly see that the only difference from this matrix element from that of the lepton number violating process is the order of the matrices in the second vertex. The overall result of this swap is preserving the momentum of the virtual particle rather than its mass. Thus

$$\mathcal{M} = \frac{g_W^2 (U_{ei}^*)^2 \epsilon_\mu(p_1)\epsilon_\nu(p_2)}{4(q^2 - m_{\nu_i}^2)} \bar{u}_e(p_3)\gamma^\mu(\mathbb{1}_4 - \gamma^5)\not{q}\gamma^\nu v_e(p_4) \tag{A.2}$$

As for the averaged matrix element squared, we use Casimir's trick by defining the matrices

$$\Gamma_1 = \gamma^\mu \not{q} \gamma^\nu (1 - \gamma^5); \quad \bar{\Gamma}_2 = (1 + \gamma^5)\gamma^\sigma \not{q} \gamma^\rho$$

which results in

$$\left\langle |\mathcal{M}|^2 \right\rangle = \frac{g_W^4 |U_{ei}|^4}{288(q^2 - m_{\nu_i}^2)^2} \left(-g_{\mu\rho} + \frac{p_{1\mu}p_{1\rho}}{m_W^2}\right)\left(-g_{\nu\sigma} + \frac{p_{2\nu}p_{2\sigma}}{m_W^2}\right) Tr\left[(\mathbb{1}_4 + \gamma^5)\gamma^\mu \not{q} \gamma^\nu \not{p}_4 \gamma^\sigma \not{q} \gamma^\rho \not{p}_3\right] \tag{A.3}$$

Evaluating this trace and contracting the indices on Mathematica, we obtain

$$\begin{aligned}
\left\langle |\mathcal{M}|^2 \right\rangle = \frac{g_w^4 \left|U_{ei}\right|^4}{72m_W^4 \left(t - m_{\nu_i}^2\right)^2} \Big[& (p_1 \cdot p_3)^2 \left(\left(2m_W^2 - p_2^2\right)(p_3 \cdot p_4) + 2(p_2 \cdot p_3)(p_2 \cdot p_4)\right) \\
& + 2(p_1 \cdot p_3)\left(2m_W^2 - p_3^2\right)\left(\left(2m_W^2 - p_2^2\right)(p_1 \cdot p_4) + 2(p_1 \cdot p_2)(p_2 \cdot p_4)\right) \\
& + 4p_1^2(p_1 \cdot p_3)\left(\left(p_2^2 - 2m_W^2\right)(p_3 \cdot p_4) - 2(p_2 \cdot p_3)(p_2 \cdot p_4)\right) \\
& - p_3^2\left(2m_W^2 - p_1^2\right)\left(2m_W^2 - p_2^2\right)(2(p_1 \cdot p_4) - p_3 \cdot p_4) \\
& + 2p_3^2\left(2m_W^2 - p_1^2\right)(2(p_1 \cdot p_2) - p_2 \cdot p_3)(p_2 \cdot p_4) \\
& - p_1^2\left(2m_W^2 - p_1^2\right)\left(\left(2m_W^2 - p_2^2\right)(p_3 \cdot p_4) + 2(p_2 \cdot p_3)(p_2 \cdot p_4)\right)\Big]
\end{aligned} \tag{A.4}$$

Upon adopting the Mandelstam variables in Eq. (4.8), this lengthy expression becomes

$$\begin{aligned}
\left\langle |\mathcal{M}|^2 \right\rangle = \frac{g_w^4 \left|U_{ei}\right|^4}{144m_W^4 \left(t - m_{\nu_i}^2\right)^2} \Big[& m_e^8 + m_e^6\left(6m_W^2 - s - 3t - u\right) \\
& + m_e^4\left(m_W^4 + m_W^2(3s - 13t - 5u) + 2st + 3t(t + u)\right) \\
& + m_e^2\left(2m_W^4(5s - t - 5u) + 2m_W^2 t(-3s + 4t + 5u) - t^2(s + t + 3u)\right) \\
& + 4m_W^6(s - u) + m_W^4 t(-8s + t + 8u) - m_W^2 t^2(-3s + t + 5u) + t^3 u\Big]
\end{aligned} \tag{A.5}$$

which is the final averaged matrix element squared.

B The Standard Double Beta Decay

In this work we have calculated exotic contributions to double beta decay, but not the actual standard double beta decay. As we aim to compare the exotic processes to the corresponding well known standard process, we will now briefly calculate the leptonic current of $2\nu\beta\beta$.

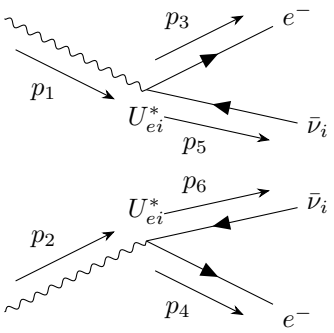

Figure 20: ...

Differently from the exotic processes, the $2\nu\beta\beta$ Feynman diagram is not a single connected diagram, but two individual diagrams occurring simultaneously. This can be seen as a "and" association of probabilities, which is acquired by multiplying the individual probabilities. A sing beta decay yields the current

$$\mathcal{M}_\beta = \frac{g_W U_{ei}^*}{2\sqrt{2}} \left[\bar{u}_e(p_3)\gamma^\mu(\mathbb{1}_4 - \gamma^5)v_{\nu_i}(p_5)\right] \tag{B.1}$$

Combining two beta decays into a double beta decay results in

$$\mathcal{M}_{2\nu\beta\beta} = \frac{g_W^2 (U_{ei}^*)^2}{8} \left[\bar{u}_e(p_3)\gamma^\mu(\mathbb{1}_4 - \gamma^5)v_{\nu_i}(p_5)\right] \left[\bar{u}_e(p_4)\gamma^\nu(\mathbb{1}_4 - \gamma^5)v_{\nu_i}(p_6)\right] \tag{B.2}$$

The averaged squared matrix element is then easily obtained using Casimir's trick, as usual:

$$\begin{aligned}\left\langle|\mathcal{M}_{2\nu\beta\beta}|^2\right\rangle =& \frac{1}{2^2\times 3}\frac{g_W^4|U_{ei}|^4}{16}\mathrm{Tr}\left[(\mathbb{1}_4+\gamma^5)\gamma^\mu \not{p}_5 \gamma^\rho \not{p}_3\right]\mathrm{Tr}\left[(\mathbb{1}_4+\gamma^5)\gamma^\nu \not{p}_6 \gamma^\sigma \not{p}_4\right] \\ =& \frac{g_W^4|U_{ei}|^4}{192}\mathrm{Tr}\left[(\mathbb{1}_4+\gamma^5)\gamma^\mu \not{p}_5 \gamma^\rho \not{p}_3\right]\mathrm{Tr}\left[(\mathbb{1}_4+\gamma^5)\gamma^\nu \not{p}_6 \gamma^\sigma \not{p}_4\right]\end{aligned} \tag{B.3}$$

The trace can be evaluated either by using the standard trace identities for gamma matrices [36] or directly with Mathematica, resulting in

$$\begin{aligned}\left\langle|\mathcal{M}_{2\nu\beta\beta}|^2\right\rangle = \frac{g_W^4|U_{ei}|^4}{12}\big[&\left((p_3\cdot p_5)\, g^{\mu\sigma} - p_5{}^\mu p_3{}^\rho - p_3{}^\mu p_5{}^\rho + i\epsilon^{\mu\rho p_3 p_5}\right) \\ &\times \left((p_4\cdot p_6)\, g^{\nu\sigma} - p_6{}^\nu p_4{}^\sigma - p_4{}^\nu p_6{}^\sigma + i\epsilon^{\nu\sigma p_4 p_6}\right)\big]\end{aligned} \tag{B.4}$$

Although there is an imaginary term arising from each trace, they will ultimately vanish when contracted with the hadronic current as the matrix element squared is a real number.

As for the phase space, it is given similarly as in the previous processes by

$$\Gamma_{2\nu\beta\beta} \approx \frac{1}{2M} |\mathcal{M}_{2\nu\beta\beta}|^2 \int \frac{d^3\vec{P}}{2(2\pi)^3 M} \frac{d^3\vec{p}_{e_1}}{2(2\pi)^3\epsilon_{e_1}} \frac{d^3\vec{p}_{e_2}}{2(2\pi)^3\epsilon_{e_2}} \frac{d^3\vec{p}_{\nu_1}}{2(2\pi)^3\epsilon_{\nu_1}} \frac{d^3\vec{p}_{\nu_2}}{2(2\pi)^3\epsilon_{\nu_2}} (p_{e_1} \cdot p_{\nu_1}) \\ \times (p_{e_2} \cdot p_{\nu_2})(2\pi)^4 \delta^{(4)}(P - p_{e_1} - p_{e_2} + p_{\nu_1} + p_{\nu_2} - \tilde{P}) a(\epsilon_{e_1}, \epsilon_{e_2}) \tag{B.5}$$

Since this calculation follows pretty much the same techniques used in the previous calculations, we will skip through repetitive steps. Integrating over P, using the usual substitution $d^3\vec{p}_j \to |\vec{p}_j|^2 d|\vec{p}_j| d\phi d\cos(\theta)$, and integrate over the solid angles, we obtain

$$\Gamma_{2\nu\beta\beta} \approx \frac{1}{4(2\pi)^7 M^2} \left(\frac{|\mathcal{M}_{2\nu\beta\beta}|}{1 - e^{-2\pi a Z}} \right)^2 \int \epsilon_{e_1}^2 d\epsilon_{e_1} \epsilon_{e_2}^2 d\epsilon_{e_2} \epsilon_{\nu_1}^2 d\epsilon_{\nu_1} \epsilon_{\nu_2}^2 d\epsilon_{\nu_2} \delta(Q + 2m_e - \epsilon_{e_1} - \epsilon_{e_2} + \epsilon_{\nu_1} + \epsilon_{\nu_2})$$

Where we have taken the neutrinos to be approximately massless. We may now use again the variable substitution defined by Eq. (5.30) and Eq. (5.31), resulting in

$$\Gamma_{2\nu\beta\beta} \approx \frac{1}{4(2\pi)^7 M^2} \left(\frac{|\mathcal{M}_{2\nu\beta\beta}|}{1 - e^{-2\pi a Z}} \right)^2 \int \epsilon_{e_1}^2 d\epsilon_{e_1} \epsilon_{e_2}^2 d\epsilon_{e_2} \frac{\epsilon^5 \sin^5(2\xi)}{4} d\epsilon d\xi \delta(Q + 2m_e - \epsilon_{e_1} - \epsilon_{e_2} + \epsilon)$$

Integrating the angle ξ, we are left with only the integral over the energies

$$\Gamma_{2\nu\beta\beta} \approx \frac{1}{30(2\pi)^7 M^2} \left(\frac{|\mathcal{M}_{2\nu\beta\beta}|}{1 - e^{-2\pi a Z}} \right)^2 \int \epsilon_{e_1}^2 d\epsilon_{e_1} \epsilon_{e_2}^2 d\epsilon_{e_2} \epsilon^5 d\epsilon \delta(Q + 2m_e - \epsilon_{e_1} - \epsilon_{e_2} + \epsilon)$$

We then integrate over the neutrinos' energy and get rid of the remaining delta function

$$\Gamma_{2\nu\beta\beta} \approx \frac{1}{30(2\pi)^7 M^2} \left(\frac{|\mathcal{M}_{2\nu\beta\beta}|}{1 - e^{-2\pi a Z}} \right)^2 \int_{m_e}^{Q+m_e} \int_{m_e}^{Q+2m_e-\epsilon_{e_2}} \epsilon_{e_1}^2 \epsilon_{e_2}^2 (Q + 2m_e - \epsilon_{e_1} - \epsilon_{e_2})^5 d\epsilon_{e_1} d\epsilon_{e_2} \tag{B.6}$$

What is left is the integral over the energies of each electron. Integrating over the first electron energy, we obtain

$$\Gamma_{2\nu\beta\beta} \approx \frac{1}{30(2\pi)^7 M^2} \left(\frac{|\mathcal{M}_{2\nu\beta\beta}|}{1 - e^{-2\pi a Z}} \right)^2 \\ \times \int_{m_e}^{Q+m_e} \frac{1}{168} \epsilon_{e_2}^2 \left(37m^2 + 10m(Q - \epsilon_{e_2}) + (Q - \epsilon_{e_2})^2 \right) (m + Q - \epsilon_{e_2})^6 d\epsilon_{e_2}$$

Finally, integrating over the second electron energy, the total decay rate is

$$\Gamma_{2\nu\beta\beta} \approx \frac{1}{(2\pi)^7 M^2} \left(\frac{|\mathcal{M}_{2\nu\beta\beta}|}{1 - e^{-2\pi a Z}} \right)^2 \frac{Q^{11} + 22mQ^{10} + 220m^2Q^9 + 990m^3Q^8 + 1980m^4Q^7}{2494800} \tag{B.7}$$

References

[1] G. Aad *et al.*, "Observation of a new particle in the search for the Standard Model Higgs boson with the ATLAS detector at the LHC," *Phys. Lett. B*, vol. 716, pp. 1–29, 2012. DOI: 10.1016/j.physletb.2012.08.020. arXiv: 1207.7214 [hep-ex].

[2] S. Chatrchyan *et al.*, "Observation of a New Boson at a Mass of 125 GeV with the CMS Experiment at the LHC," *Phys. Lett. B*, vol. 716, pp. 30–61, 2012. DOI: 10.1016/j.physletb.2012.08.021. arXiv: 1207.7235 [hep-ex].

[3] T. Kajita, E. Kearns, and M. Shiozawa, "Establishing atmospheric neutrino oscillations with Super-Kamiokande," *Nucl. Phys. B*, vol. 908, pp. 14–29, 2016. DOI: 10.1016/j.nuclphysb.2016.04.017.

[4] Q. Ahmad *et al.*, "Direct evidence for neutrino flavor transformation from neutral current interactions in the Sudbury Neutrino Observatory," *Phys. Rev. Lett.*, vol. 89, p. 011 301, 2002. DOI: 10.1103/PhysRevLett.89.011301. arXiv: nucl-ex/0204008.

[5] W. Pauli, "Dear radioactive ladies and gentlemen," *Phys. Today*, vol. 31N9, p. 27, 1978.

[6] R. Arnold *et al.*, "Measurement of the double-beta decay half-life and search for the neutrinoless double-beta decay of ^{48}Ca with the NEMO-3 detector," *Phys. Rev. D*, vol. 93, no. 11, p. 112 008, 2016. DOI: 10.1103/PhysRevD.93.112008. arXiv: 1604.01710 [hep-ex].

[7] C. Patrignani *et al.*, "Review of Particle Physics," *Chin. Phys. C*, vol. 40, no. 10, p. 100 001, 2016, See p. 768. DOI: 10.1088/1674-1137/40/10/100001.

[8] C. Cowan, F. Reines, F. Harrison, H. Kruse, and A. McGuire, "Detection of the free neutrino: A Confirmation," *Science*, vol. 124, pp. 103–104, 1956. DOI: 10.1126/science.124.3212.103.

[9] F. Reines and C. L. Cowan, "The neutrino," *Nature*, vol. 178, pp. 446–449, 1956. DOI: 10.1038/178446a0.

[10] G. Danby, J. Gaillard, K. Goulianos, L. Lederman, N. Mistry, M. Schwartz, and J. Steinberger, "Observation of High-Energy Neutrino Reactions and the Existence of Two Kinds of Neutrinos," *Physical Review Letters*, vol. 9, pp. 36–44, 1962.

[11] C. S. Wu, E. Ambler, R. W. Hayward, D. D. Hoppes, and R. P. Hudson, "Experimental Test of Parity Conservation in Beta Decay," *Phys. Rev.*, vol. 105, pp. 1413–1415, 4 Feb. 1957. DOI: 10.1103/PhysRev.105.1413. [Online]. Available: https://link.aps.org/doi/10.1103/PhysRev.105.1413.

[12] B. Pontecorvo, "Mesonium and Antimesonium," *Soviet Journal of Experimental and Theoretical Physics*, vol. 6, p. 429, 1958.

[13] *Sudbury Neutrino Observatory*, https://falcon.phy.queensu.ca/SNO/, [Online].

[14] *Kamioka Observatory*, http://www-sk.icrr.u-tokyo.ac.jp/index-e.html, [Online].

[15] Z. Maki, M. Nakagawa, and S. Sakata, "Remarks on the Unified Model of Elementary Particles," *Progress of Theoretical Physics*, vol. 28, pp. 870–880, Nov. 1962. DOI: 10.1143/PTP.28.870.

[16] P. de Salas, D. Forero, S. Gariazzo, P. Martínez-Miravé, O. Mena, C. Ternes, M. Tórtola, and J. Valle, "2020 Global reassessment of the neutrino oscillation picture," Jun. 2020. arXiv: 2006.11237 [hep-ph].

[17] K. S. Krane, *Introductory Nuclear Physics*. 1987.

[18] B. Pontecorvo, "Electron and Muon Neutrinos," *Sov. Phys. JETP*, vol. 10, pp. 1236–1240, 1960.

[19] *Ettore Majorana: Scientific Papers*. Germany: Springer, 2006, pp. 201–233, ISBN: 3540480919.

[20] F. F. Deppisch, L. Graf, J. Harz, and W.-C. Huang, "Neutrinoless Double Beta Decay and the Baryon Asymmetry of the Universe," *Phys. Rev. D*, vol. 98, no. 5, p. 055 029, 2018. DOI: 10.1103/PhysRevD.98.055029. arXiv: 1711.10432 [hep-ph].

[21] M. Doi, T. Kotani, and E. Takasugi, "Double beta Decay and Majorana Neutrino," *Prog. Theor. Phys. Suppl.*, vol. 83, p. 1, 1985. DOI: 10.1143/PTPS.83.1.

[22] E. L. Fireman, "Double Beta Decay," *Physical Review*, vol. 74, pp. 1201–1253, 9 Nov. 1948. DOI: 10.1103/PhysRev.74.1201. [Online]. Available: https://link.aps.org/doi/10.1103/PhysRev.74.1201.

[23] D. Adams *et al.*, "Improved Limit on Neutrinoless Double-Beta Decay in ^{130}Te with CUORE," *Phys. Rev. Lett.*, vol. 124, no. 12, p. 122 501, 2020. DOI: 10.1103/PhysRevLett.124.122501. arXiv: 1912.10966 [nucl-ex].

[24] M. Agostini *et al.*, "Probing Majorana neutrinos with double-β decay," *Science*, vol. 365, p. 1445, 2019. DOI: 10.1126/science.aav8613. arXiv: 1909.02726 [hep-ex].

[25] Y. Gando, "Neutrinoless double beta decay search with liquid scintillator experiments," in *Prospects in Neutrino Physics*, Apr. 2019. arXiv: 1904.06655 [physics.ins-det].

[26] R. Arnold *et al.*, "Results of the search for neutrinoless double-β decay in ^{100}Mo with the NEMO-3 experiment," *Phys. Rev. D*, vol. 92, no. 7, p. 072 011, 2015. DOI: 10.1103/PhysRevD.92.072011. arXiv: 1506.05825 [hep-ex].

[27] ——, "Final results on ^{82}Se double beta decay to the ground state of ^{82}Kr from the NEMO-3 experiment," *Eur. Phys. J.*, vol. C78, no. 10, p. 821, 2018. DOI: 10.1140/epjc/s10052-018-6295-x. arXiv: 1806.05553 [hep-ex].

[28] T. Brune and H. Päs, "Majoron Dark Matter and Constraints on the Majoron-Neutrino Coupling," 2018. arXiv: 1808.08158 [hep-ph].

[29] M. Doi, T. Kotani, and E. Takasugi, "The Neutrinoless Double Beta Decay With Majoron Emission," *Phys. Rev. D*, vol. 37, p. 2575, 1988. DOI: 10.1103/PhysRevD.37.2575.

[30] K. Blum, Y. Nir, and M. Shavit, "Neutrinoless double-beta decay with massive scalar emission," *Phys. Lett. B*, vol. 785, pp. 354–361, 2018. DOI: 10.1016/j.physletb.2018.08.022. arXiv: 1802.08019 [hep-ph].

[31] M. D. Schwartz, *Quantum Field Theory and the Standard Model*. Cambridge University Press, 2014, ISBN: 9781107034730. [Online]. Available: http://www.cambridge.org/us/academic/subjects/physics/theoretical-physics-and-mathematical-physics/quantum-field-theory-and-standard-model.

[32] P. B. Pal, *An introductory course of particle physics*. Boca Raton: CRC Press, 2014, ISBN: 978-1482216981.

[33] D. Griffiths, *Introduction to Elementary Particles*. Weinheim, Germany: Wiley-VCH (2008) 454 p, 2008, ISBN: 9783527406012.

[34] *Wolfram Mathematica*, https://www.wolfram.com/mathematica/, [Online].

[35] *Feyncalc*, https://feyncalc.github.io/, [Online].

[36] M. Thomson, *Modern Particle Physics*. New York: Cambridge University Press, 2013, ISBN: 9781107034266. [Online]. Available: http://www-spires.fnal.gov/spires/find/books/www?cl=QC793.2.T46::2013.

[37] *Neutrino Ettore Majorana Observatory*, http://nemo.in2p3.fr/nemow3/, [Online].

[38] L. Kells, W. Kern, and J. Bland, *Plane and Spherical Trigonometry*. Creative Media Partners, LLC, 2018, pp. 323–326, ISBN: 9780343252373. [Online]. Available: https://books.google.co.uk/books?id=d4OJvQEACAAJ.